SSRDM 2011

Advanced Summer School in Radiation Detection and Measurements

München, Germany, July 25-29, 2011

Advanced Concepts in the Readout and Signal Processing

Helmuth Spieler

helmuth.spieler@gmail.com

Additional tutorials at [*http://www-physics.lbl.gov/~spieler*](http://www-physics.lbl.gov/~spieler)

or simply Google "spieler detectors"

More detailed discussions in
H. Spieler: Semiconductor Detector Systems, Oxford University Press, 2005

Course Contents

I. Why Understand Front-End Electronics?

II. Signals and Noise

III. Signal Processing

- Analog
- Digital

IV. Examples

- Strip and Pixel Detectors
- Time Projection Chambers
- Micro-Calorimeters

I. Why Understand Front-End Electronics?

Energy resolution enables recognition of structure in energy spectra.

Optimizing energy resolution often depends on electronics.

Comparison of NaI(Tl) scintillation detector and Ge semiconductor diode detector.

- Resolution in NaI(Tl) is determined by the scintillator.
- Resolution of the Ge detector depends significantly on electronics.

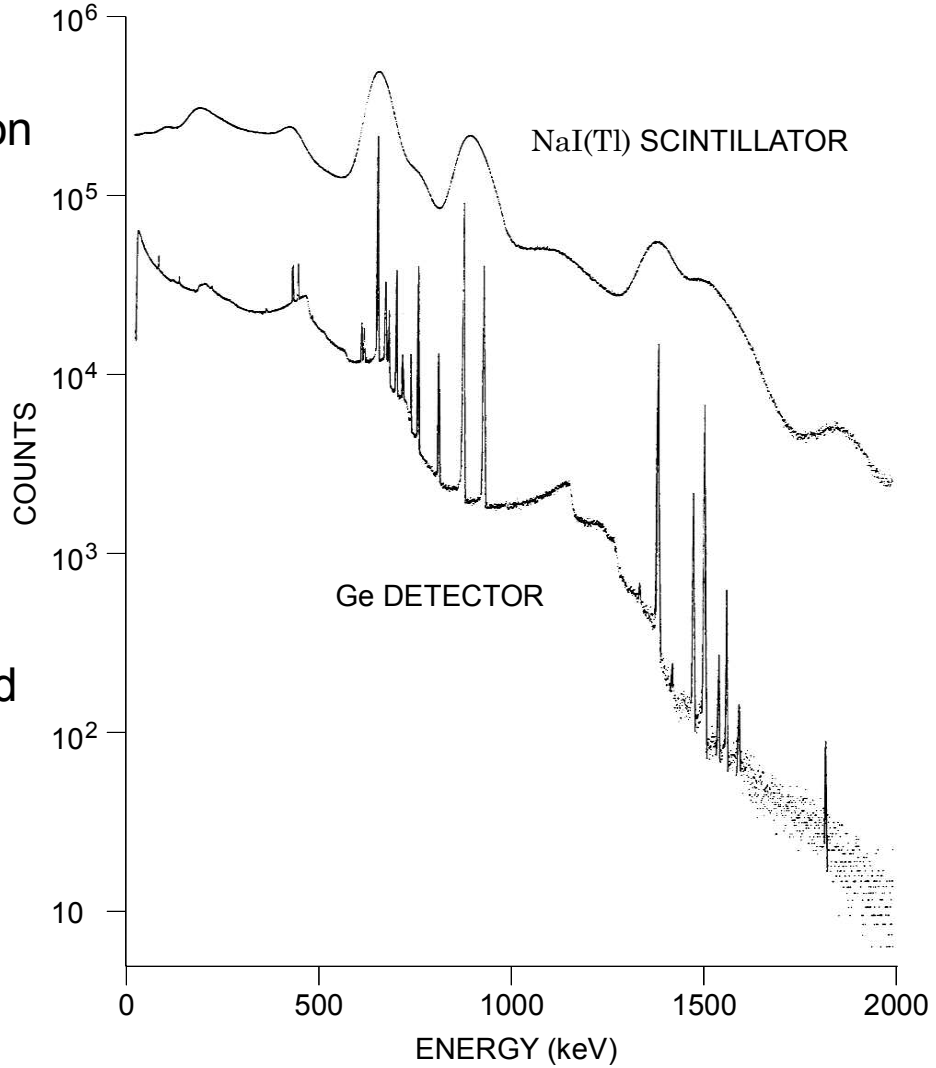

J.Cl. Philippot, IEEE Trans. Nucl. Sci. **NS-17/3** (1970) 446

Energy resolution is also important in experiments that don't measure energy.

Energy resolution improves sensitivity because

signal-to-background ratio improves with better resolution.

(signal counts in fewer bins compete with fewer background counts)

In tracking detectors a minimum signal-to-background ratio is essential to avoid fake hits.

Achieving the required signal-to-noise ratio with minimized power dissipation is critical in large-scale tracking detectors.

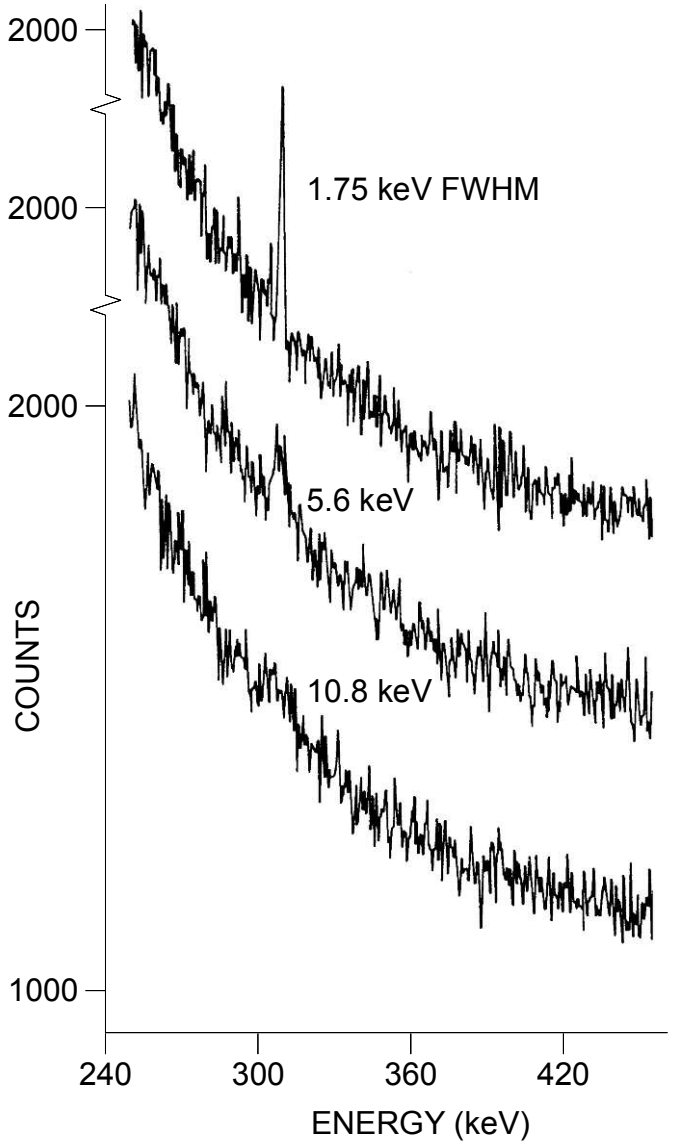

G.A. Armantrout *et al.*, IEEE Trans. Nucl. Sci. **NS-19/1** (1972) 107

Recognizing overall contributions to signal sensitivity does not require detailed knowledge of electronics engineering.

It does require a real understanding of basic classical physics,

i.e. recognize which aspects of physics apply in practical situations.

… nope, real life doesn't tell you which chapter to follow!

For physicists and electronics engineers to work together efficiently it is necessary that physicists understand basic principles so that they don't request things that cannot work.

A common problem is "wouldn't it be nice to have this ...", which often adds substantial effort and costs

– without real benefits.

What determines Resolution?

1. Signal variance (e.g. statistical fluctuations) >> Baseline Variance

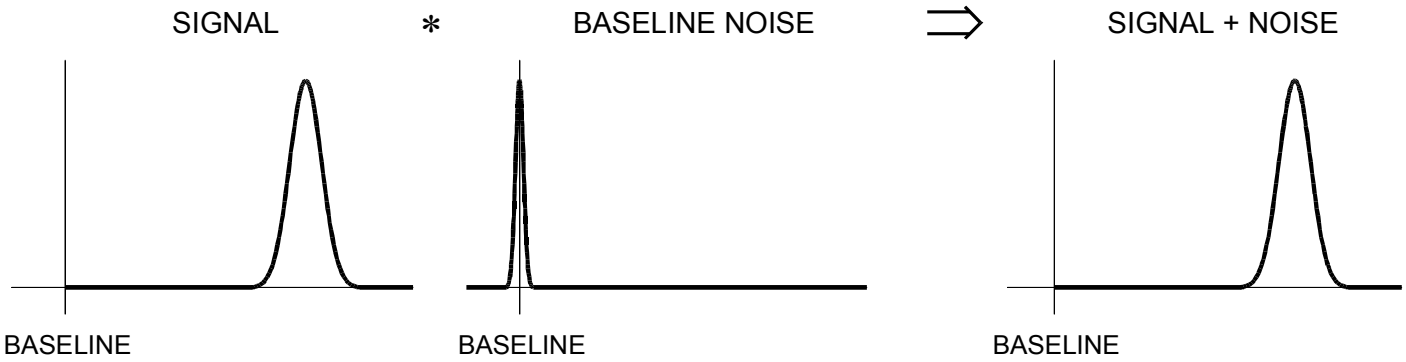

$\Rightarrow$ Electronic (baseline) noise not important

Examples:
- High-gain proportional chambers
- Scintillation Counters with High-Gain PMTs

e.g. 1 MeV γ-rays absorbed by $\mathrm{NaI(Tl)}$ crystal

Number of photoelectrons: $N_{pe} \approx 8{\cdot}10^4$ [MeV^{-1}] $\times E_\gamma \times QE \approx 2.4{\cdot}10^4$

Variance typically: $\sigma_{pe} = \sqrt{N_{pe}} \approx 160$ and $\sigma_{pe} / N_{pe} \approx 5$ - 8%

Signal at PMT anode (assume Gain= 10^4): $Q_{sig} = G_{PMT} N_{pe} \approx 2.4{\cdot}10^8$ el

and $\sigma_{sig} = G_{PMT} \sigma_{pe} \approx 1.2{\cdot}10^7$ el

whereas electronic noise easily < 10^4 el

2. Signal Variance << Baseline Variance

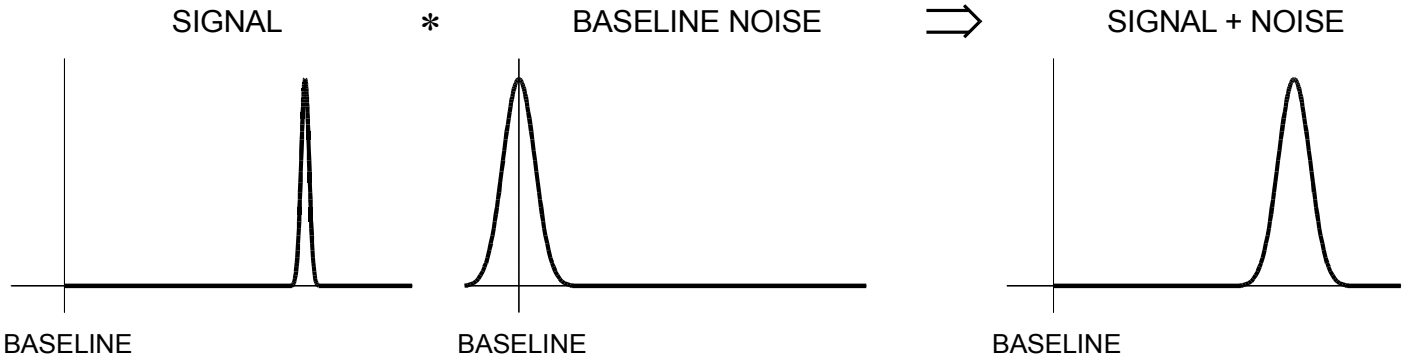

$\Rightarrow$ Electronic (baseline) noise critical for resolution

Examples:
- Gaseous ionization chambers (no internal gain)
- Semiconductor detectors

e.g. in Si : Number of electron-hole pairs $N_{ep} = \dfrac{E_{dep}}{3.6\ \text{eV}}$

Variance $\sigma_{ep} = \sqrt{F \cdot N_{ep}}$ (where F = Fano factor ≈ 0.1)

For 50 keV photons: $\sigma_{ep} \approx 40$ el $\Rightarrow \sigma_{ep} / N_{ep} = 7.5 \cdot 10^{-4}$

Obtainable noise levels are 10 to 1000 el.

Baseline fluctuations can have many origins ...

pickup of external interference

artifacts due to imperfect electronics

… etc.,

but the (practical) fundamental limit is electronic noise.

Depends on noise sources and signal processing.

Sources of electronic noise:
- Thermal fluctuations of carrier motion
- Statistical fluctuations of currents

Both types of fluctuations are random in amplitude and time

⇒ Power distributed over wide frequency range

⇒ Contribution to energy fluctuations depends on signal processing

Many different types of detectors are used for radiation detection.

Nearly all rely on electronics.

Although detectors appear to be very different, basic principles of the readout apply to all.

- The sensor signal is a current.
- The integrated current $Q_S = \int i_S(t)dt$ yields the signal charge.
- The total charge is proportional to the absorbed energy.

Readout systems include the following functions:

- Signal acquisition
- Pulse shaping
- Digitization
- Data Readout

1. Basic Functions of Front-End Electronics

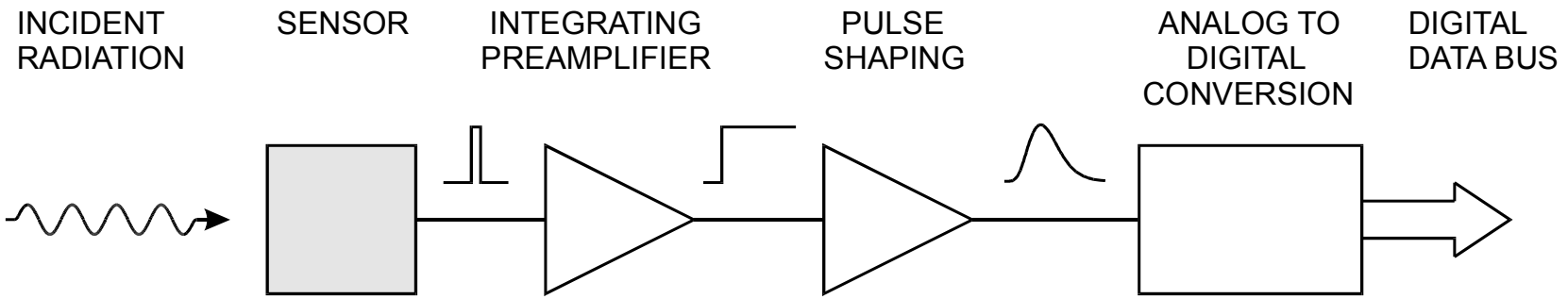

Pulse shaping can also be performed with digital circuitry:

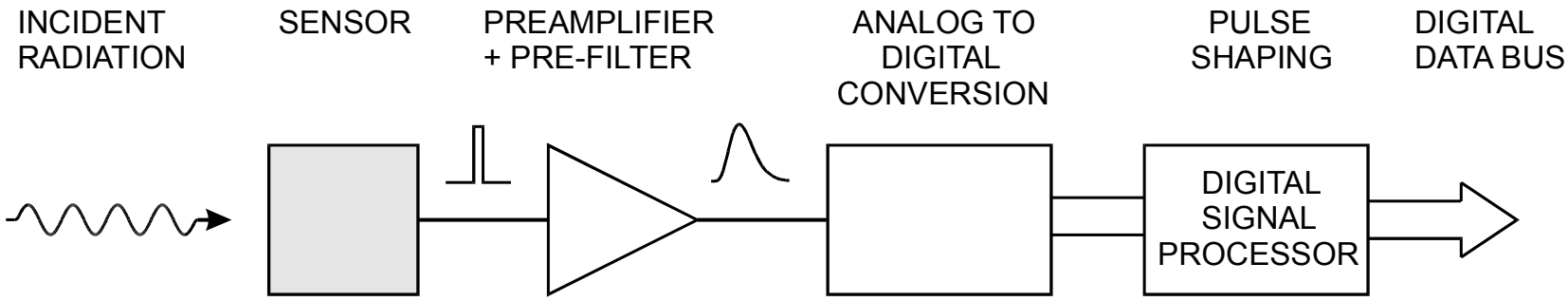

Many Different Implementations

"Traditional" Si detector system
for charged particle measurements

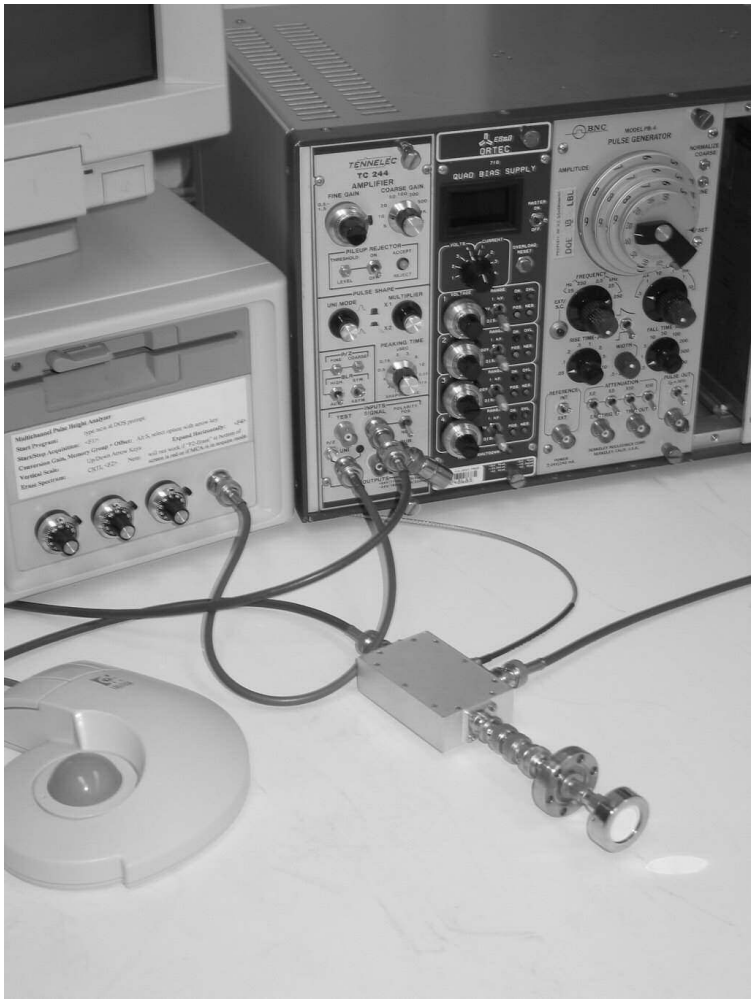

Tracking Detector Module (CDF SVX)
512 electronics channels on 50 μm pitch

Spectroscopy systems highly optimized!

By the late 1970s improvements were measured in single %.

Separate system components:

1. detector
2. preamplifier
3. amplifier
   - adjustable gain
   - adjustable shaping
     - (unipolar + bipolar)
   - adjustable pole-zero cancellation
   - baseline restorer

Nuclear Physics beam times were typically a few days with changing configurations, so equipment required to be modular and adaptable.

Today, systems with many channels are required in many fields.

In large systems power dissipation and size are critical, so systems are not necessarily designed for optimum noise, but *adequate* noise, and circuitry is tailored to specific detector requirements.

Large-Scale Readout Systems

Example: Si strip detector

On-chip Circuits

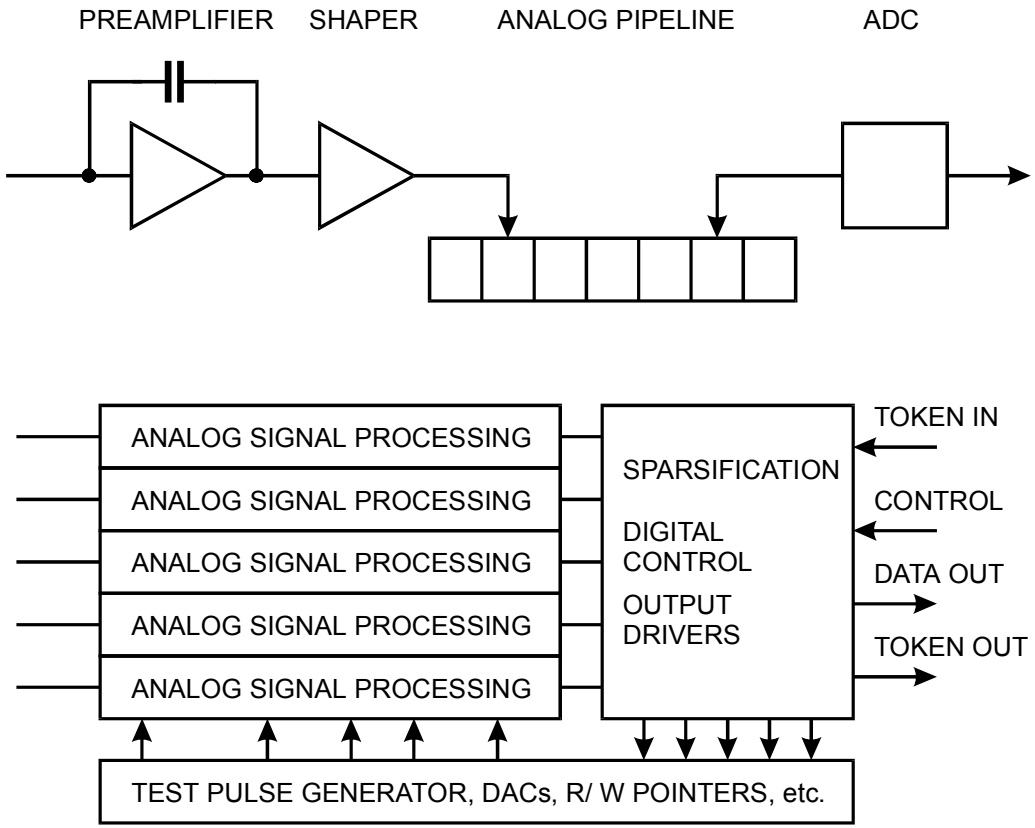

Inside a typical readout IC: 128 parallel channels of analog front-end electronics
Logic circuitry to decode control signals, load DACs, etc.
Digital circuitry for zero-suppression, readout

Readout of Multiple ICs

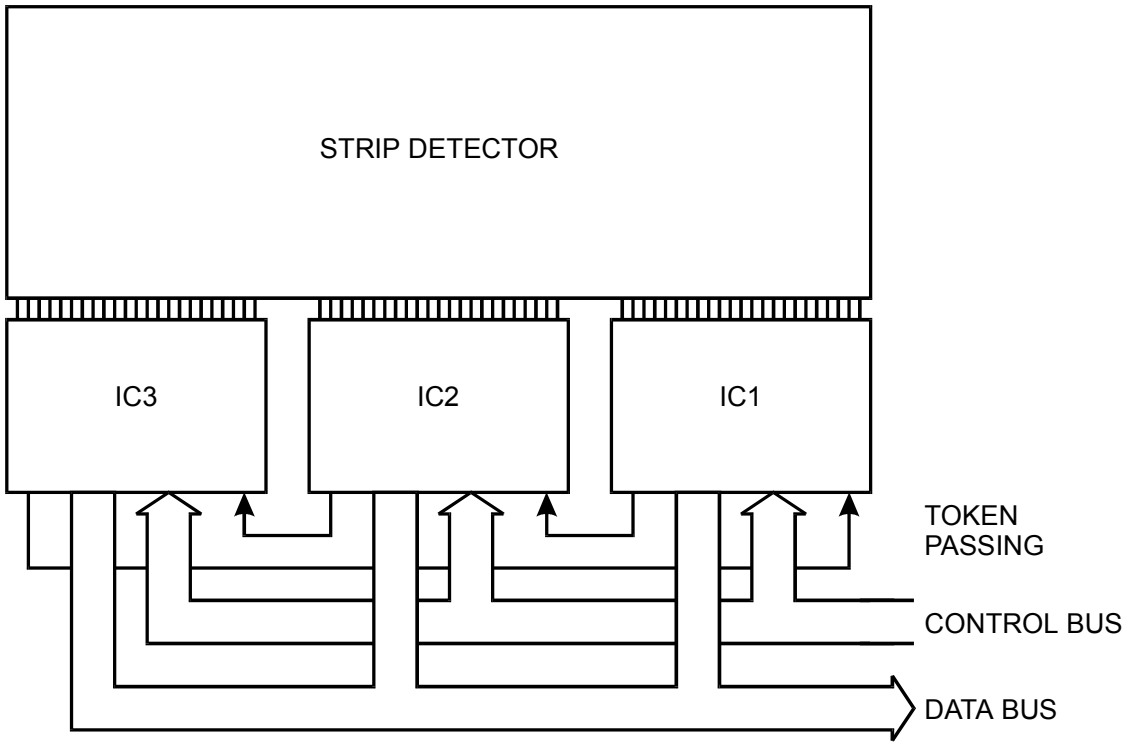

IC1 is designated as master.

Readout is initiated by a trigger signal selecting appropriate time stamp to IC1.

When all data from IC1 have been transferred, a token is passed to IC2.

When IC3 has finished, the token is passed back to IC1, which can begin a new cycle.

ATLAS Silicon Strip system (SCT): ABCD chips mounted on hybrid

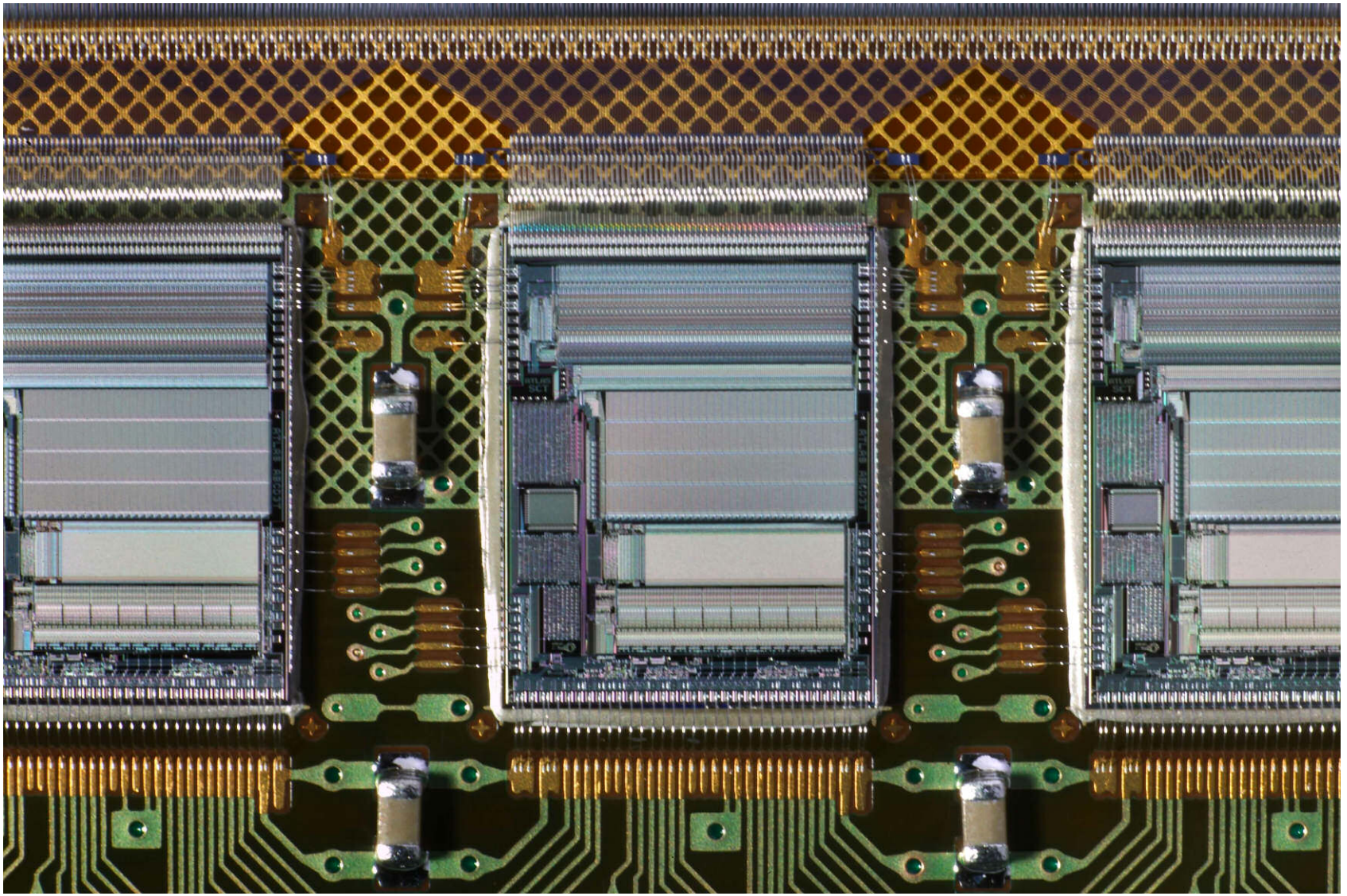

ATLAS SCT Detector Module

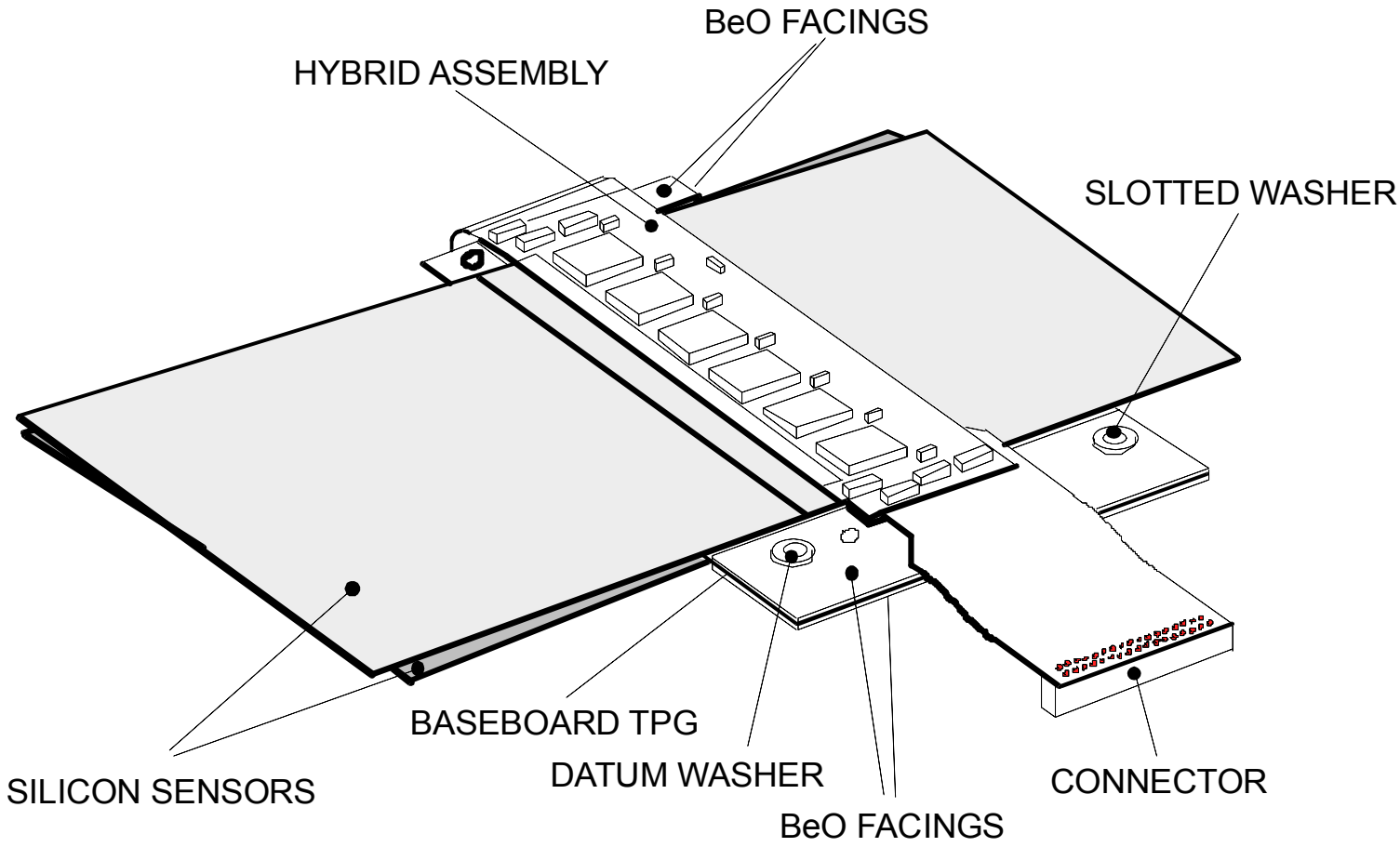

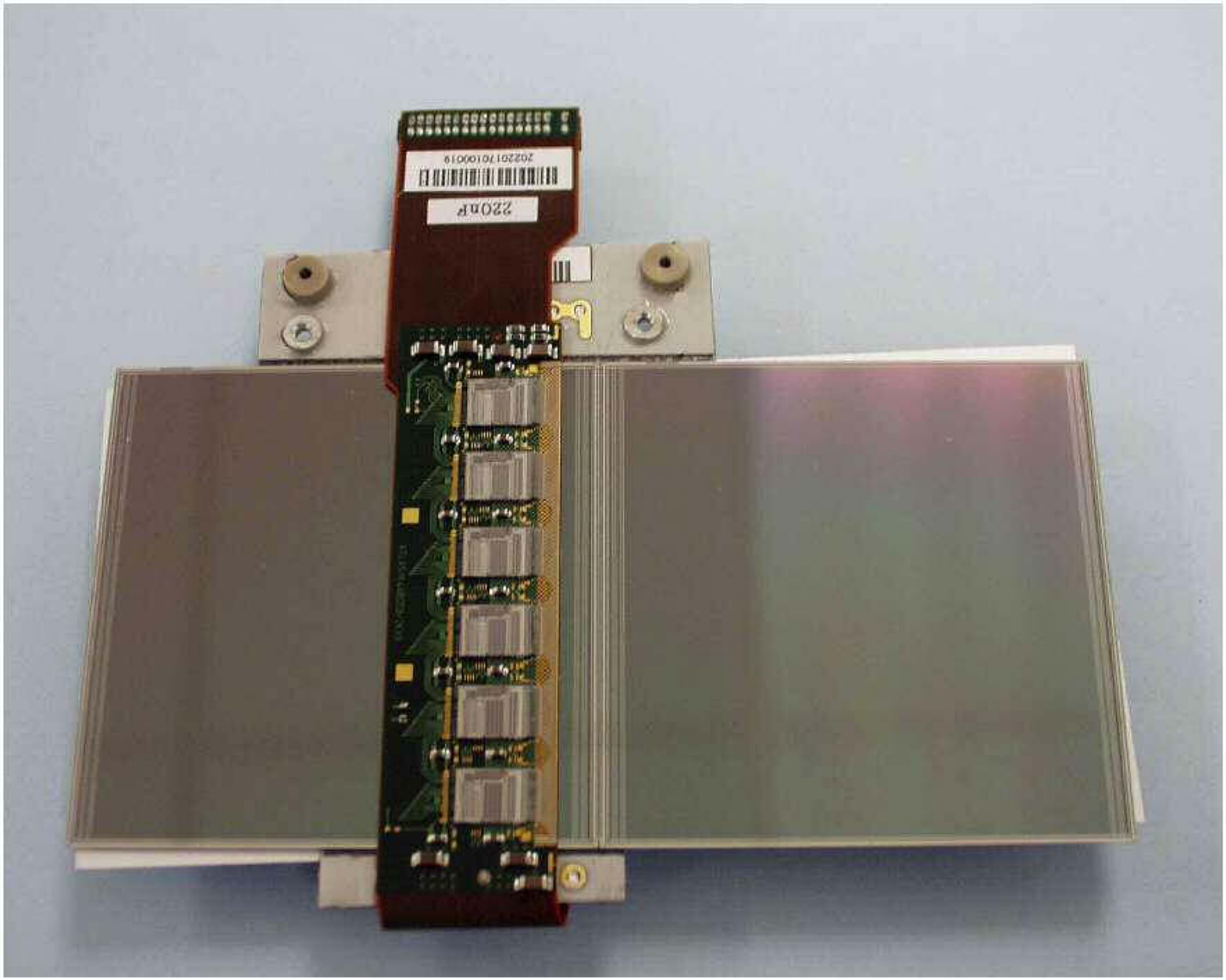
220nF

Cross Section of Module

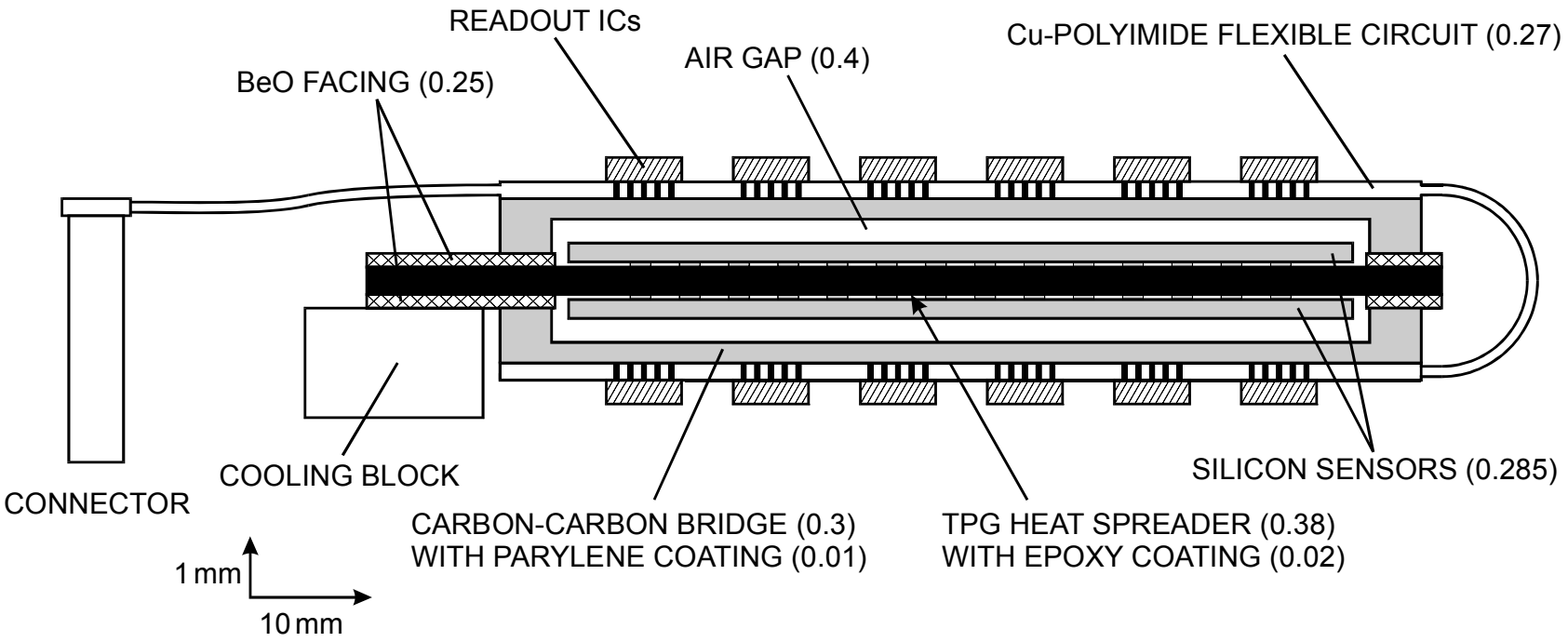

Design criteria depend on application

1. Energy resolution
2. Rate capability
3. Timing information
4. Position sensing

Large-scale systems impose compromises

1. Power consumption
2. Scalability
3. Straightforward setup + monitoring
4. Cost

Technology choices

1. Discrete components – low design cost
   fix “on the fly”
2. Full-custom ICs – high density, low power, but
   better get it right!

Successful systems rely on many details that go well beyond “headline specs”!

II. Signals and Noise

We consider detectors that provide electrical signal outputs.

To extract the amplitude or timing information the electrical signal is coupled to an amplifier, sent through gain and filtering stages, and finally digitized to allow data storage and analysis.

Optimal signal processing depends on the primary signal.

In general, the signal can be

1. a continuously varying current or voltage
2. a sequence of pulses, occurring
   - periodically
   - at known times
   - randomly

All of these affect the choice of signal processing techniques.

First steps in signal processing:
- Formation of the signal in the detector
- Coupling the sensor to the amplifier

Radiation detectors use either
- direct detection (e.g. ionization chambers)

  or
- indirect detection (e.g. scintillators)

1. Signal Formation

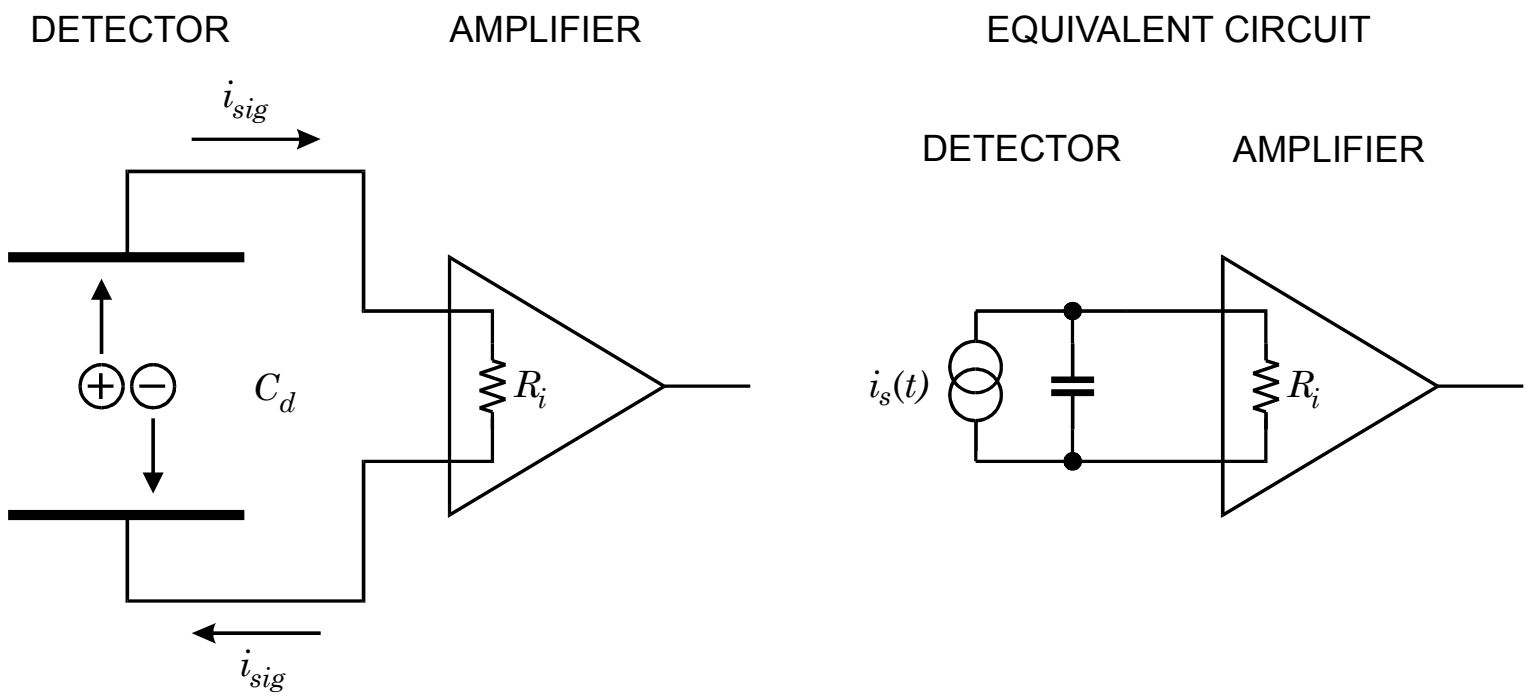

The signal current $i_{sig}(t)$ begins when a charge particle starts moving.

The time for the signal charges to reach the corresponding electrodes is the collection time T_C.

The signal charge is proportional to the energy: $E \propto Q_S = \int_0^{T_C} i_{sig}(t)dt$

Induced Charge

Consider a charge q in a parallel plate capacitor:

When the charge is midway between the two plates, the charge induced on one plate is determined by applying Gauss' law. The same number of field lines intersect both S_1 and S_2, so equal charge is induced on each plate (= q / 2).

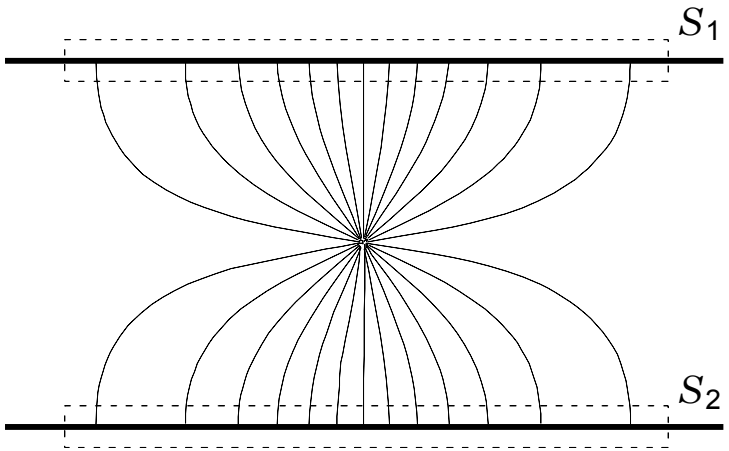

When the charge is close to one plate, most of the field lines terminate on that plate and the induced charge is much greater.

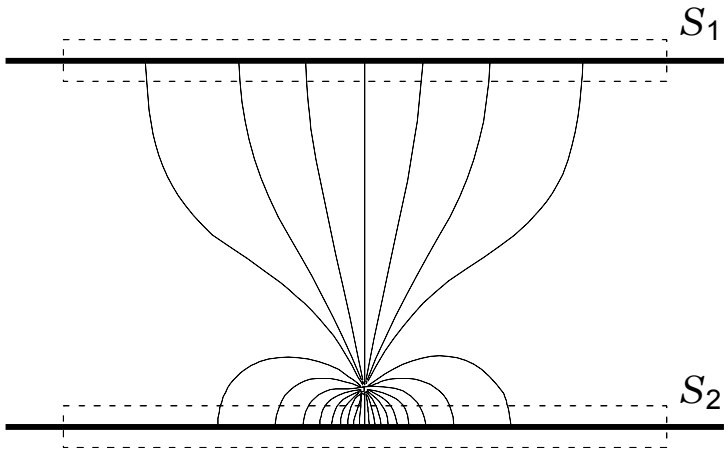

As a charge traverses the space between the two plates the induced charge changes continuously, so current flows in the external circuit as soon as the charges begin to move.

Induced Signal Currents in a Strip Detector

Consider a charge originating near the upper contiguous electrode and drifting down towards the strips.

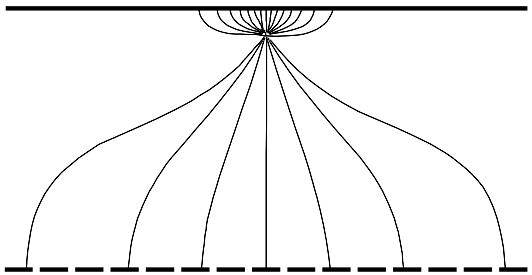

Initially, charge is induced over many strips.

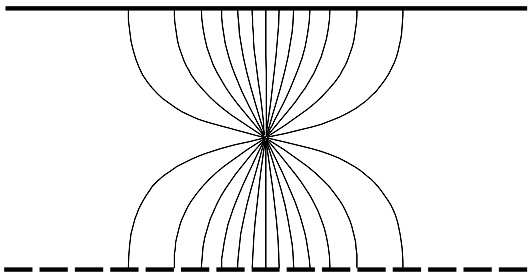

As the charge approaches the strips, the signal distributes over fewer strips.

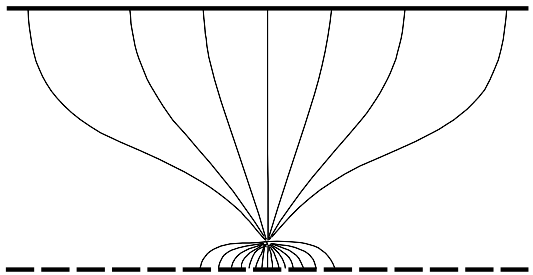

When the charge is close to the strips, the signal is concentrated over few strips

The magnitude of the induced current due to the moving charge depends on the coupling between the charge and the individual electrodes.

For a quantitative description see Spieler website or Chapter 2, pp 71-82

For a discussion of an incorrect, but popular derivation of signal charge based on “energy conservation”, see www-physics.lbl.gov/~spieler/EDIT_2011/Silicon_Readout.pdf

The pulse shapes depend on the charge carrier velocities, but also on the electrode configuration.

These signals are from a 300 μm thick silicon detector with simple parallel-plate electrodes and a track traversing the detector.

The left plot is with the detector biased at the depletion voltage, whereas the right is at over-depletion, which reduces the collection time.

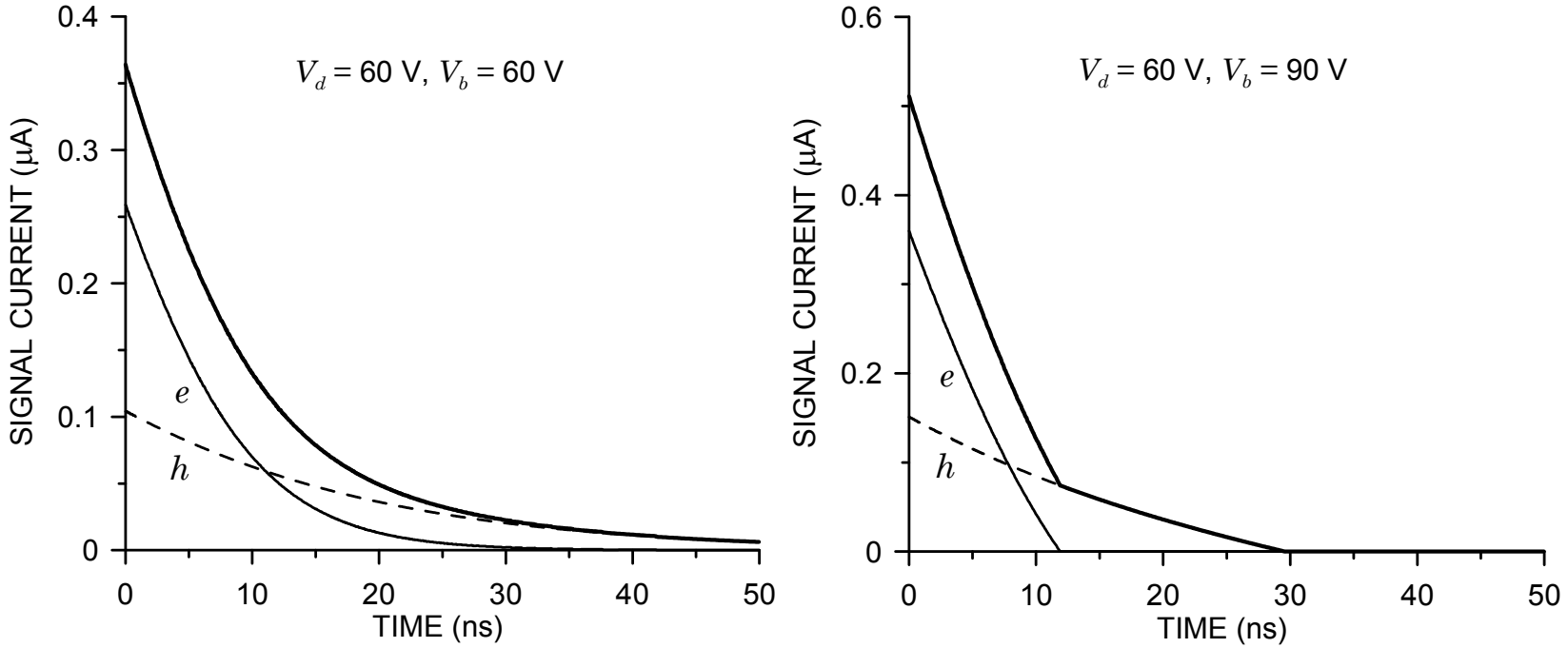

Current pulses in strip detectors of the same thickness and also with the track traversing the detector)
(V_d = 60V, V_b = 90V)

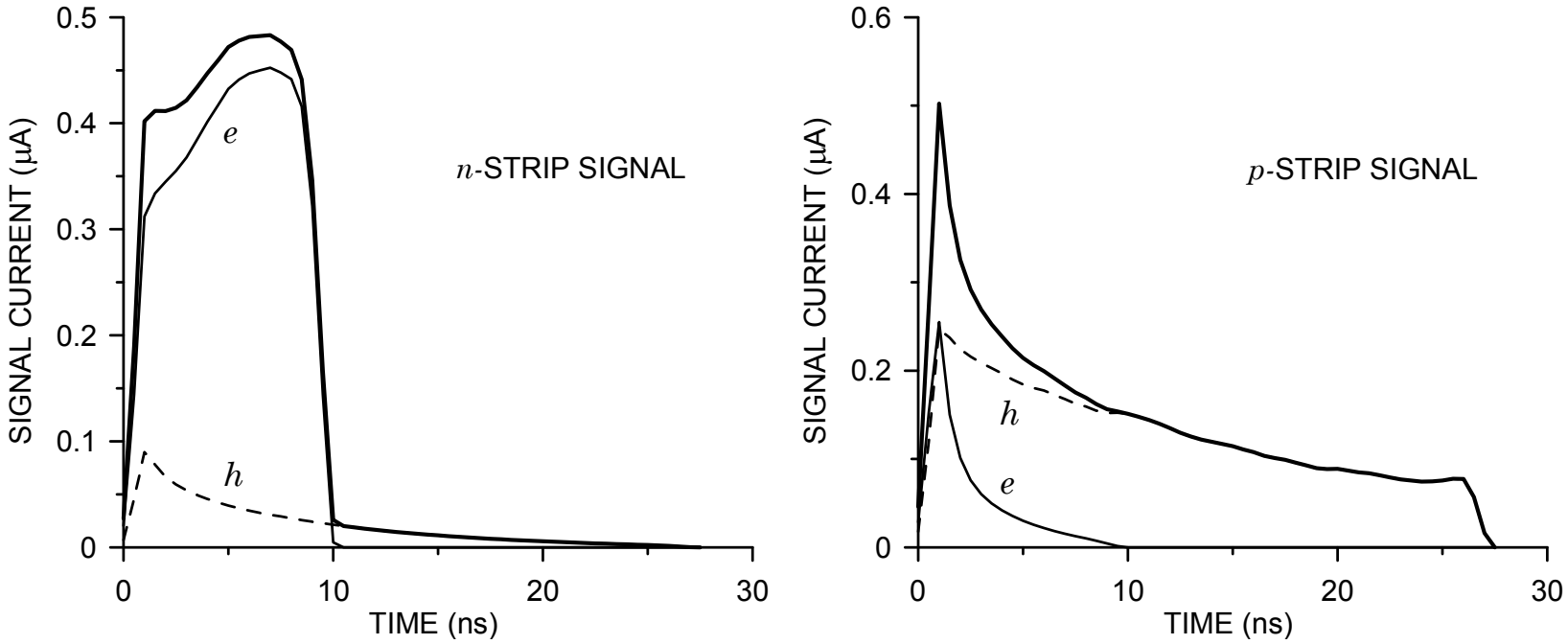

The duration of the electron and hole pulses is determined by the time required to traverse the detector as in the parallel-plate detector, but the shapes are very different.

This is because in segmented detectors the weighting fields are very different.

Induced current is a common phenomenon, e.g. in a photomultiplier tube

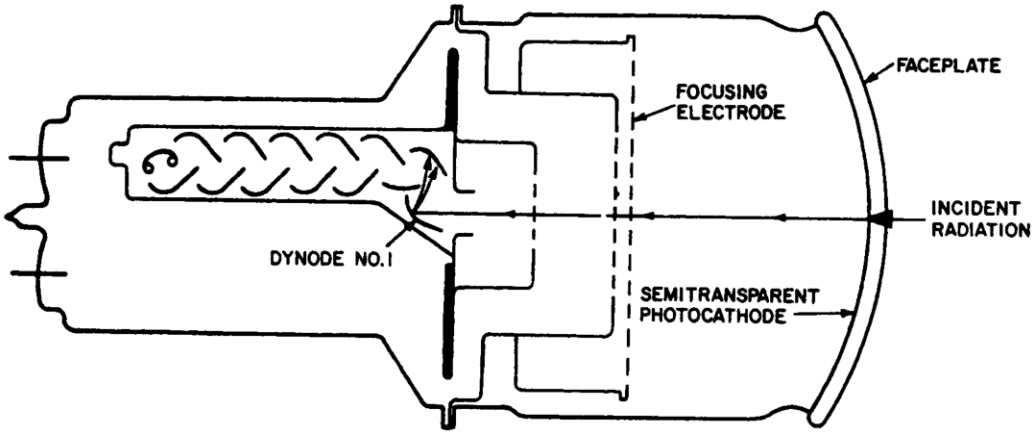

Detail of output circuit

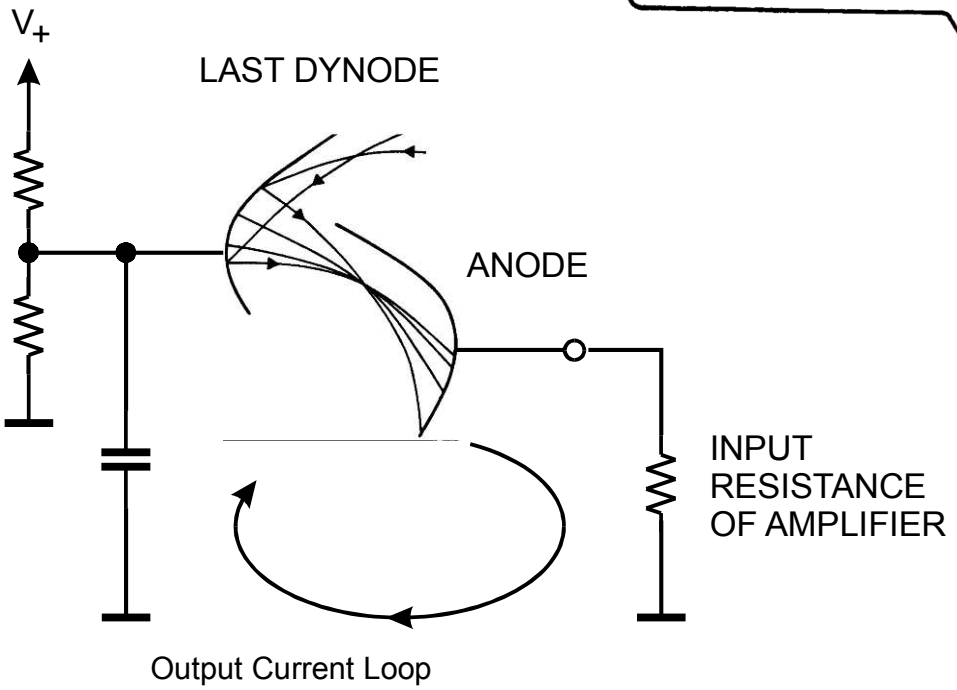

Model

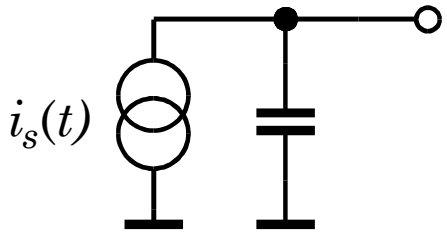

The closed current path from the last dynode to the anode must be well configured.

Signal Magnitude and Fluctuations

Any form of elementary excitation can be used to detect the radiation signal.

An electrical signal can be formed directly by ionization.

> Incident radiation quanta impart sufficient energy to individual atomic electrons to form electron-ion pairs (in gases) or electron-hole pairs (in semiconductors and metals).

Other detection mechanisms are

- Excitation of optical states (scintillators)
- Excitation of lattice vibrations (phonons)
- Breakup of Cooper pairs in superconductors
- Formation of superheated droplets in superfluid He

The number of Signal Quanta for a signal energy E: $N_{SQ} = \frac{E}{E_{SQ}}$

Typical excitation energies E_{SQ}

Ionization in gases	~30 eV
Ionization in semiconductors	1 – 5 eV
Scintillation	~10 – 1000 eV
Phonons	meV
Breakup of Cooper Pairs	meV

Signal Fluctuations: Intrinsic Resolution of Semiconductor Detectors

The number of charge-pairs: $N_Q = \frac{E}{E_i}$

The corresponding energy fluctuation: $\Delta E = E_i \sqrt{F N_Q} = E_i \sqrt{F \frac{E}{E_i}} = \sqrt{F E E_i}$

F is the Fano factor (Chapter 2, pp 52-55).

Si: $E_i = 3.6$ eV $\quad F = 0.1$

Ge: $E_i = 2.9$ eV $\quad F = 0.1$

E_i is greater than the band gap because for >keV energies momentum conservation requires additional excitation of phonons.

Since the total energy must be conserved,

a) the fluctuation cannot exceed the absorbed energy

b) any fluctuation in the number of signal charges must be balanced by the fluctuation in the number of phonons. As the number of phonons is much greater, its relative variance is small and this reduces the overall fluctuations.

The magnitude of the Fano factor depends on the energy paths that lead to the signal quanta. It often is >1:

In Xe gas $F = 0.15$, but in liquid Xe $F \approx 20$.

Inherent Detector Energy Resolution

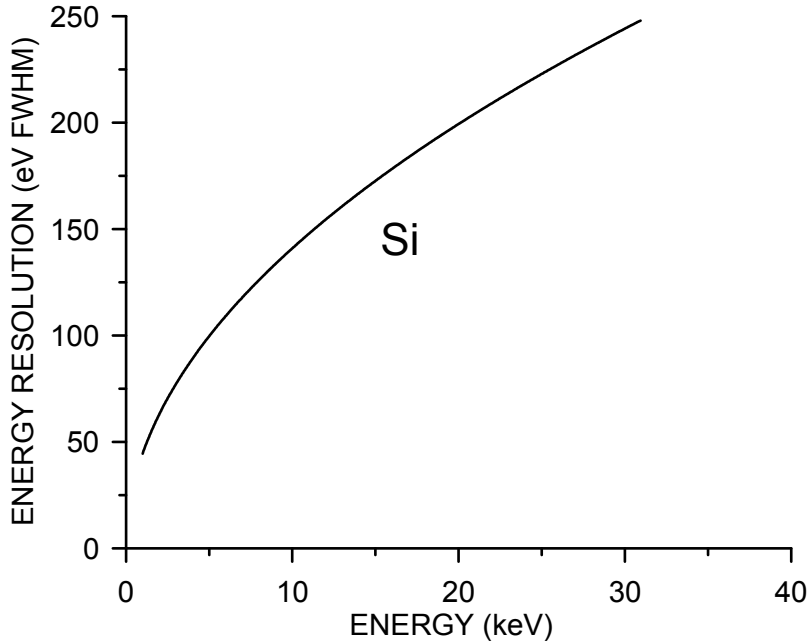

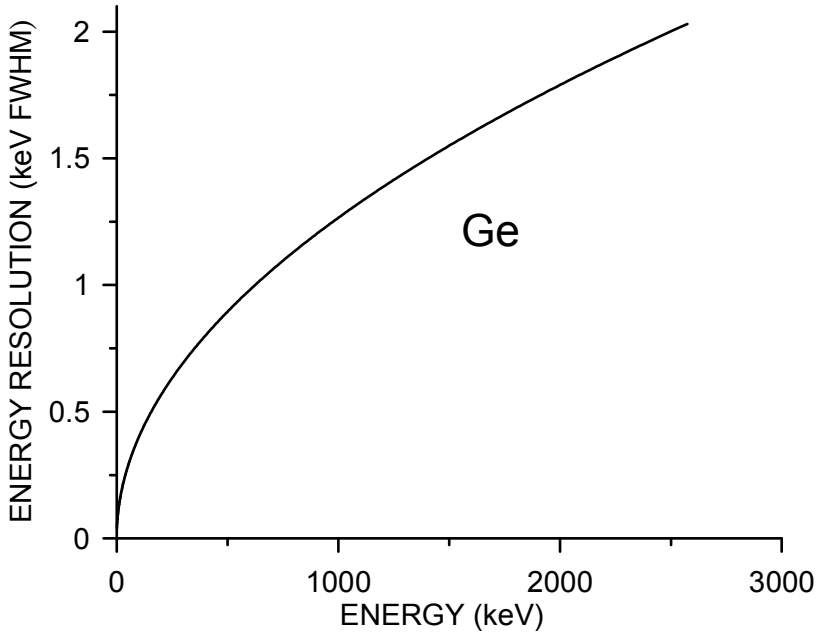

Detectors with good efficiency in the tens of keV range can have sufficiently small capacitance to allow electronic noise of ~100 eV FWHM, so the variance of the detector signal is a significant contribution.

At energies >100 keV the detector sizes required tend to increase the electronic noise to dominant levels.

3. Signal Acquisition

Amplifier Types

a) Voltage-Sensitive Amplifier

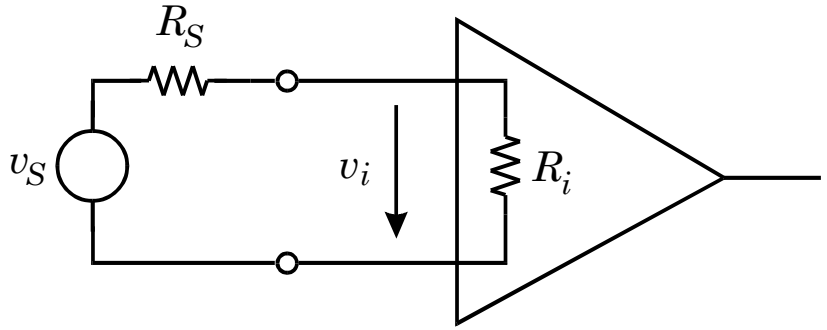

The signal voltage at the amplifier input

$$v_i = \frac{R_i}{R_S + R_i} v_S$$

If the signal voltage at the amplifier input is to be approximately equal to the signal voltage

$$v_i \approx v_S \quad \Rightarrow \quad R_i \gg R_S$$

To operate in the voltage-sensitive mode, the amplifier's input resistance (or impedance) must be large compared to the source resistance (impedance).

In ideal voltage amplifiers one sets $R_i = \infty$, although this is never true in reality, although it can be fulfilled to a good approximation.

To provide a voltage output, the amplifier should have a low output resistance, i.e. its output resistance should be small compared to the input resistance of the following stage.

b) Current-Sensitive Amplifier

The signal current divides into the source resistance and the amplifier's input resistance. The fraction of current flowing into the amplifier

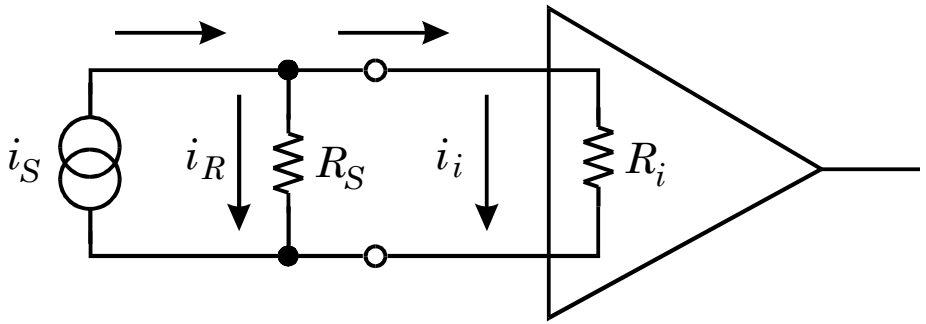

$$i_i = \frac{R_s}{R_s + R_i} i_S$$

If the current flowing into the amplifier is to be approximately equal to the signal current

$$i_i \approx i_S \qquad \Rightarrow \qquad R_i \ll R_S$$

To operate in the current-sensitive mode, the amplifier's input resistance (or impedance) must be small compared to the source resistance (impedance).

One can also model a current source as a voltage source with a series resistance. For the signal current to be unaffected by the amplifier input resistance, the input resistance must be small compared to the source resistance, as derived above.

At the output, to provide current drive the output resistance should be high, i.e. large compared to the input resistance of the next stage.

- Whether a specific amplifier operates in the current or voltage mode depends on the source resistance.

- Amplifiers can be configured as current mode input and voltage mode output or, conversely, as voltage mode input and current mode output. The gain is then expressed as V/A or A/V.

Although an amplifier has a pair of input and a second pair of output connections, since the two have a common connection a simplified representation is commonly used:

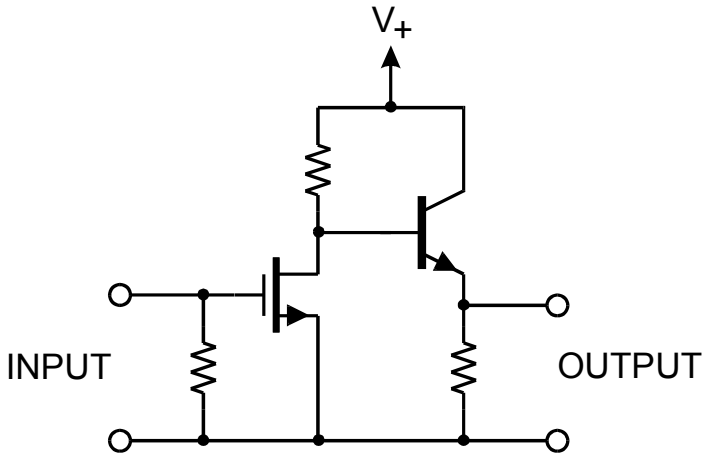

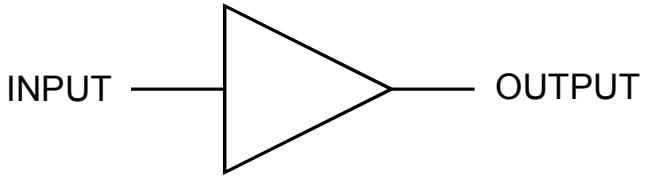

c) Voltage and Current Mode with Capacitive Sources

Output voltage:

v_o = (voltage gain A_v) × (input voltage v_i).

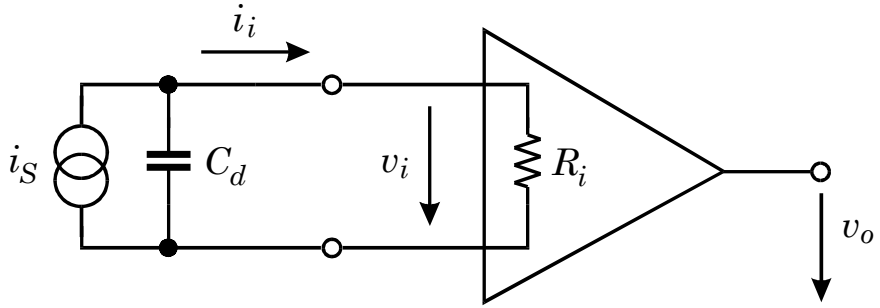

Operating mode depends on charge collection time t_c and the input time constant R_iC_d :

a) $R_iC_d \ll t_c$

detector capacitance discharges rapidly

$\Rightarrow \quad v_o \propto i_s(t)$

current sensitive amplifier

b) $R_iC_d \gg t_c$

detector capacitance discharges slowly

$\Rightarrow \quad v_o = A_v \cdot (Q_S / C) \propto \int i_s(t)dt$

voltage sensitive amplifier

Note that in both cases the amplifier is providing voltage gain, so the output signal voltage is determined directly by the input voltage. The difference is that the shape of the input voltage pulse is determined either by the instantaneous current or by the integrated current and the decay time constant.

Goal is to measure signal charge, so it is desirable to use a system whose response is independent of detector capacitance (can vary with bias voltage or strip length).

Active Integrator ("charge-sensitive amplifier")

Start with an ideal inverting voltage amplifier

Voltage gain $dv_o / dv_i = -A$

$\Rightarrow \quad v_o = -Av_i$

Input impedance = ∞ (i.e. no signal current flows into amplifier input)

Connect feedback capacitor C_f between output and input.

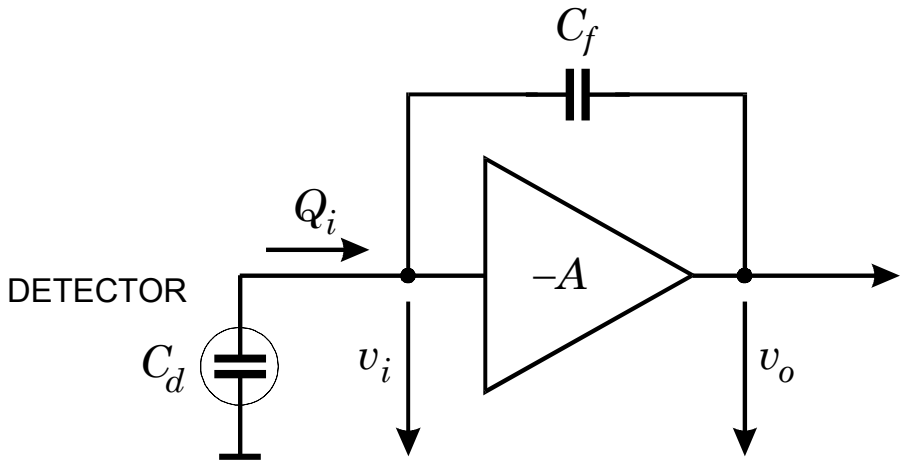

Voltage difference across C_f: $\quad v_f = (A+1)v_i$

$\Rightarrow$ Charge deposited on C_f: $\quad Q_f = C_f v_f = C_f(A+1)v_i$

$Q_i = Q_f \quad$ (since $Z_i = \infty$)

$\Rightarrow$ Effective input capacitance $\quad C_i = \dfrac{Q_i}{v_i} = C_f(A+1)$ $\quad$ ("dynamic" input capacitance)

Gain $\quad A_Q = \dfrac{dV_o}{dQ_i} = \dfrac{A \cdot v_i}{C_i \cdot v_i} = \dfrac{A}{C_i} = \dfrac{A}{A+1} \cdot \dfrac{1}{C_f} \approx \dfrac{1}{C_f} \quad (A >> 1)$

Charge gain is set by a well-controlled quantity, the feedback capacitance.

Q_i is the charge flowing into the preamplifier .... but some charge remains on C_d.

What fraction of the signal charge is measured?

$$\frac{Q_i}{Q_s} = \frac{C_i v_i}{Q_d + Q_i} = \frac{C_i}{Q_s} \cdot \frac{Q_s}{C_i + C_d}$$

$$= \frac{1}{1 + \frac{C_d}{C_i}} \approx 1 \quad (\text{if } C_i >> C_d)$$

Example: $A = 10^3$

$C_f = 1$ pF $\Rightarrow$ $C_i = 1$ nF

$C_{det} = 10$ pF: $Q_i / Q_s = 0.99$

$C_{det} = 500$ pF: $Q_i / Q_s = 0.67$

↑

Si Det.: 50 μm thick, 250 mm^2 area

Note: Input coupling capacitor must be $\gg C_i$ for high charge transfer efficiency.

Calibration

Inject specific quantity of charge – measure system response

Use voltage pulse (can be measured conveniently with oscilloscope)

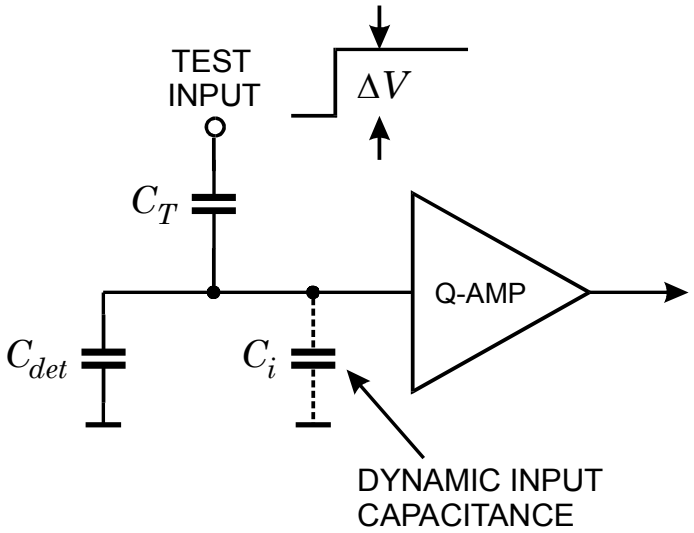

$C_i >> C_T \Rightarrow$ Voltage step applied to test input develops over C_T.

$\Rightarrow \quad Q_T = \Delta V \cdot C_T$

Accurate expression:

$$Q_T = \frac{C_T}{1+\frac{C_T}{C_i}} \cdot \Delta V \approx C_T \left(1 - \frac{C_T}{C_i}\right) \Delta V$$

Typically: $C_T / C_i = 10^{-3} - 10^{-4}$

Realistic Charge-Sensitive Preamplifiers

The preceding discussion assumed idealized amplifiers with infinite speed.

In reality, amplifiers may be too slow to follow the instantaneous detector pulse.

Does this incur a loss of charge?

Equivalent Circuit:

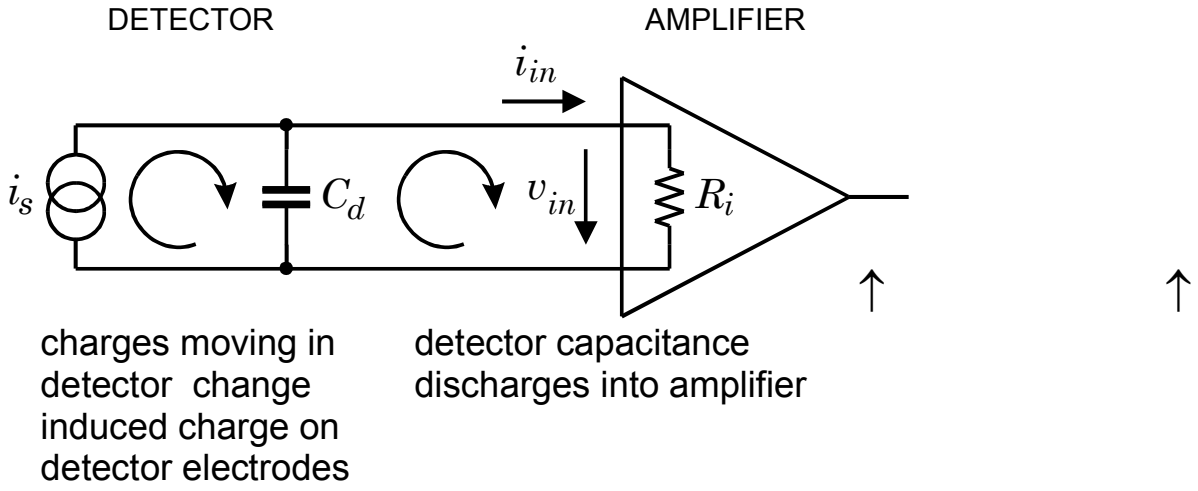

Signal is preserved even if the amplifier responds much more slowly than the detector signal.

However, the response of the amplifier affects the measured pulse shape.

- How do “real” amplifiers affect the measured pulse shape?
- How does the detector affect amplifier response?

Frequency and phase response of a simple amplifier:

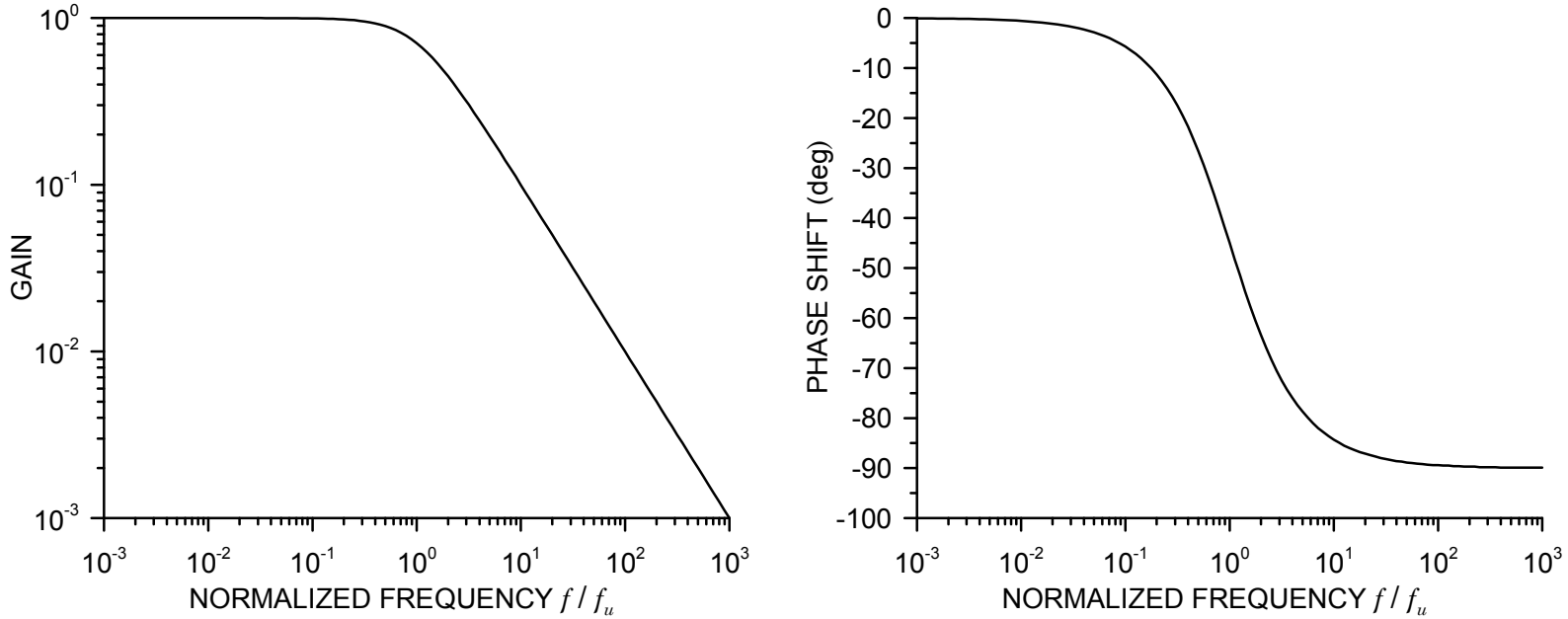

Phase shows change from low-frequency response. For an inverting amplifier add 180°.

The corner (cutoff) frequency is often called a “pole”.

Pulse Response of the Simple Amplifier

A voltage step $v_i(t)$ at the input causes a current step $i_o(t)$ at the output of the transistor.

For the output voltage to change, the capacitance C_O at the output must first charge up.

$\Rightarrow$ The output voltage changes with a time constant $\tau = R_L C_O$ (R_L is the load resistance)

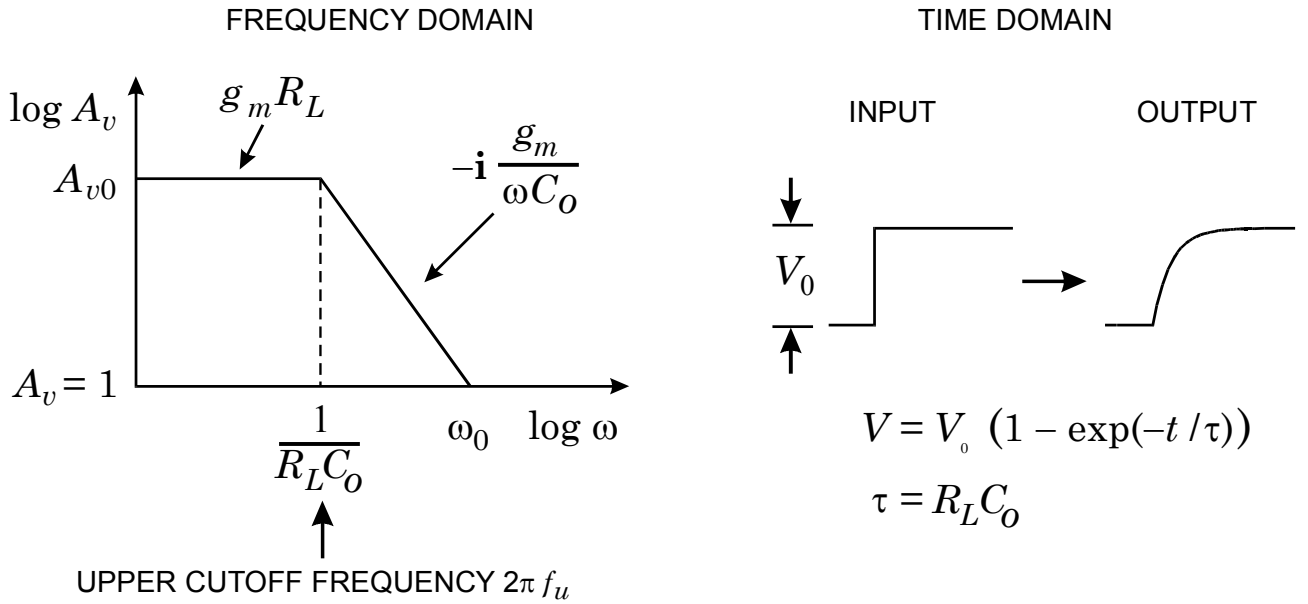

The imaginary term above the cutoff frequency indicates the 90° phase shift.

The time constant τ corresponds to the upper cutoff frequency : $\tau = \frac{1}{2\pi f_u}$

Input Impedance of a Charge-Sensitive Amplifier

Input impedance $$Z_i = \frac{Z_f}{A+1} \approx \frac{Z_f}{A} \quad (A >> 1)$$

Amplifier gain vs. frequency beyond the upper cutoff frequency

$$A = -\mathbf{i}\ \frac{\omega_0}{\omega}$$

Feedback impedance $$Z_f = -\mathbf{i}\ \frac{1}{\omega\ C_f}$$

$\Rightarrow$ Input Impedance $$Z_i = -\frac{\mathbf{i}}{\omega\ C_f} \cdot \frac{1}{-\mathbf{i}\frac{\omega_0}{\omega}} = \frac{1}{\omega_0 C_f}$$

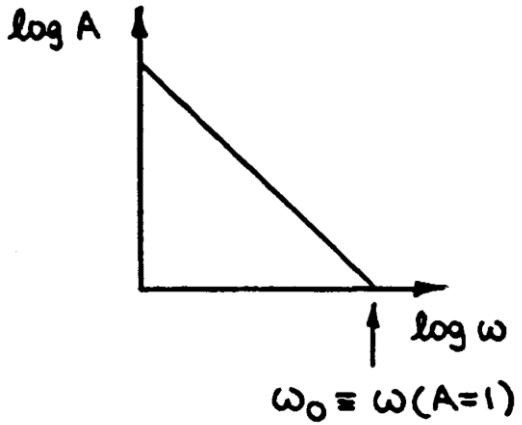

Gain-Bandwidth Product

Imaginary component vanishes $\Rightarrow$ *Resistance:* $Z_i \rightarrow R_i$

$\Rightarrow$ low frequencies ($f < f_u$): capacitive input
high frequencies ($f > f_u$): resistive input

Practically all charge-sensitive amplifiers operate in the 90° phase shift regime.
$\Rightarrow$ Resistive input

However ... Note that the input impedance varies with frequency.

Example: cutoff frequencies at 10 kHz and 100 MHz, low frequency gain = 10^3

OPEN LOOP GAIN AND PHASE

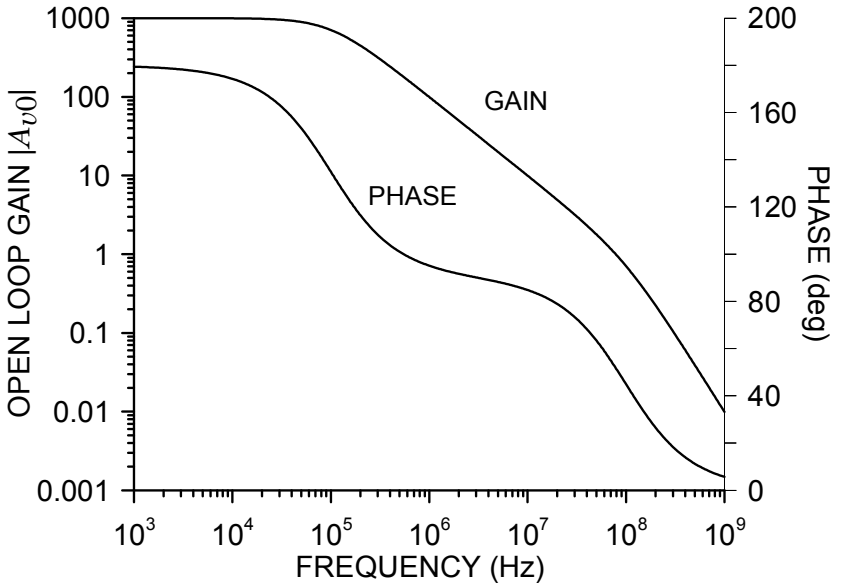

INPUT IMPEDANCE (C_f = 1 pF)

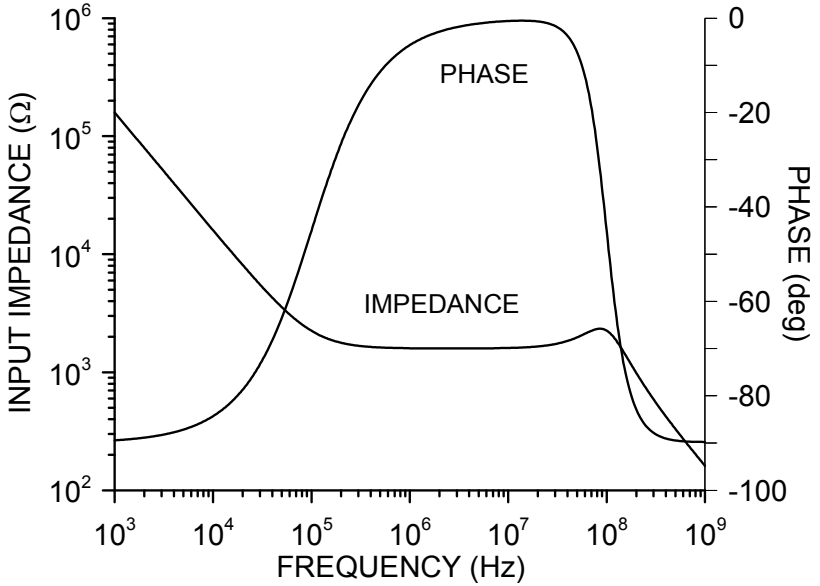

The relevant frequency range is determined by the frequency passband of the pulse shaper. This is 5 – 15 MHz for a typical 20 ns shaper, so in this example the ohmic input is effective at much longer shaping times.

In the resistive regime the input impedance

$$Z_i = \frac{1}{\omega_0 C_f} ,$$

where C_f is the feedback capacitance and ω_0 is the extrapolated unity gain frequency in the 90° phase shift regime.

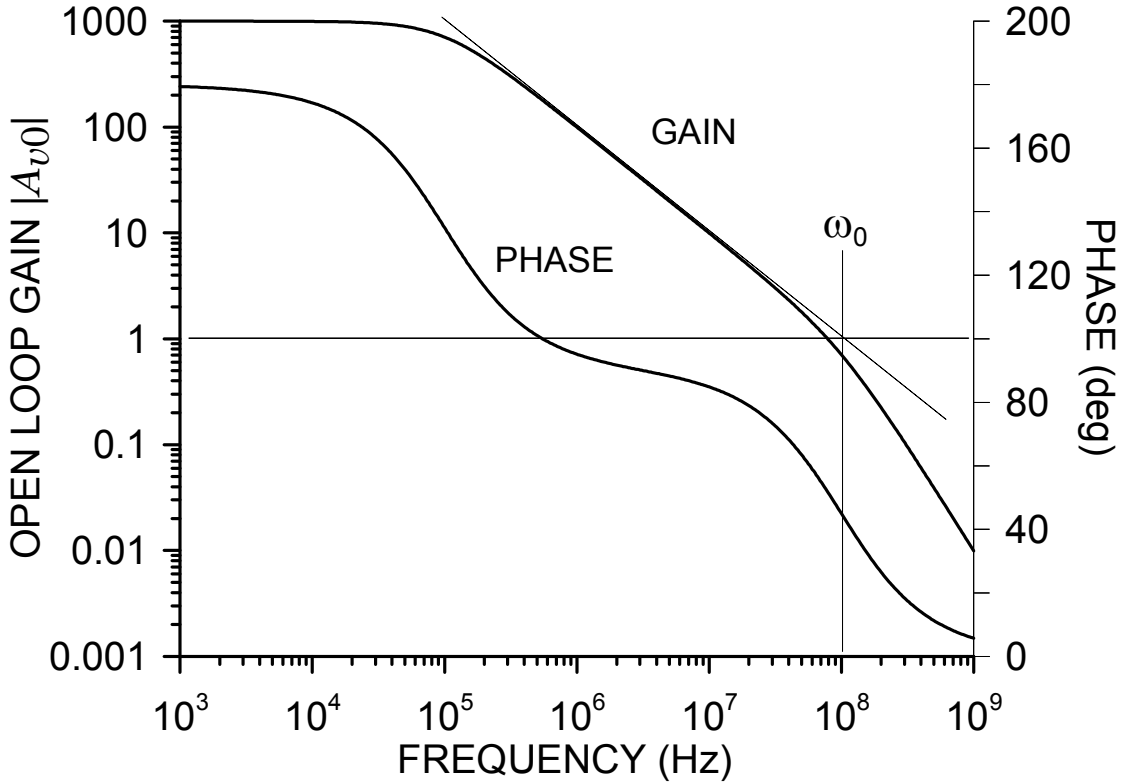

Low-power amplifiers with a gain-bandwidth product much greater than in this example are quite practical, so smaller feedback capacitances are also possible.

Importance of input impedance in strip and pixel detectors:

Amplifiers must have a low input impedance to reduce transfer of charge through capacitance to neighboring strips

In the previous example at
10 MHz ($\hat{=}$ ~20 ns peaking time)
$Z_i \approx$1.6 kΩ, corresponding to 12 pF

$\Rightarrow$ with 6 cm long strips about half of the signal current will go to the neighbors.

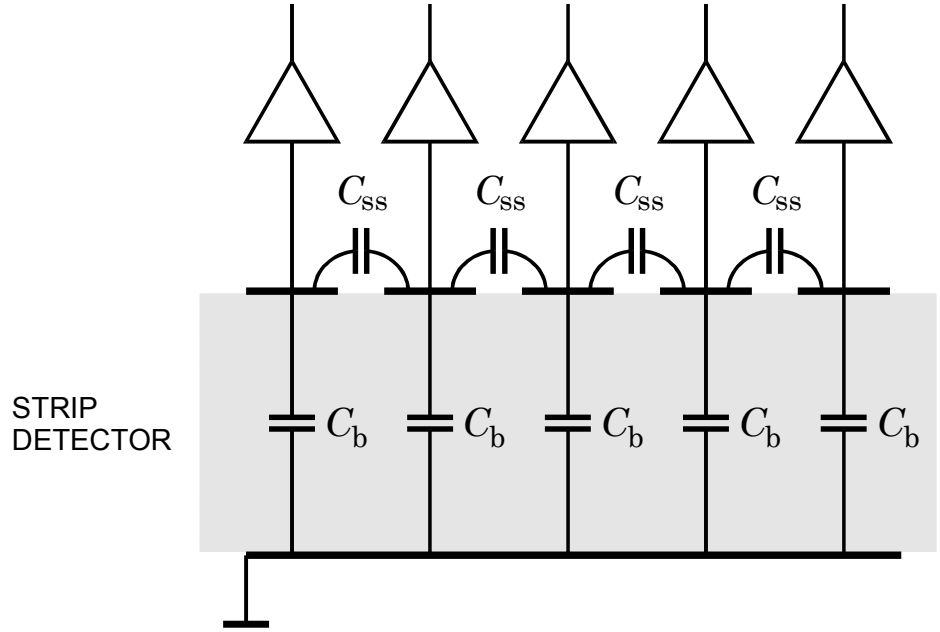

For strip pitches that are smaller than the bulk thickness, the capacitance is dominated by the fringing capacitance to the neighboring strips C_{SS}.

Typically: 1 – 2 pF/cm for strip pitches of 25 – 100 μm on Si.

The backplane capacitance C_b is typically 20% of the strip-to-strip capacitance.

Negligible cross-coupling at shaping times $T_P > (2 \ldots 3) \times R_i C_D$ and if $C_i \gg C_D$.

2. Electronic Noise

1. Signals and Noise
2. Basic Noise Mechanisms
   - Shot Noise
   - Thermal Noise
   - Low Frequency ("$1/f$") Noise
3. Signal-to-Noise Ratio vs. Detector Capacitance
   - Voltage Amplifier
   - Charge-Sensitive Amplifier
4. Complex Sensors
   - Strip Detector Model
5. Noise Summary

1. Signals and Noise

Choose a time when no signal is present.

Amplifier's quiescent output level (baseline):

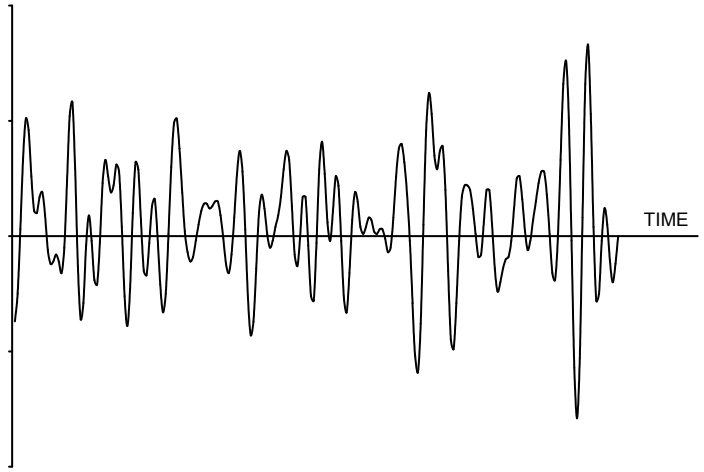

In the presence of a signal, noise + signal add.

Signal

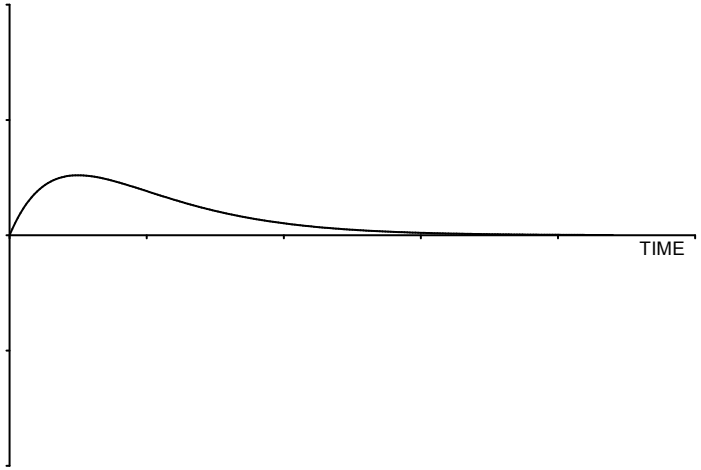

Signal+Noise (S/N = 1)

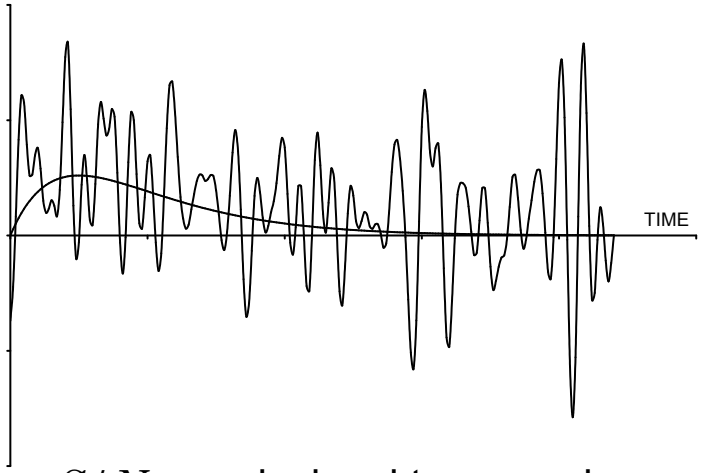

$S/N \equiv$ peak signal to rms noise

Measurement of peak amplitude yields signal amplitude + noise fluctuation

The preceding example could imply that the fluctuations tend to increase the measured amplitude, since the noise fluctuations vary more rapidly than the signal.

In an optimized system, the time scale of the fluctuation is comparable to the signal peaking time.

Then the measured amplitude fluctuates positive and negative relative to the ideal signal.

Measurements taken at 4 different times:

noiseless signal superimposed for comparison

S/N = 20

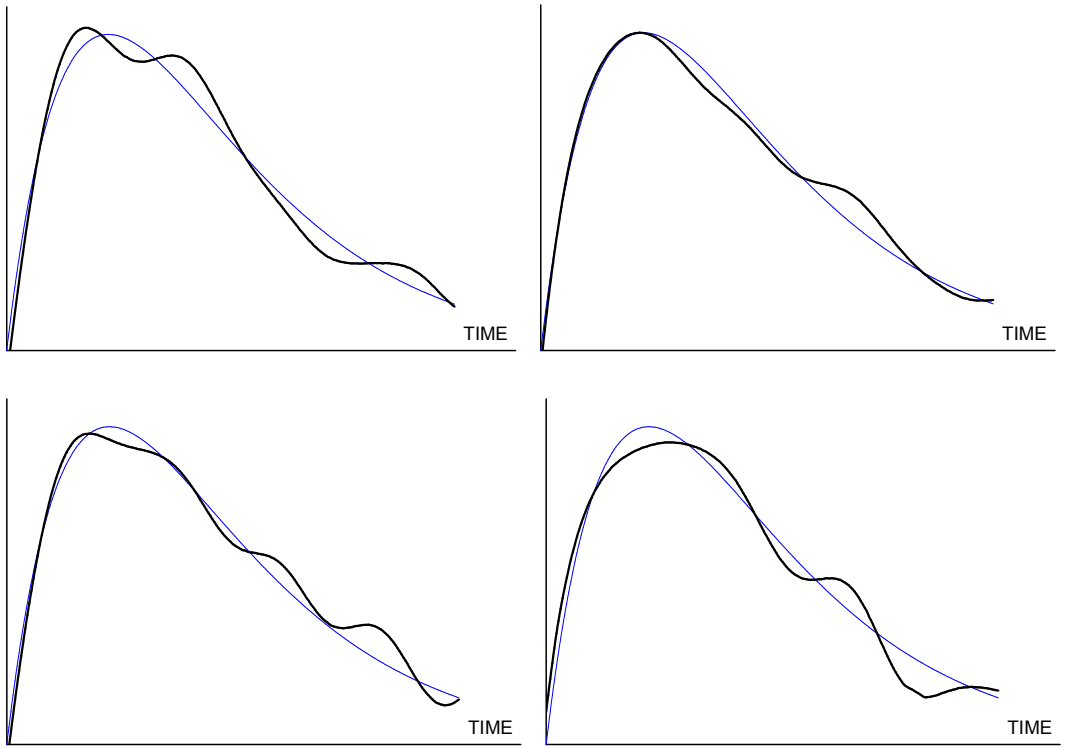

Noise affects

Peak signal

Time distribution

Electronic noise is purely random.

⇒ amplitude distribution is Gaussian

⇒ noise modulates baseline

⇒ baseline fluctuations superimposed on signal

⇒ output signal has Gaussian distribution

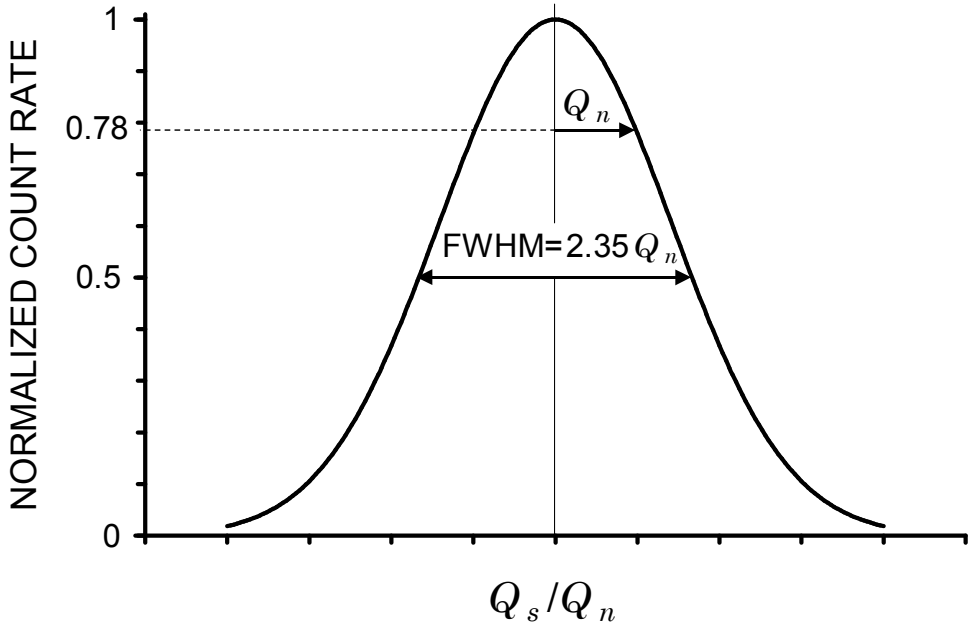

Measuring Resolution

Inject an input signal with known charge using a pulse generator set to approximate the detector signal shape.

Measure the pulse height spectrum.

peak centroid ⇒ signal magnitude
peak width ⇒ noise (FWHM= 2.35 Q_n)

2. Basic Noise Mechanisms and Characteristics

Consider n carriers of charge e moving with a velocity v through a sample of length l. The induced current i at the ends of the sample is

$$i = \frac{n\ e\ v}{l}$$

The fluctuation of this current is given by the total differential

$$\langle di \rangle^2 = \left(\frac{ne}{l} \langle dv \rangle \right)^2 + \left(\frac{ev}{l} \langle dn \rangle \right)^2,$$

where the two terms are added in quadrature since they are statistically uncorrelated.

Two mechanisms contribute to the total noise:

- velocity fluctuations, *e.g.* thermal noise
- number fluctuations, *e.g.* shot noise
  excess or "1/f" noise

Thermal noise and shot noise are both "white" noise sources, i.e.

power per unit bandwidth (≡ spectral density) is constant: $\frac{dP_{noise}}{df} = const.$

Shot noise

A common example of noise due to number fluctuations is “shot noise”, which occurs whenever carriers are injected into a sample volume independently of one another.

Example: current flow in a semiconductor diode (emission over a barrier)

Its effect is easy to understand in the time domain. Since the signal charge is the result of an integrated current, the fluctuations of any additional “background” current will introduce fluctuations to the measured signal charge.

The noise current I_n will introduce statistical fluctuations equal to the square root of the number of carriers measured during the readout integration time

$$\sigma_n = \sqrt{N_n} = \sqrt{\frac{I_n T_{int}}{q_e}} \ ,$$

so it increases with integration time.

Note: Shot noise does not occur in “ohmic” conductors. Since the number of available charges is not limited, the fields caused by local fluctuations in the charge density draw in additional carriers to equalize the total number.

Thermal Noise (Johnson Noise)

Two approaches can be used to derive the spectral distribution of thermal noise.

1. The thermal velocity distribution of the charge carriers is used to calculate the time dependence of the induced current, which is then transformed into the frequency domain.
2. Application of Planck's theory of black body radiation.

The first approach clearly shows the underlying physics, whereas the second "hides" the physics by applying a general result of statistical mechanics. However, the first requires some advanced concepts that go well beyond the standard curriculum, so the "black body" approach will be used.

In Planck's theory of black body radiation the energy per mode

$$\bar{E} = \frac{h\nu}{e^{h\nu/kT} - 1}$$

and the spectral density of the radiated power

$$\frac{dP}{d\nu} = \frac{h\nu}{e^{h\nu/kT} - 1}.$$

This is the power that can be extracted in equilibrium.

At low frequencies $h\nu \ll kT$:

$$\frac{dP}{d\nu} \approx \frac{h\nu}{\left(1+\frac{h\nu}{kT}\right)-1} = kT \ ,$$

so at low frequencies the spectral density is independent of frequency and for a total bandwidth B the noise power that can be transferred to an external device

$$P_n = kTB \, .$$

To apply this result to the noise of a resistor, consider a resistor R whose thermal noise gives rise to a noise voltage V_n. To determine the power transferred to an external device consider the circuit

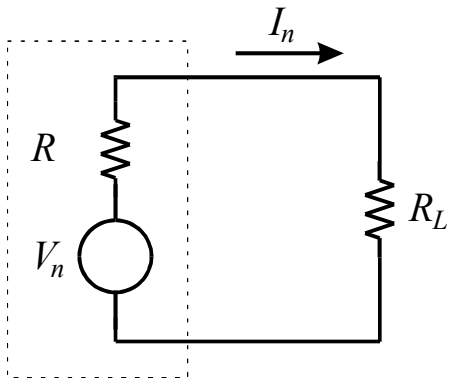

The dotted box encloses the equivalent circuit of the resistive noise source.

The power dissipated in the load resistor R_L

$$\frac{V_{nL}^2}{R_L} = I_n^2 R_L = \frac{V_n^2 R_L}{(R + R_L)^2}$$

The maximum power transfer occurs when the load resistance equals the source resistance $R_L = R$, so

$$V_{nL}^2 = \frac{V_n^2}{4} .$$

Since the maximum power that can be transferred to R_L is kTB ,

$$\frac{V_{nL}^2}{R} = \frac{V_n^2}{4R} = kTB$$

$$P_n = \frac{V_n^2}{R} = 4kTB$$

and the spectral density of the noise power in the resistor

$$\frac{dP_n}{d\nu} = 4kT .$$

Note that this noise is most practically analyzed in the frequency domain.

Total noise increases with bandwidth.

Total noise is the integral over the shaded region.

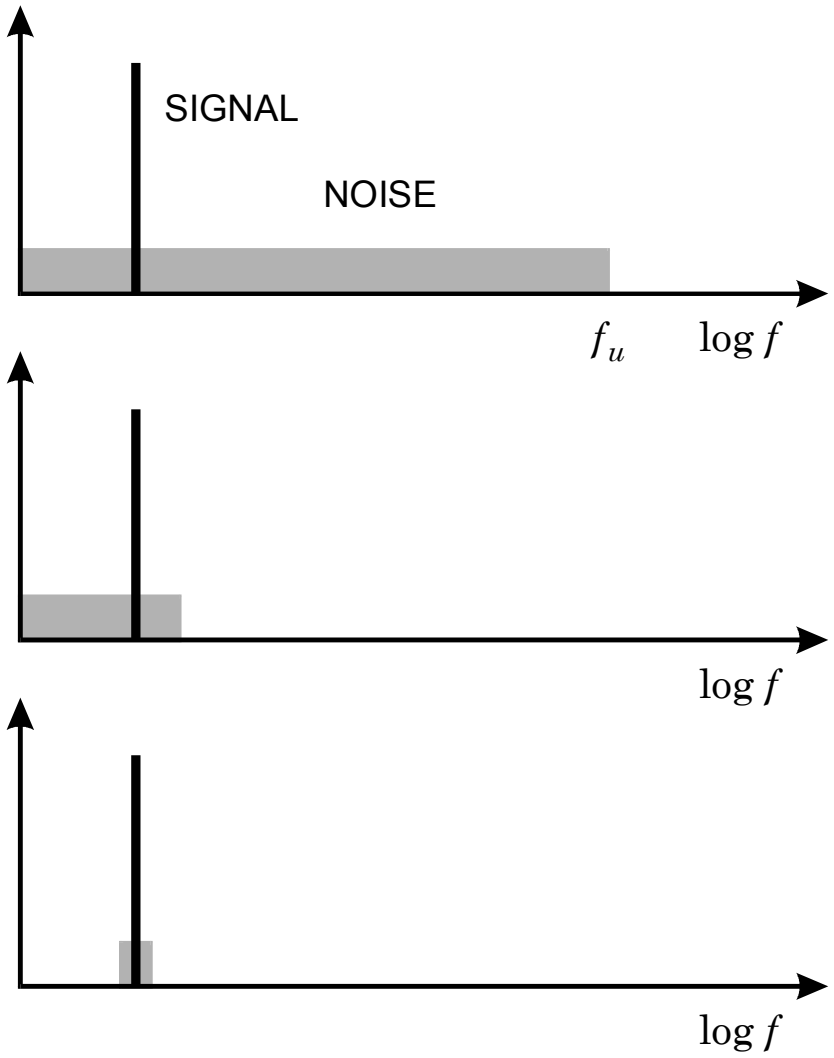

S/N increases as noise bandwidth is reduced until signal components are attenuated significantly.

Low Frequency ("$1/f$") Noise

Charge can be trapped and then released after a characteristic lifetime τ.

The spectral density for a single lifetime

$$S(f) \propto \frac{\tau}{1+(2\pi f\tau)^2} \ .$$

For $2\pi f\tau \gg 1$: $S(f) \propto \frac{1}{f^2}$.

However,
several traps with different time constants can yield a "$1/f$" distribution:

Traps with three time constants of 0.01, 0.1 and 1 s yield a $1/f$ distribution over two decades in frequency.

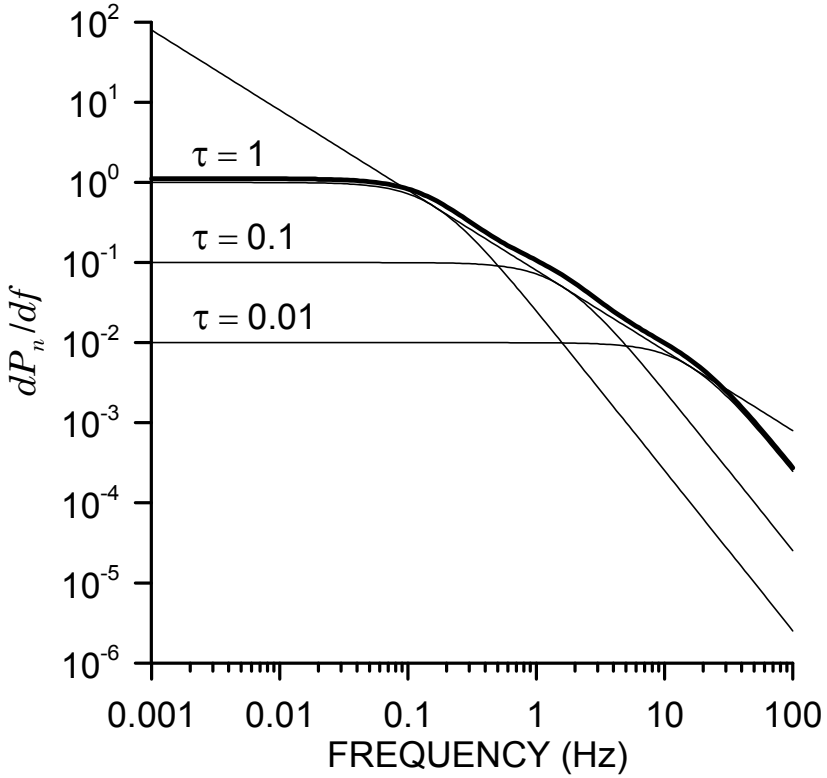

Low frequency noise is ubiquitous – must not have $1/f$ dependence, but commonly called $1/f$ noise.

Spectral power density: $\frac{dP_{noise}}{df} = \frac{1}{f^{\alpha}}$ (typically α = 0.5 – 2)

3. Signal-to-Noise Ratio vs. Detector Capacitance

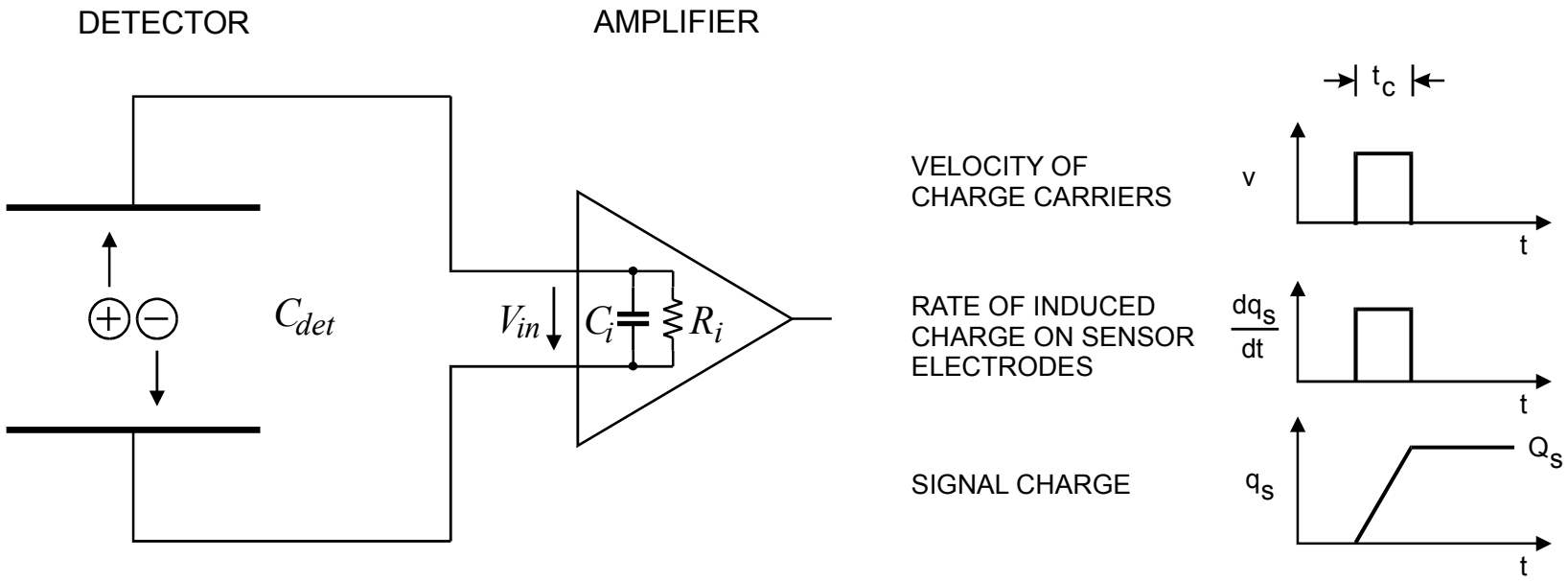

if $R_i \times (C_{det} + C_i) \gg$ collection time,

the peak voltage at amplifier input $V_{in} = \frac{Q_s}{C} = \frac{\int i_s dt}{C} = \frac{Q_s}{C_{det} + C_i}$

↑

Magnitude of voltage depends on total capacitance at input!

The peak amplifier signal V_S is inversely proportional to the **total capacitance at the input**, i.e. the sum of

1. detector capacitance,
2. input capacitance of the amplifier, and
3. stray capacitances.

Assume an amplifier with a noise voltage v_n at the input.

Then the signal-to-noise ratio

$$\frac{S}{N} = \frac{V_S}{v_n} \propto \frac{1}{C}$$

- However, S/N does not become infinite as $C \to 0$
  (then front-end operates in current mode)

- The result that $S/N \propto 1/C$ generally applies to systems that measure signal charge.

Noise vs. Detector Capacitance – Charge-Sensitive Amplifier

In a voltage-sensitive preamplifier

- noise voltage at the output is essentially independent of detector capacitance,
- input signal decreases with increasing input capacitance, so signal-to-noise ratio depends on detector capacitance.

In a charge-sensitive preamplifier, the signal at the amplifier output is independent of detector capacitance (if $C_i \gg C_d$).

What is the noise behavior?

- Noise appearing at the output of the preamplifier is fed back to the input, decreasing the output noise from the open-loop value $v_{no} = v_{ni} A_v$.
- The magnitude of the feedback depends on the shunt impedance at the input, i.e. the detector capacitance.

Although specified as an equivalent input noise, the dominant noise sources are typically internal to the amplifier.

Only in a fed-back configuration is some of this noise actually present at the input. In other words, the primary noise signal is not a physical charge (or voltage) at the amplifier input to which the loop responds in the same manner as to a detector signal.

$\Rightarrow$ **S/N at the amplifier output depends on feedback.**

Noise in charge-sensitive preamplifiers

Start with an output noise voltage v_{no}, which is fed back to the input through the capacitive voltage divider $C_f - C_d$.

$$v_{no} = v_{ni}\frac{X_{C_f} + X_{C_d}}{X_{C_d}} = v_{ni}\frac{\dfrac{1}{\omega\, C_f} + \dfrac{1}{\omega\, C_d}}{\dfrac{1}{\omega\, C_d}}$$

$$v_{no} = v_{ni}\left(1 + \frac{C_d}{C_f}\right)$$

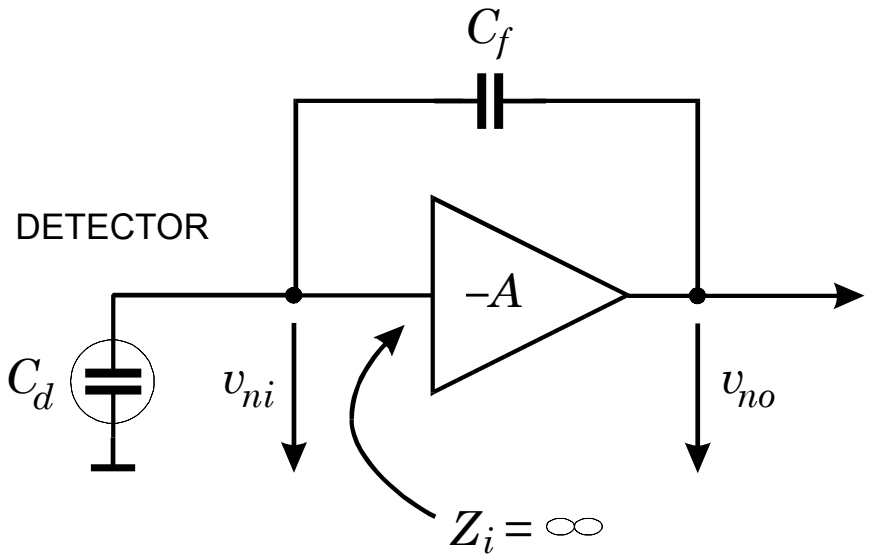

Equivalent input noise charge

$$Q_{ni} = \frac{v_{no}}{A_Q} = v_{no}C_f$$

$$Q_{ni} = v_{ni}\left(C_d + C_f\right)$$

Signal-to-noise ratio $$\frac{Q_s}{Q_{ni}} = \frac{Q_s}{v_{ni}(C_d + C_f)} = \frac{1}{C}\ \frac{Q_s}{v_{ni}}$$

Same result as for voltage amplifier, but here

- *the signal is constant and*
- *the noise grows with increasing* C.

As shown previously, the pulse rise time at the amplifier output also increases with total capacitive input load C, because of reduced feedback.

In contrast, the rise time of a voltage sensitive amplifier is not affected by the input capacitance, although the equivalent noise charge increases with C just as for the charge-sensitive amplifier.

In an ideal current-sensitive amplifier the signal-to-noise ratio can be independent of capacitance, but the effect of external noise sources often increases with detector capacitance.

Conclusion

In general

- optimum S/N is independent of whether the voltage, current, or charge signal is sensed.
- S/N cannot be ***improved*** by feedback.

Practical considerations, i.e. type of detector, amplifier technology, can favor one configuration over the other.

4. Complex Sensors

Strip Detector Model for Noise Simulations

Noise coupled from neighbor channels.

Analyze signal and noise in center channel.

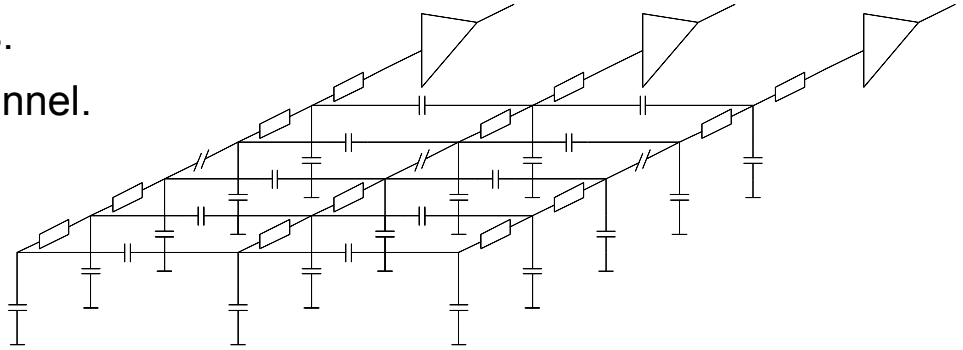

Includes:
a) Noise contributions from
neighbor channels
b) Signal transfer to
neighbor channels
c) Noise from distributed strip resistance
d) Full SPICE model of preamplifier

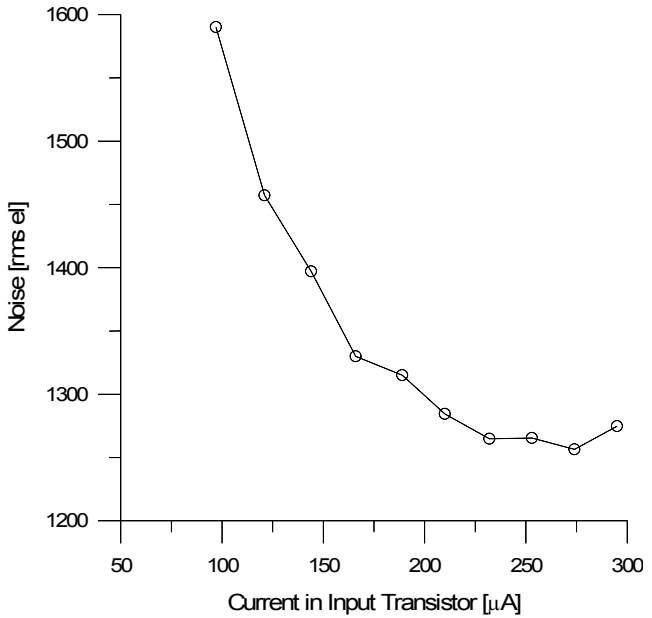

Measured Noise of Module:

p-strips on n-bulk, BJT input transistor

Simulation Results: 1460 el (150 μA)
1230 el (300 μA)

⇒ Noise can be predicted with good accuracy.

5. Noise Summary

The contribution of the various noise sources to signal-to-noise ratio depends on the frequency response of the pulse processor.

- A large bandwidth will increase the contribution of “white” noise.
- However, reducing the bandwidth corresponds to increasing the effective time duration of the signal pulse, so shot noise will increase.
- Low frequency response will also increase the contribution of low-frequency (“1/f”) noise.

In analyzing the effect of electronics – often the major noise contribution – the noise has to be expressed in terms of the relevant electronics parameters: voltage and current.

The noise of an electronic amplifier can be fully expressed as the combination of voltage and current noise sources referred to the input.

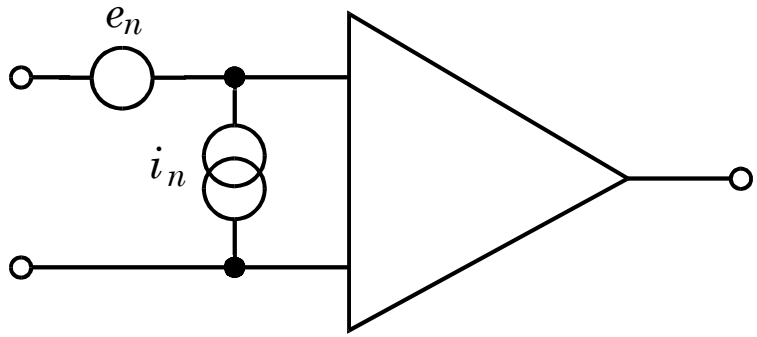

The noise sources are expressed in terms of

- spectral density of voltage $e_n(f)$ and
- spectral density current $i_n(f)$

IV. Signal Processing

1. The Problem
   - "Optimum" Filtering
   - Pulse Shaping Objectives
2. Pulse Shaping and Signal-to-Noise Ratio
   - Equivalent Noise Charge
   - Ballistic Deficit
   - Noise vs. Shaping Time
   - Analytical Analysis of a Detector Front-End
   - Other Types of Shapers
   - Examples
   - Detector Noise Summary
3. Noise vs. Power Dissipation

1. The Problem

Radiation impinges on a sensor and creates an electrical signal.

The signal level is low and must be amplified to allow digitization and storage.

Both the sensor and amplifiers introduce signal fluctuations – noise.

1. Fluctuations in signal introduced by sensor
2. Noise from electronics superimposed on signal

The detection limit and measurement accuracy are determined by the signal-to-noise ratio.

Electronic noise affects all measurements:

1. Detect presence of hit: Noise level determines minimum threshold.
   If threshold too low, output dominated by noise hits.
2. Energy measurement: Noise “smears” signal amplitude.
3. Time measurement: Noise alters time dependence of signal pulse.

How to optimize the signal-to-noise ratio?

1. Increase signal and reduce noise
2. For a given sensor and signal: reduce electronic noise

Assume that the signal is a pulse.

The time distribution of the signal corresponds to a frequency spectrum (Fourier transform).

Examples:

1. The pulse is unipolar, so it has a DC component and the frequency spectrum extends down to zero.

2. This bipolar pulse carries no net charge, so the frequency spectrum falls to zero at low frequencies, but extends to higher frequencies because of the faster slope.

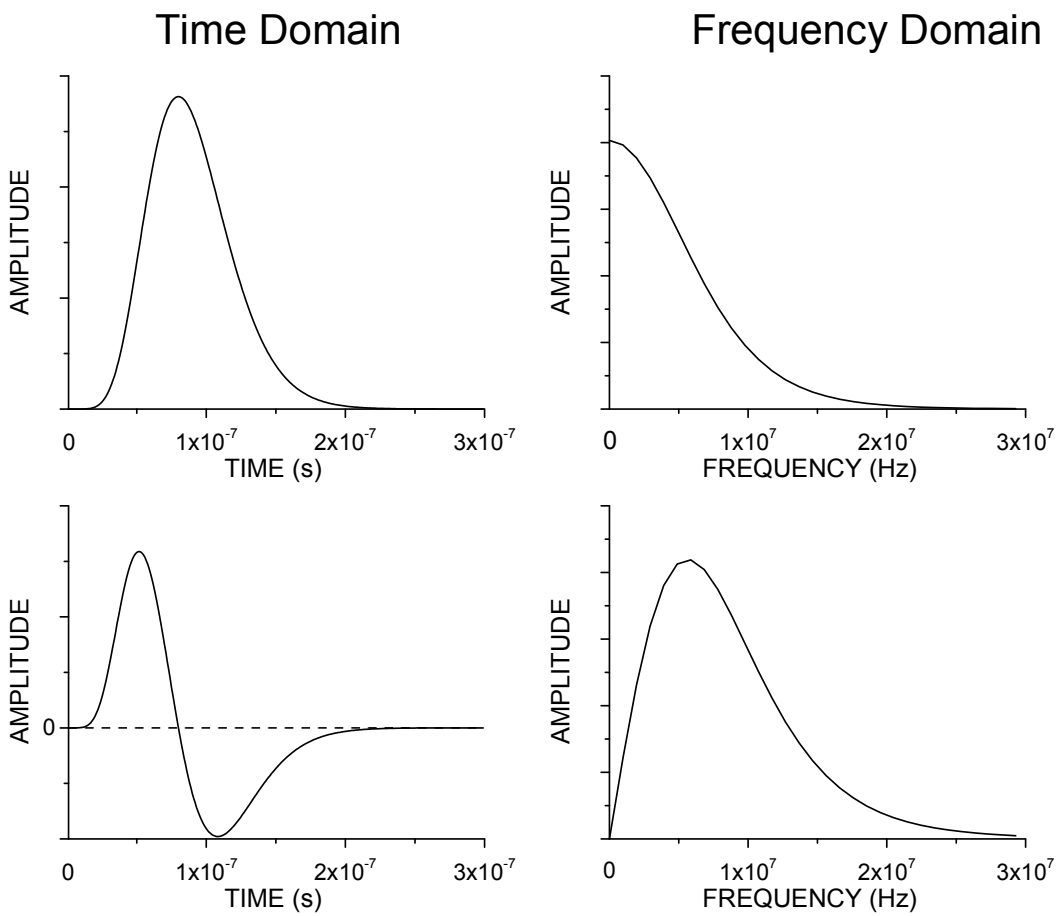

The noise spectrum is generally not the same as the signal spectrum.

Typical Noise Spectrum:

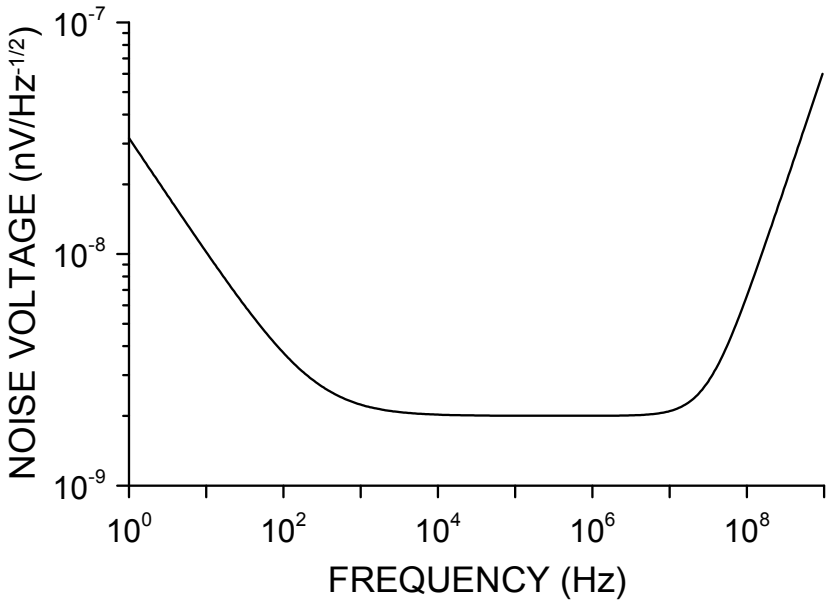

⇒ Tailor frequency response of measurement system to optimize signal-to-noise ratio.

Frequency response of the measurement system affects both

- signal amplitude and
- noise.

Signal Processing Objectives

Two conflicting objectives:

1. Improve Signal-to-Noise Ratio S/N

Restrict bandwidth to match measurement time ⇒ Increase pulse width

Typically, the pulse shaper transforms a narrow detector current pulse to

a broader pulse (to reduce electronic noise),

with a gradually rounded maximum at the peaking time T_P
(to facilitate measurement of the peak amplitude)

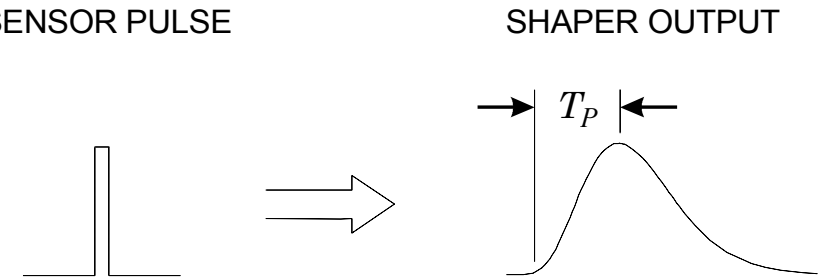

If the shape of the pulse does not change with signal level, the peak amplitude is also a measure of the energy, so one often speaks of pulse-height measurements or pulse height analysis. The pulse height spectrum is the energy spectrum.

2. Improve Pulse Pair Resolution ⇒ Decrease pulse width

Pulse pile-up distorts amplitude measurement.

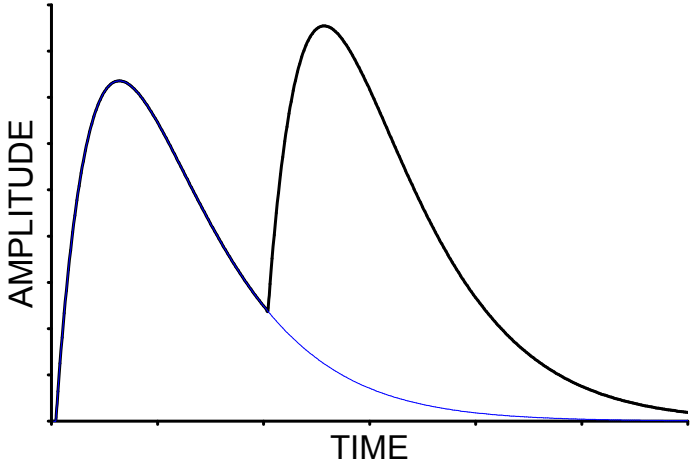

Reducing pulse shaping time to 1/3 eliminates pile-up.

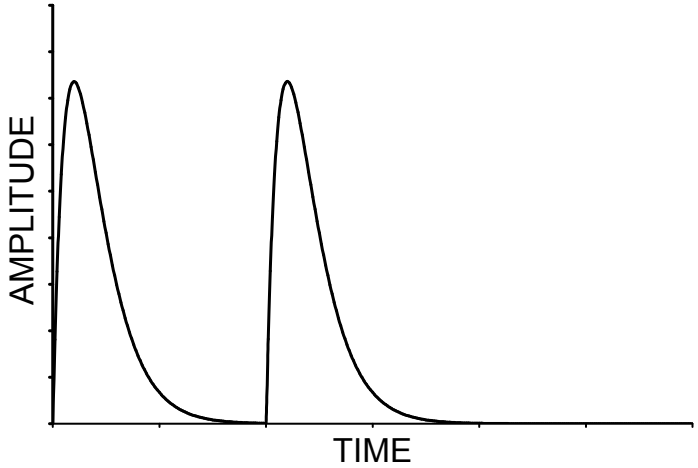

Necessary to find balance between these conflicting requirements. Sometimes minimum noise is crucial, sometimes rate capability is paramount.

Usually, many considerations combined lead to a “non-textbook” compromise.

- *“Optimum shaping” depends on the application!*
- Shapers need not be complicated – *Every amplifier is a pulse shaper!*

Goal: Improve energy resolution

Procedure: Integrate detector signal current $\Rightarrow$ Step impulse

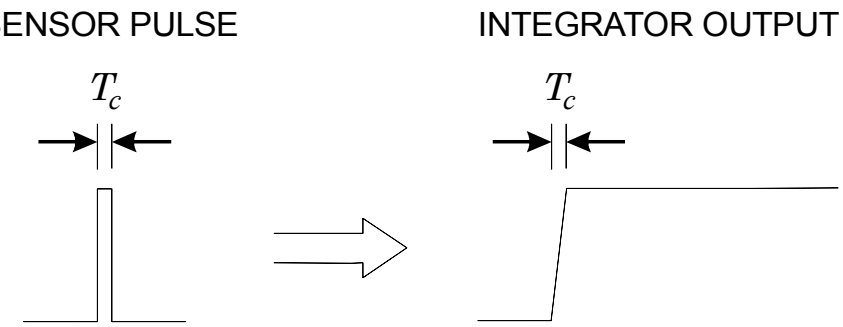

Commonly approximated as
"step" response (zero rise time).

Long "flat top" allows measurements at times well beyond the collection time T_C.

$\Rightarrow$ Allows reduced bandwidth and great flexibility in selecting shaper response.

Optimum for energy measurements, but not for fast timing!

"Fast-slow" systems utilize parallel processing chains to optimize both timing and energy resolution (see Timing Measurements in other tutorials).

Simple Example: CR-RC Shaping

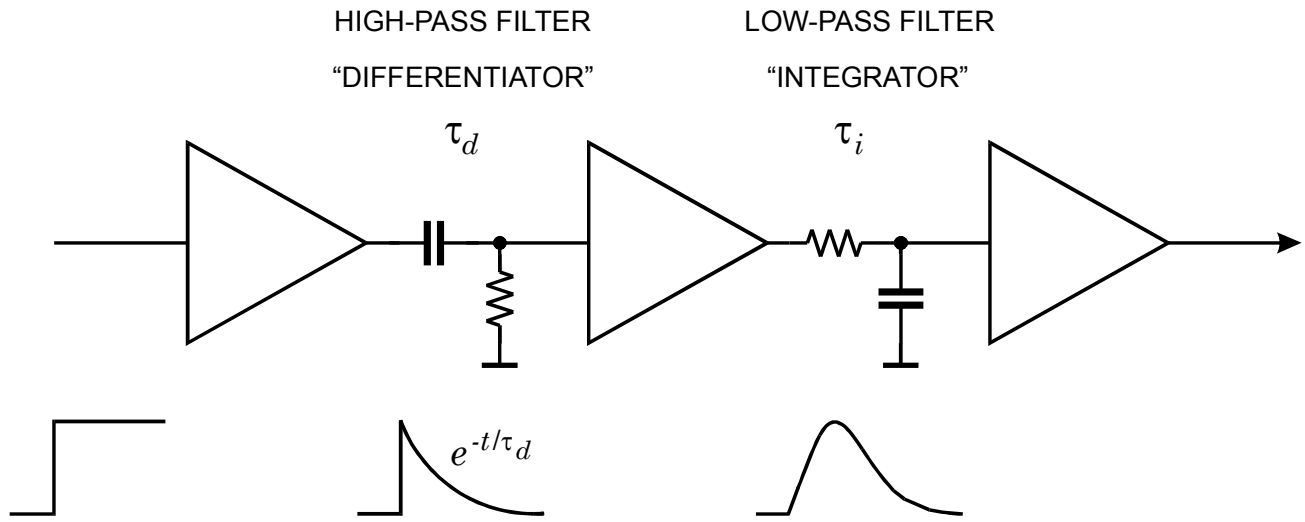

Simple arrangement: Noise performance only 36% worse than optimum filter with same time constants.

⇒ Useful for estimates, since simple to evaluate

Key elements:
- lower frequency bound ($\hat{=}$ pulse duration)
- upper frequency bound ($\hat{=}$ rise time)

are common to all shapers.

2. Pulse Shaping and Signal-to-Noise Ratio

Pulse shaping affects both the

- total noise

and

- peak signal amplitude

at the output of the shaper.

Equivalent Noise Charge

Inject known signal charge into preamp input
(either via test input or known energy in detector).

Determine signal-to-noise ratio at shaper output.

Equivalent Noise Charge $\equiv$ Input charge for which $S/N = 1$

Shapers with Multiple Integrators

Start with simple CR-RC shaper and add additional integrators (n= 1 to n= 2, ... n= 8).

Change integrator time constants to preserve the peaking time $\tau_n = \tau_{n=1} / n$

Increasing the number of integrators makes the output pulse more symmetrical with a faster return to baseline.

$\Rightarrow$ improved rate capability at the same peaking time

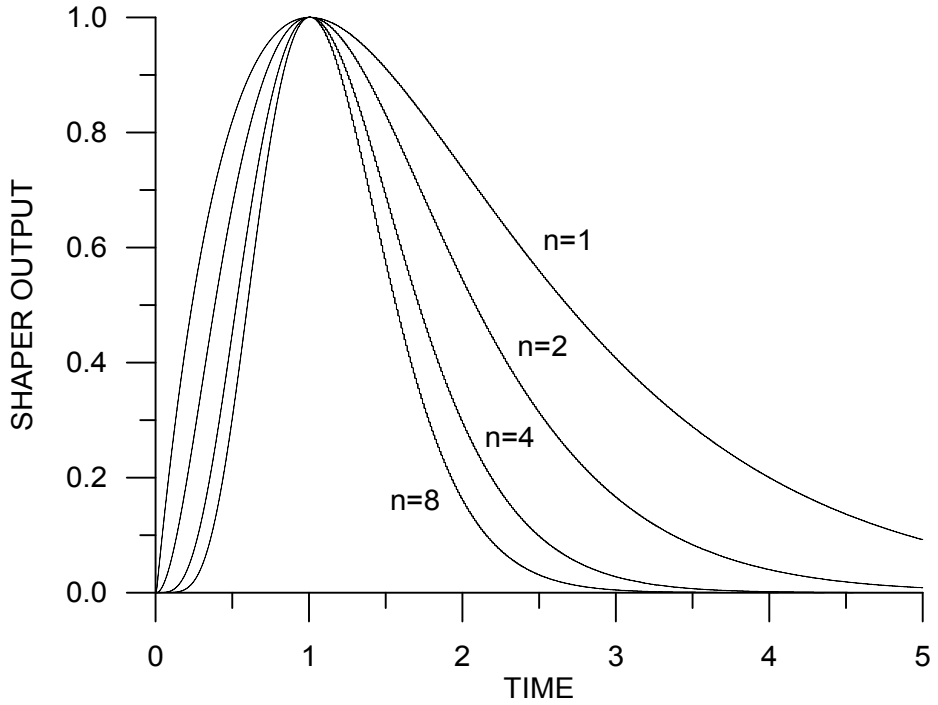

Multiple integrators often do not require additional circuitry. Several gain stages are typically necessary to bring the signal to the level required for a threshold discriminator or analog-to-digital converter. Their bandwidth can be set to provide the desired pulse shaping.

In γ-spectroscopy systems shapers with the equivalent of 8 RC integrators are common. Usually, this is achieved with active filters.

Noise Charge vs. Shaping Time

Assume that in a CR-RC shaper the differentiator and integrator time constants are equal $\tau_i = \tau_d \equiv \tau$.

$\Rightarrow$ Both cutoff frequencies equal: $f_U = f_L \equiv f_P = 1/2\pi\tau$.

Frequency response of individual pulse shaping stages

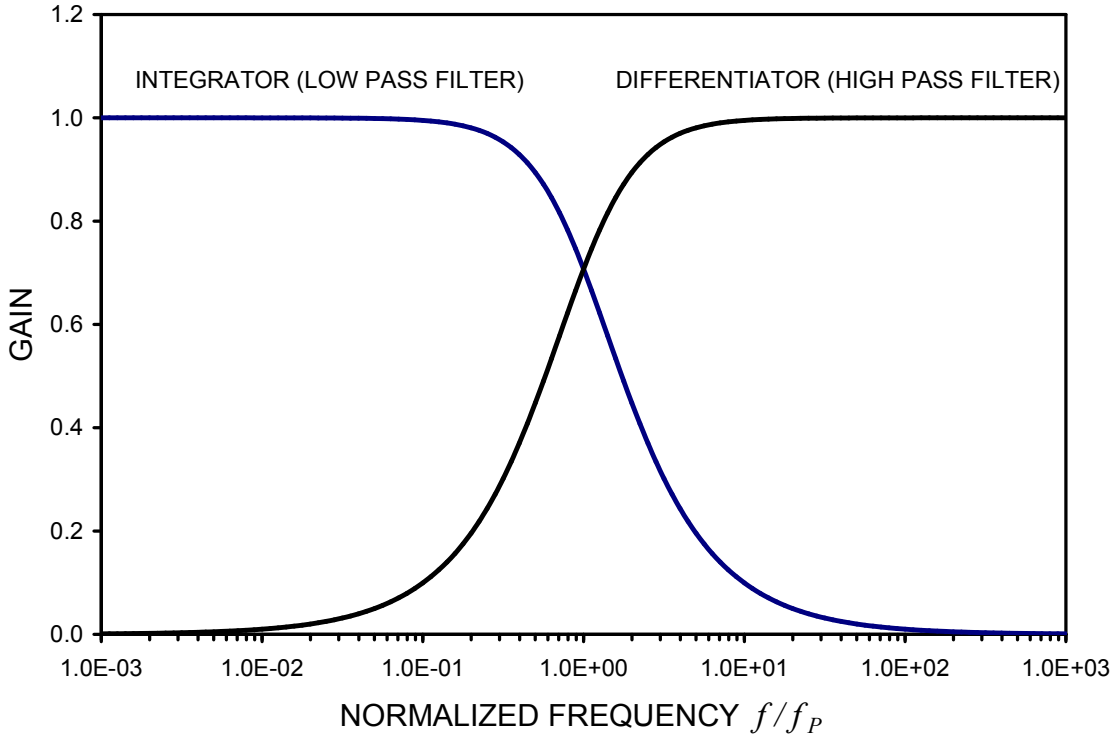

Combined frequency response

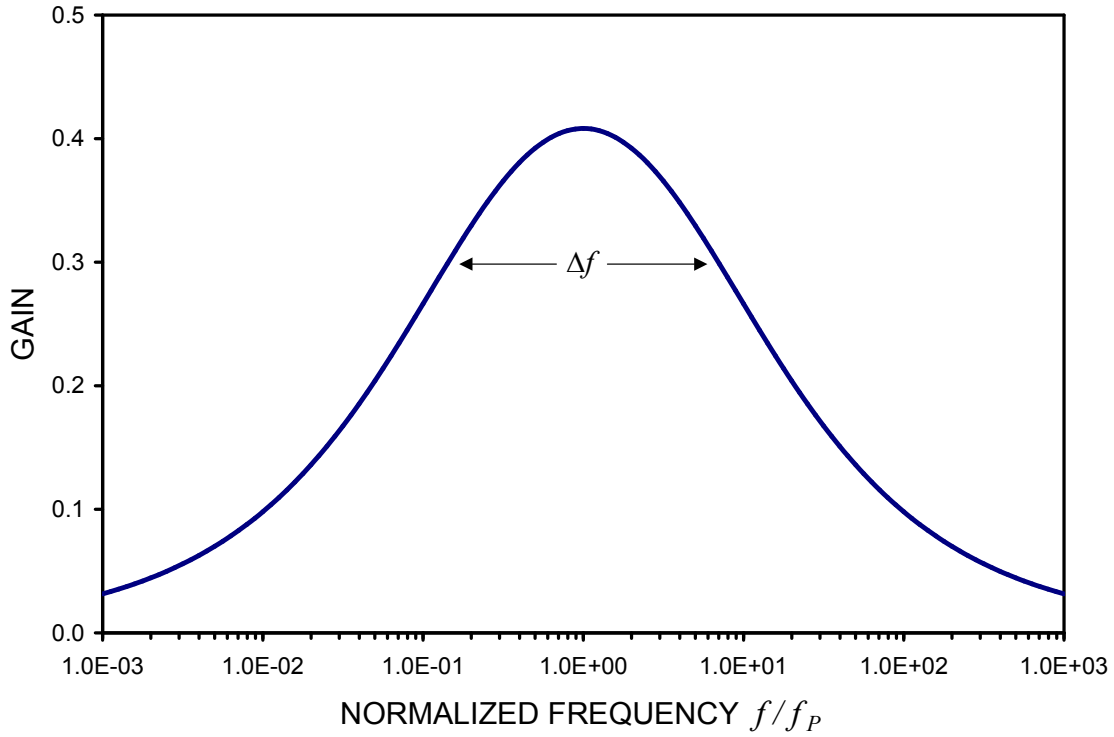

Logarithmic frequency scale $\Rightarrow$ shape of response independent of the shaping time.

The frequency scale is normalized to the peaking frequency f_P of the pulse.

Bandwidth Δf decreases with increasing shaping time.

Comparison with CR-$4RC$ shaper

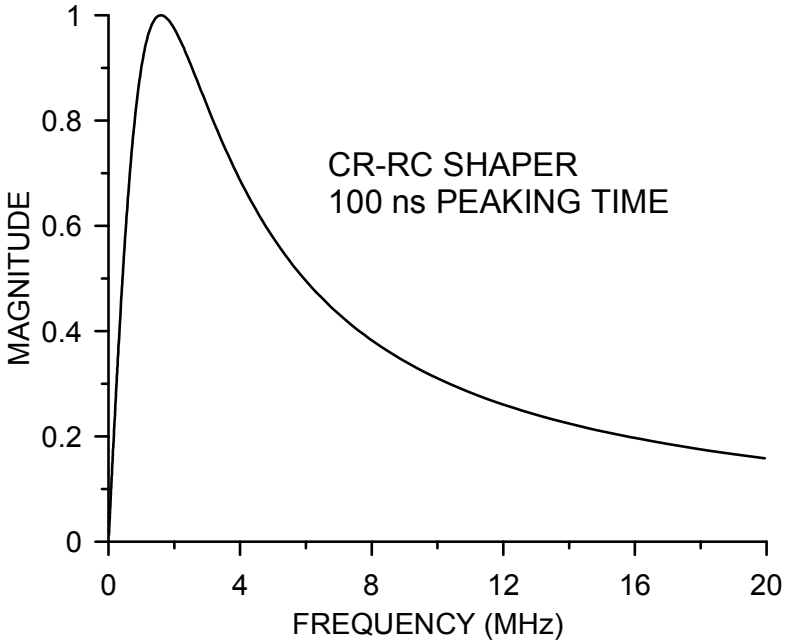

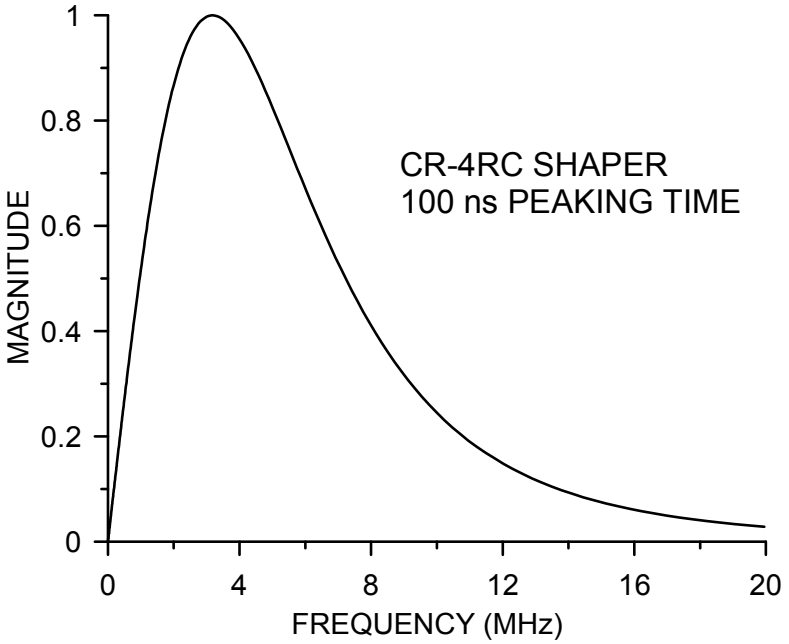

Both have a 100 ns peaking time.

The peaking frequencies are 1.6MHz for the CR-RC shaper and 3.2 MHz for the CR-4RC.

The bandwidth, i.e. the difference between the upper and lower half-power frequencies is 3.2 MHz for the CR-RC shaper and 4.3 MHz for the CR-4RC shaper.

The peaking frequency and bandwidth scale with the inverse peaking time.

Result of typical noise measurement vs. shaping time

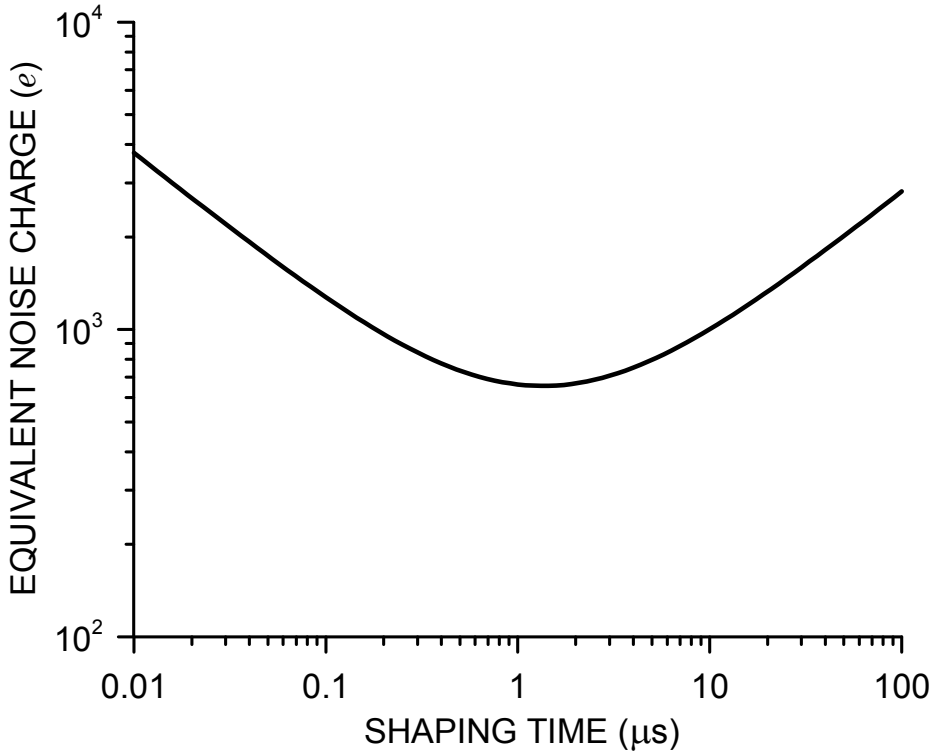

Short shaping times correspond to high frequencies, so the contribution of “white” noise dominates and the overall noise decreases with increasing shaping time.

Long shaping times correspond to a large pulse width, so the contribution of shot noise current increases.

Detector Noise Summary

Two basic noise mechanisms: input noise current i_n [$\mathrm{A}/\sqrt{\mathrm{Hz}}$]
input noise voltage e_n [$\mathrm{V}/\sqrt{\mathrm{Hz}}$]

Equivalent Noise Charge: $$Q_n^2 = i_n^2 \, T_S \, F_i + C^2 \, e_n^2 \, \frac{F_v}{T_S} + C^2 \, A_f \, F_f$$

T_S Characteristic shaping time (*e.g.* peaking time)

F_i , F_v, F_f "Shape Factors" that are determined by the shape of the pulse.

C Total capacitance at the input (detector capacitance + input capacitance of preamplifier + stray capacitance + …)

The third term is 1/f noise, dependent not on bandwidth, but ratio of upper to lower cutoff frequencies (independent of shaping time)

Typical values of F_i , F_v

CR-RC shaper	F_i = 0.924	F_v = 0.924
CR-(RC)^4 shaper	F_i = 0.45	F_v = 1.02
CR-(RC)^7 shaper	F_i = 0.34	F_v = 1.27
CAFE chip	F_i = 0.4	F_v = 1.2

Note that $F_i < F_v$ for higher order shapers.

Shapers can be optimized to reduce current noise contribution relative to the voltage noise (mitigate radiation damage!).

Minimum noise obtains when the current and voltage noise contributions are equal.

Current noise

- detector bias current
  increases with detector size, strongly temperature dependent
- noise from resistors shunting the input
  increases as resistance is decreased
- input transistor –
  low for FET, higher for BJTs
- independent of detector capacitance

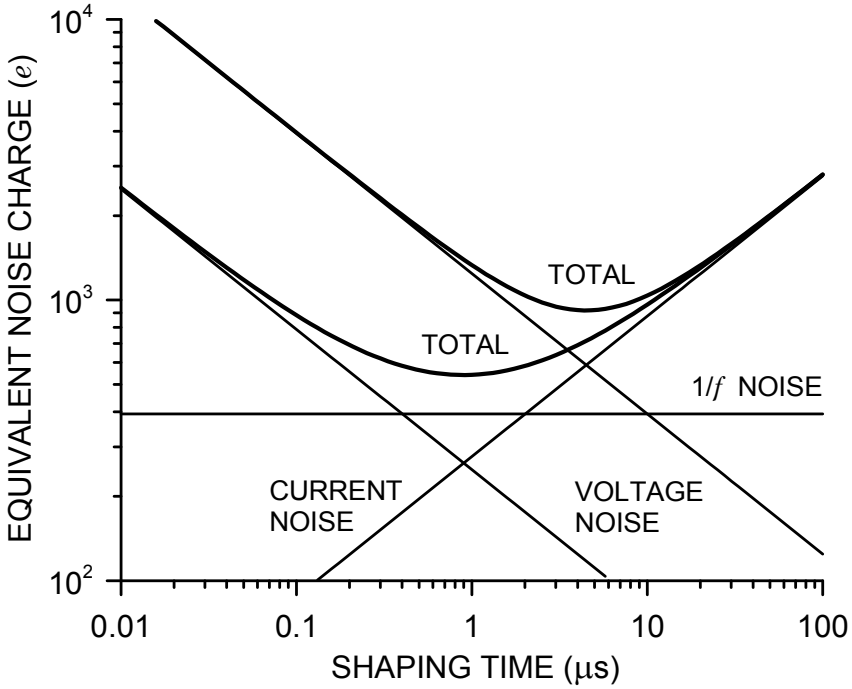

Voltage noise

- input transistor –
  noise decreases with increased current
- series resistance, e.g. detector electrode, protection circuits

FETs commonly used as input devices – improved noise when cooled ($T_{opt} \approx 130$ K)

Bipolar transistors are advantageous at short shaping times (<100 ns).
When collector current is optimized, bipolar transistor equivalent noise charge is independent of shaping time (see Chapter 6).

Practical Detector Front-End

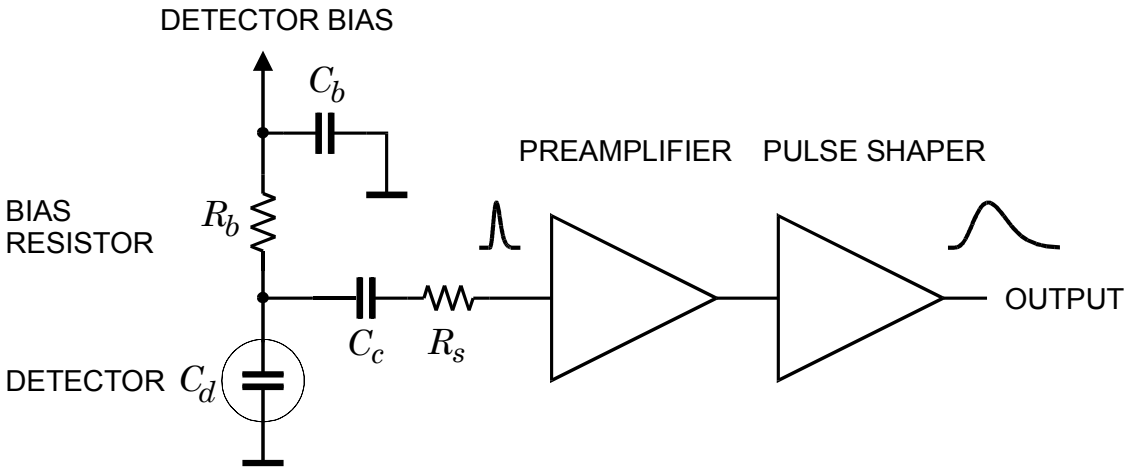

$$Q_n^2 = \left[\left(2q_e I_D + \frac{4kT}{R_b} + i_{na}^2\right)\cdot T_S F_i + \left(4kTR_S + e_{na}^2\right)\cdot C_d^2 \frac{F_v}{T_S} + A_f F_f C_d^2\right]$$

current noise	voltage noise	$1/f$ noise
$\propto T_S$	$\propto 1/T_S$	independent of T_S
independent of C_d	$\propto C_d^2$	$\propto C_d^2$

Noise parameters i_{na} and e_{na} characterize the amplifier noise.

The 3rd term is the 1/f noise contribution. A_f is the source intensity and F_f the effect of the pulse shaper. For a CR-RC shaper $F_f \approx 4$.

Numerical expression for the noise of a CR-RC shaper

(amplifier current noise and 1/*f* noise negligible)

(note that some units are "hidden" in the numerical factors)

$$Q_n^2 = 12\, I_B\, \tau \;+\; 6\cdot 10^5 \frac{\tau}{R_P} \;+\; 3.6\cdot 10^4\, e_n^2\, \frac{C^2}{\tau} \qquad \text{[rms electrons]}$$

where

τ shaping time constant [ns]

I_B detector bias current + amplifier input current [nA]

R_P input shunt resistance [kΩ]

e_n equivalent input noise voltage spectral density [nV/√Hz]

C total input capacitance [pF]

$Q_n = 1\ el$ corresponds to 3.6 eV in Si
2.9 eV in Ge

Even when more sophisticated shapers are used, this is often useful to achieve an estimate of practical noise levels and major contributions.

Digital Signal Processing

Sample detector signal with fast digitizer to reconstruct pulse:

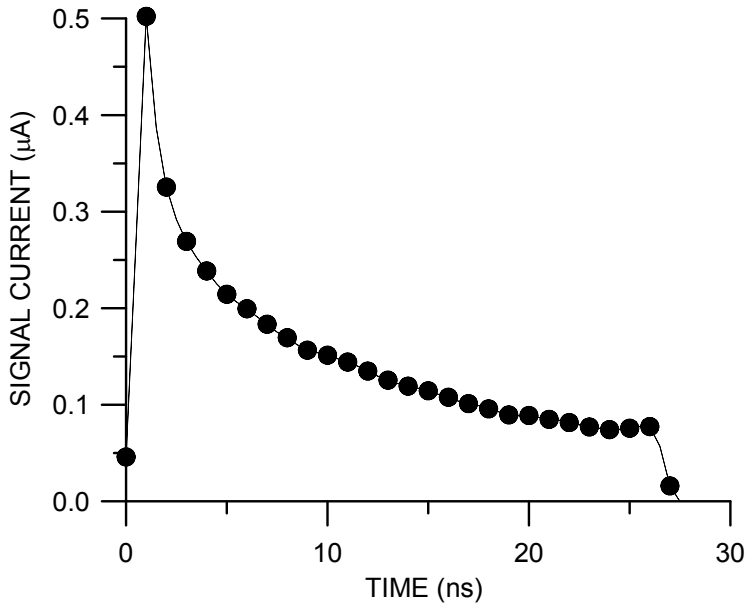

Then use digital signal processing to perform mathematical operations for desired pulse shaping.

Block Diagram

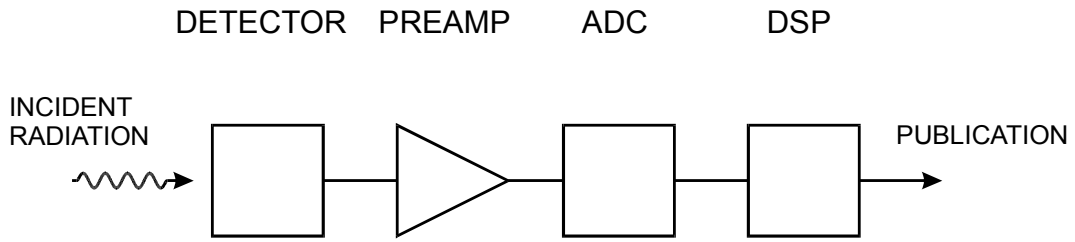

DSP allows great flexibility in implementing filtering functions

However: increased circuit complexity

increased demands on ADC, compared to traditional shaping.

Important to choose sample interval sufficiently small to capture pulse structure.

Sampling interval of 4 ns misses initial peak.

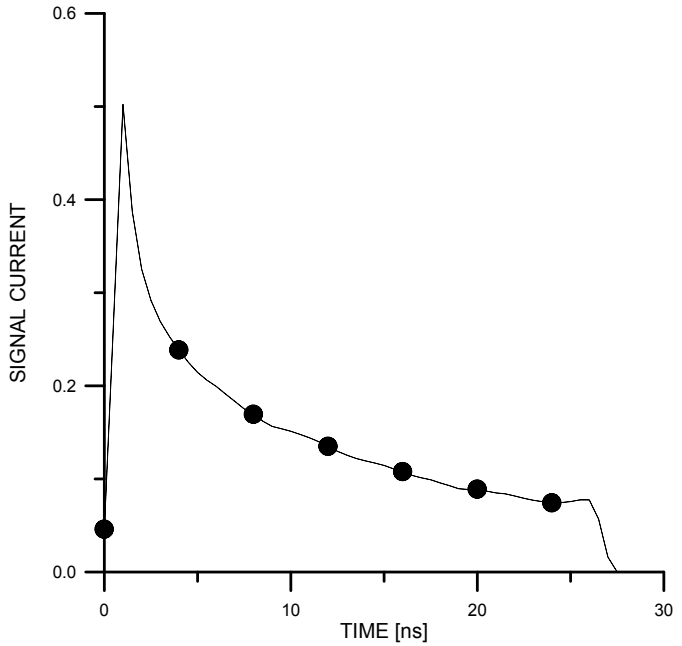

With too low a sampling rate high frequency components will be “aliased” to lower frequencies:

Applies to any form of sampling
(time waveform, image, ...)

Nyquist condition:

Sampling frequency > 2x highest signal frequency

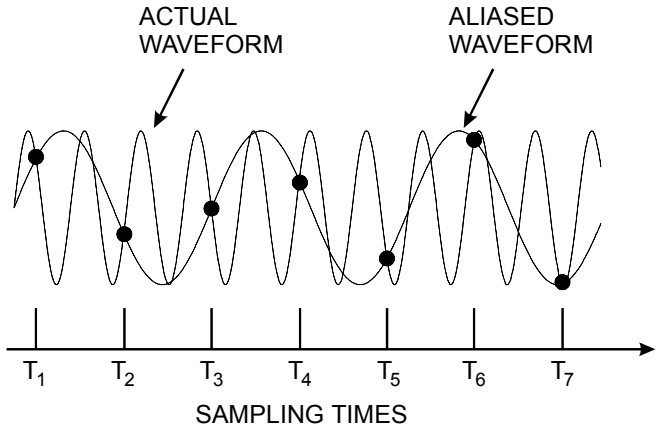

Undersampling will transfer high-frequency noise into the frequency range of the pulse shaper.

⇒ Fast ADC required + Pre-Filter to limit signal bandwidth

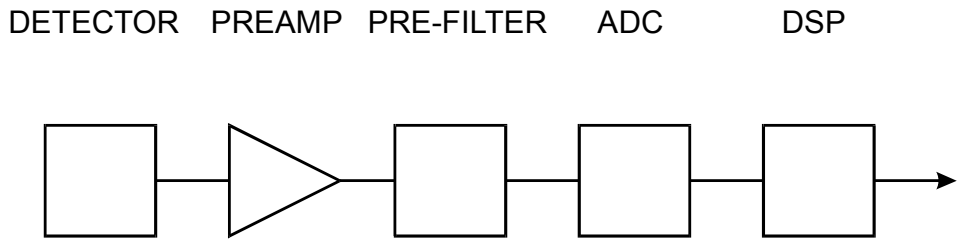

- Dynamic range requirements for ADC may be more severe than in analog filtered system (depending on pulse shape and pre-filter).
- Digitization introduces additional noise ("quantization noise")

  If one bit corresponds to an amplitude interval Δ, the quantization noise

$$\sigma_v^2 = \int_{-\Delta/2}^{\Delta/2} \frac{v^2}{\Delta}\, dv = \frac{\Delta^2}{12} .$$

  (differential non-linearity introduces additional quasi-random noise)
- If the Nyquist requirement is met, this noise will be distributed nearly uniformly up to ½ of the sampling frequency f_S and then the spectral noise density $e_n = \Delta V / \sqrt{6 f_S}$.
- Sampling at a higher frequency spreads the total noise over a larger range, so oversampling will reduce the spectral density and reduce the noise contribution within the frequency range of the pulse shaping.

Digital Filtering

Filtering is performed by convolution: $S_o(n) = \sum_{k=0}^{N-1} W(k) \cdot S_i(n-k)$

$W(k)$ is a set of coefficients that describes the weighting function yielding the desired pulse shape.

A filter performing this function is called a Finite Impulse Response (FIR) filter.

This is analogous to filtering in the frequency domain.

In the frequency domain the result of filtering is determined by multiplying the responses of the individual stages:

$$G(f) = G_1(f) \cdot G_2(f)$$

where $G_1(f)$ and $G_1(f)$ are complex numbers.

The theory of Fourier transforms states that the equivalent result in the time domain is formed by convolution of the individual time responses:

$$g(t) = g_1(t) * g_2(t) \equiv \int_{-\infty}^{+\infty} g_1(\tau) \cdot g_2(t-\tau) d\tau \,,$$

analogously to the discrete sum shown above.

Benefits of digital signal processing:

- Flexibility in implementing filter functions
- Filters possible that are impractical in hardware
- Simple to change filter parameters
- Tail cancellation and pile-up rejection easily incorporated
- Adaptive filtering can be used to compensate for pulse shape variations.

Where is digital signal processing appropriate?

- Systems highly optimized for

  Resolution

  High counting rates
- Variable detector pulse shapes

Where is analog signal processing best (most efficient)?

- Fast shaping
- Systems not sensitive to pulse shape (fixed shaper constants)
- High density systems that require small circuit area or low power

Both types of systems require careful analog design.

Performance specifications of many commercial ADCs are incomplete.

IV. Examples

1. Strip and Pixel Detectors – Conflicts and Compromises

The front-end electronics functions in strip and high-rate pixel detectors are quite similar to single detectors.

Requirements

1. low mass to reduce scattering

2. low noise
   not minimum,
   but required level

3. fast response
   timing
   high total hit rates
   (LHC: ~10^{10} s^{-1})

4. low power

5. radiation tolerance
   Reduced signal levels

+ contain costs

Conflicts

reduction in mass $\Rightarrow$ thin detector

radiation tolerance $\Rightarrow$ thin detector

thin detector $\Rightarrow$ less signal $\Rightarrow$ lower noise required

lower noise $\Rightarrow$ increased power

fast response $\Rightarrow$ increased power

increased power $\Rightarrow$ more mass in cabling + cooling

immunity to external pickup $\Rightarrow$ shielding $\Rightarrow$ mass

How to cope with ...

- High total event rate
  - a) fast electronics
    high power required for both noise and speed
  - b) segmentation
    reduce rate per detector element
    for example, at $r = 30$ cm the LHC hit rate in an area of $5 \cdot 10^{-2}$ cm^2 is about 10^5 s^{-1}, corresponding to an average time between hits of 10 μs.

    ⇒ longer shaping time allowable

    ⇒ lower power for given noise level

- Large number of events per crossing
  - a) fast electronics (high power)
  - b) segmentation
    if a detector element is sufficiently small, the probability of two tracks passing through is negligible
  - c) single-bunch timing
    reduce confusion by assigning hits to specific crossing times

⇒ Segmentation is an efficient tool to cope with high rates.

Noise vs. Power Dissipation

Under optimum scaling to maintain signal-to-noise ratio,

input transistor power ($\approx$ preamp power) scales with $(S/N)^2$.

Power Reduction

1. Segmentation reduces detector capacitance

   $\Rightarrow$ lower noise for given power

2. Segmentation reduces the hit rate per channel

   $\Rightarrow$ longer shaping time, reduce voltage noise

3. Segmentation reduces the leakage current per channel
   (smaller detector volume)

   $\Rightarrow$ reduced shot noise, increased radiation resistance

Segmentation is a key concept in large-scale detector systems.
(also to increase radiation resistance)

Example: Optimization of Si detector strip length

Assume reduced signal charge S_{rad} / S_0 due to trapping (radiation damage):

Under optimum scaling to maintain signal-to-noise ratio,

input transistor power (≈ preamp power) scales with $(S_0 / S_{rad})^2$.

see Spieler, *Semiconductor Detector Systems*, Ch. 6

Alternative: reduce sensor capacitance

Best to scale strip length by S_{rad} / S_0 to maintain required S / N at the same power per channel.

This increases number of readout ICs by S_0 / S_{rad}, so it

increases overall power by S_0 / S_{rad}

- Digital readout power per channel roughly independent of strip length
- Front-end power dominated by input transistor – scales with $\propto C_{strip}^2 \propto L_{strip}^2$

Total power: $P_{tot} = N_{strip}\left(P'_{analog}L^2 + P_{digital}\right)$

Number of strips: $N_{strip} = \frac{A}{p \cdot L}$ where $A =$ Area and $p =$ strip pitch

$\Rightarrow$ Power per unit area $\frac{P_{tot}}{A} = \frac{1}{p}\left(P'_{analog}L + \frac{P_{digital}}{L}\right)$

Assume analog power for 10 cm strip length: 0.2 mW
(SiGe design by E. Spencer, UCSC)

For comparison
ABCD chip digital power: 1.1 mW/ch at 40 MHz clock frequency, $V_{DD} = 4$V

Digital power scales $\propto$ clock frequency and $\propto$ (supply voltage)^2

Note: max strip length also constrained by occupancy

Total Power (kW) per Square Meter vs. Strip Length and Digital Power P_{dig}
(strip pitch = 80 μm, analog power 0.2 mW for 10 cm strip length)

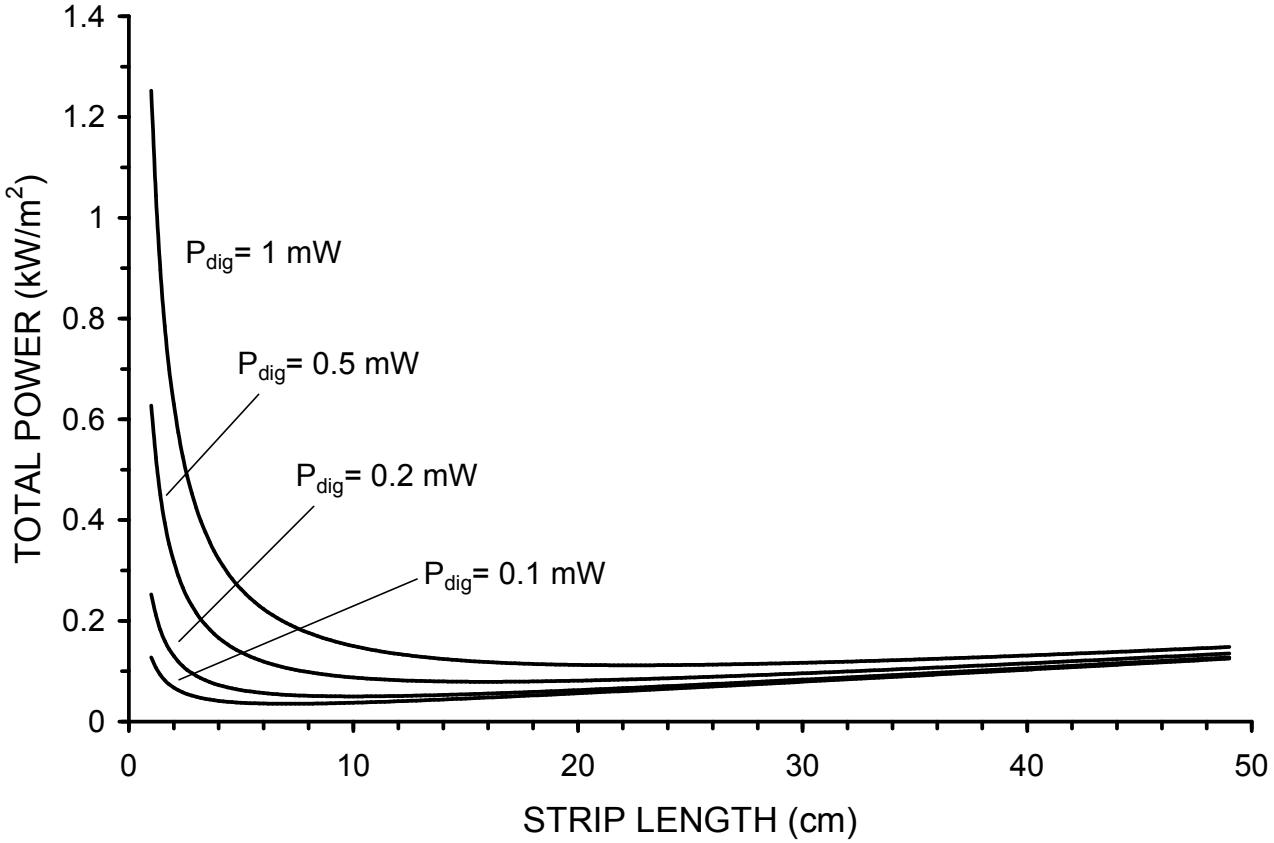

- Power increases rapidly at strip lengths below about 3 cm.
  (Dominated by digital circuitry)
- Important to streamline digital circuitry to reduce its contribution.
  e.g. analyze contributions of individual circuit blocks and assess usefulness.

Digital Power Dissipation

CMOS logic circuits requires little power, but power is absorbed during switching.

Energy dissipated in wiring resistance R:

$$E = \int i^2(t) R \, dt$$

$$i(t) = \frac{V}{R} \exp\left(-\frac{t}{RC}\right)$$

$$E = \frac{V^2}{R} \int_0^\infty \exp\left(-2t/RC\right) dt = \frac{1}{2} CV^2$$

If pulses (rising + falling edge transitions) occur at frequency f,

$$P = fCV^2$$

Power dissipation increases with clock frequency and (logic swing)^2.

The RC time constant also introduces a time delay.

This depends on the number of driven inputs and wiring lengths.

CASCADED CMOS STAGES

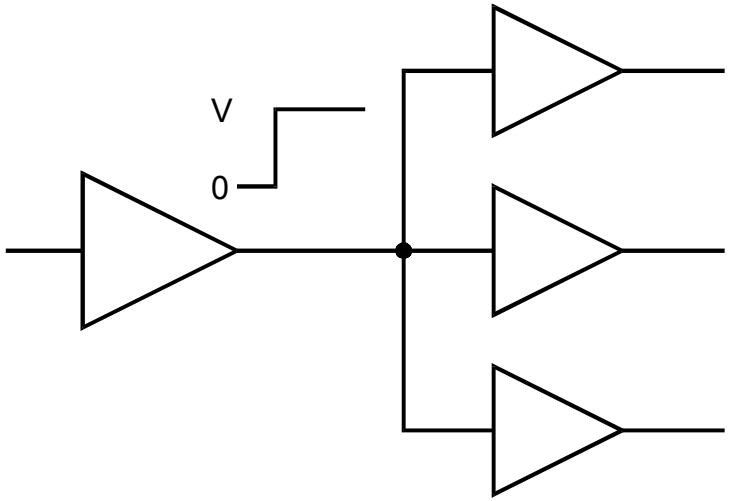

EQUIVALENT CIRCUIT

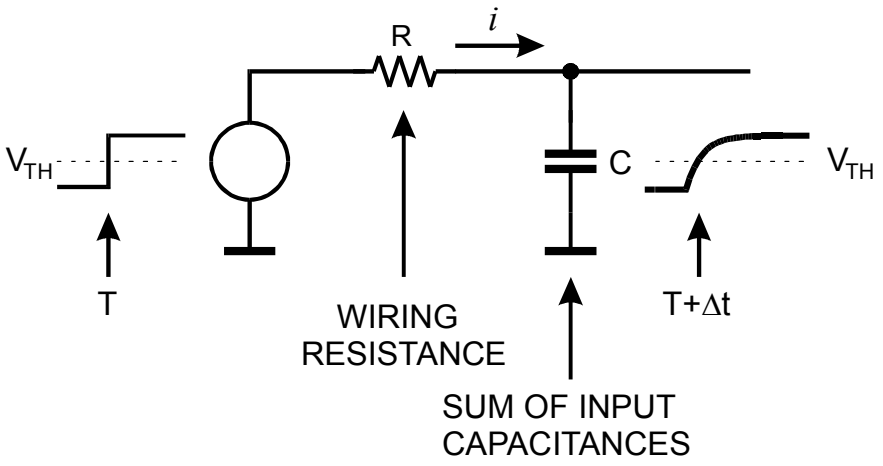

The above result is often derived from the energy stored in a capacitor.

$$E = \frac{1}{2} C V^2$$

However, this energy will be returned when the capacitor is discharged, so after the leading and trailing edges of a pulse the net energy is zero.

In reality, the power is dissipated by the charge and discharge current flow in the circuit's series resistance.

This is one of many examples where the wrong physics yields a correct result

– until one digs deeper.

Analog signal processing follows the standard procedures, but additional digital control circuitry is required to control thousands of channel per module.

Block diagram of the LHC ATLAS Silicon Tracker front-end

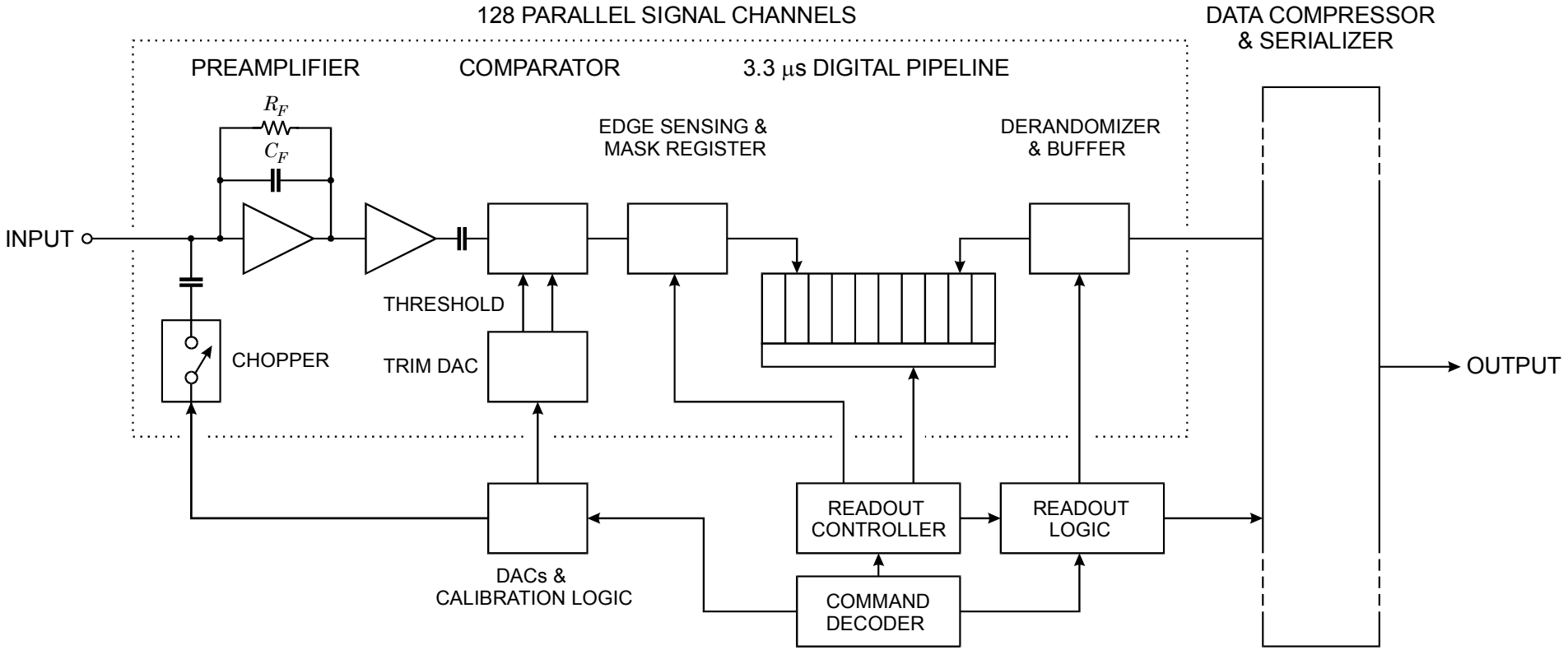

Pixel Detectors with Random Access Readout

"Smart Pixels"

Quiescent state:
no clocks or switching in pixel array

Pixel circuitry only issues signals when struck.

Struck pixels send address + time stamp to peripheral register

On receipt of trigger selectively read out pixels.

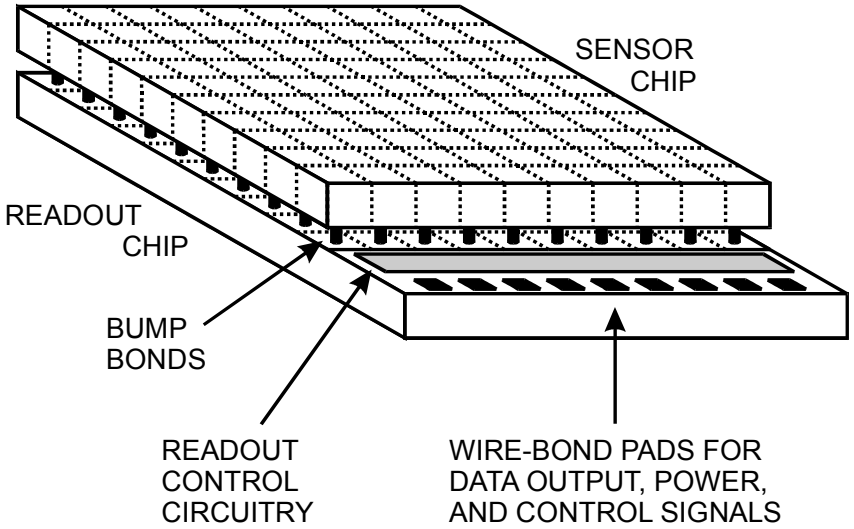

Hybrid configuration permits optimization of the detector and readout electronics.

Each ATLAS pixel cell includes:
- Q-amplifier + shaper per pixel
- threshold comparator per pixel
- trim-DAC per pixel for fine adjustment of threshold
- time-over-threshold analog digitization
- test pulse per pixel (dual range)
- bad pixels can be masked

Block Diagram of Pixel Cell

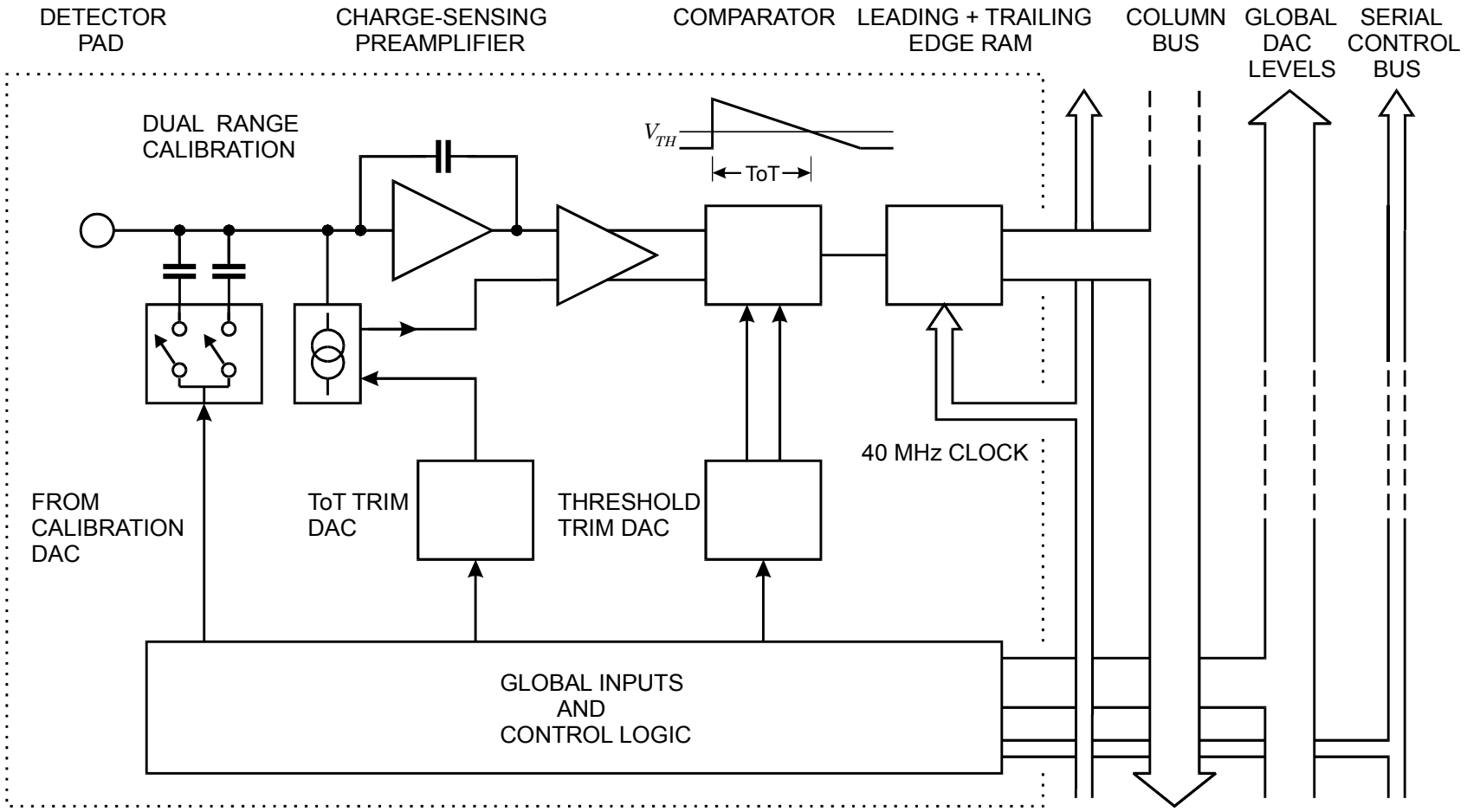

Pixel Readout

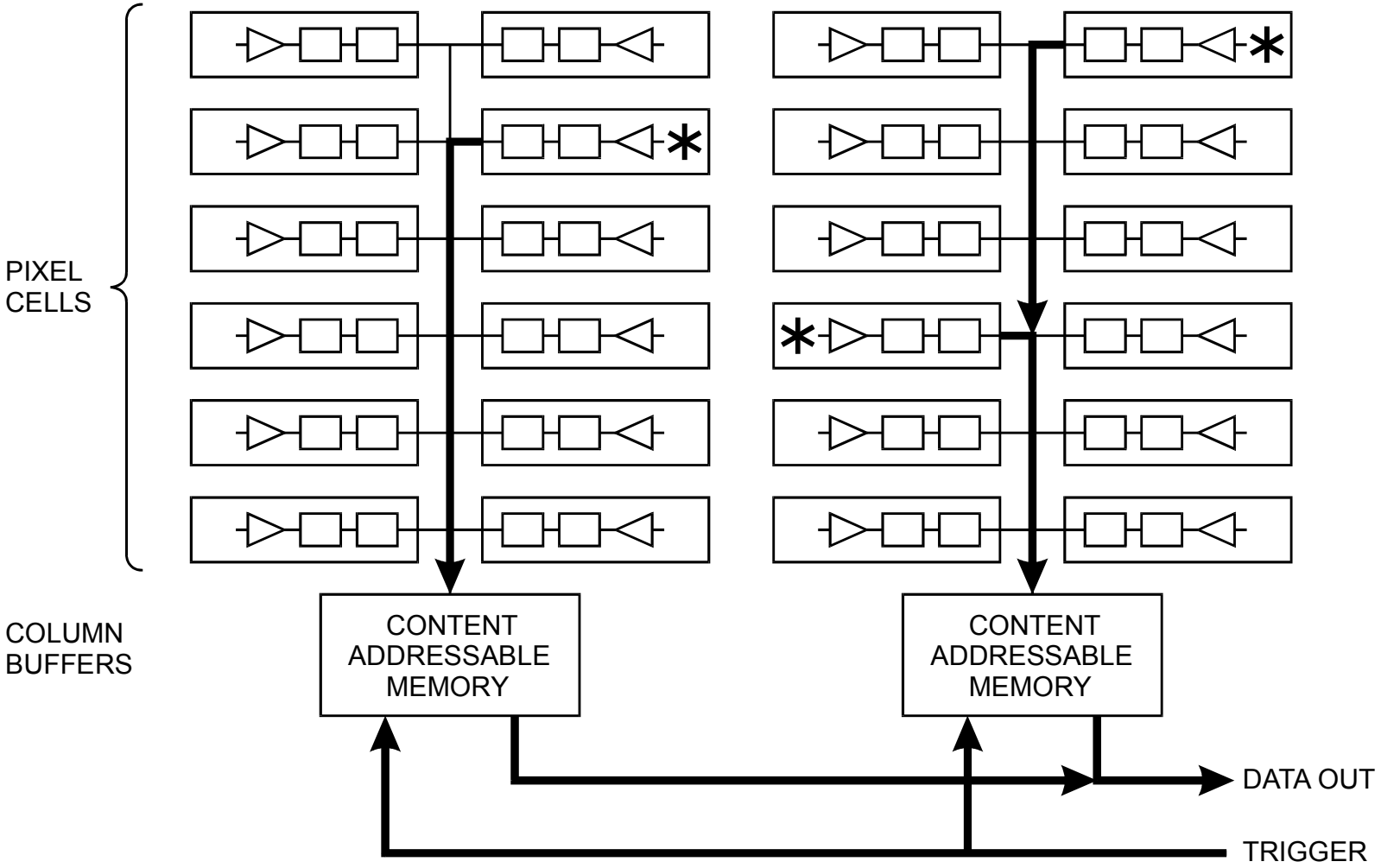

ATLAS Pixel Module

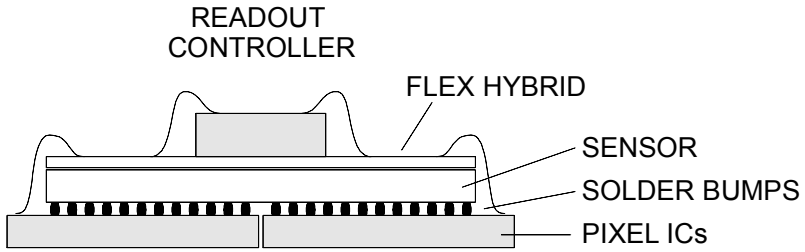

SCHEMATIC CROSS SECTION (THROUGH HERE)

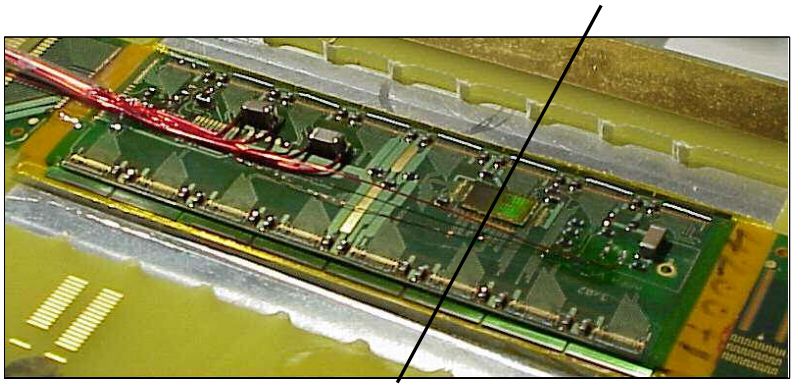

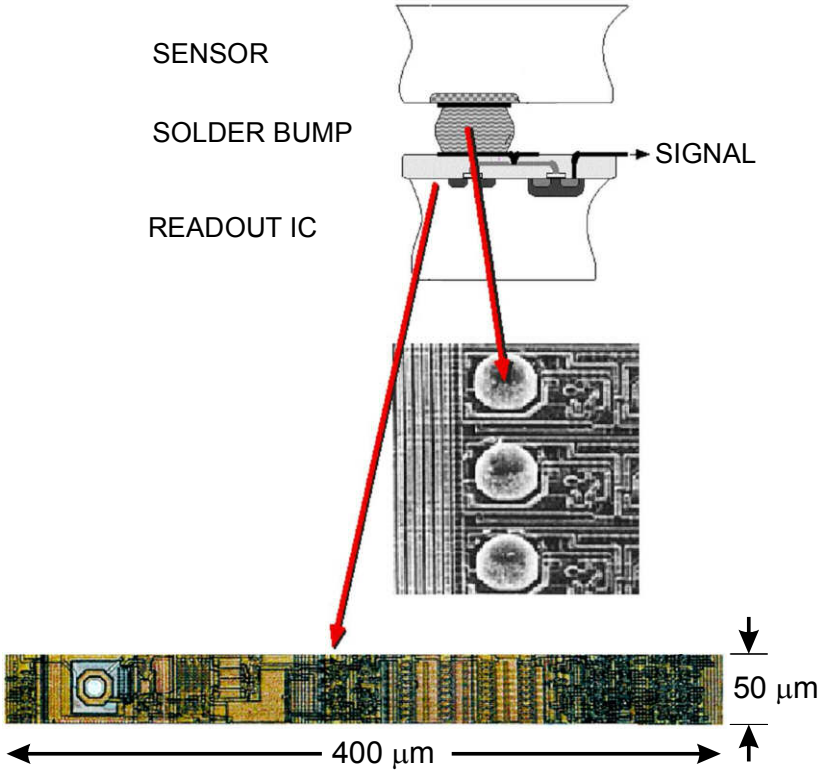

2. High Pressure Xe Gas Time Projection Chamber

Goal:

Develop a novel detector that combines high energy resolution with measurements of event topologies to separate the desired signals from backgrounds.

The design should be scalable to match a wide range of applications, including searches for ultra-rare events.

Potential Applications

1. Search for neutrinoless double-beta decay

    a) Verify that the neutrino is its own anti-particle
    b) Helps determine absolute neutrino mass
    c) If observed, lepton number not conserved

2. Large-area gamma detectors that require background suppression

These applications require separation of the desired signals from a wide range of backgrounds.

This requires

- High energy resolution for electrons and gamma rays into the MeV regime
- Reconstruction of energy deposition sequence to separate full from partial energy deposition
- Discrimination between neutron and gamma signals

High-pressure Xe gas can provide energy resolution much superior to liquid Xe.

E= 2.5 MeV (= Q ^{136}Xe):

- High-Pressure Xe: $\Delta E / E \approx 3 \cdot 10^{-3}$ (Fano factor ≈ 0.15)
- Liquid Xe (EXO prediction): $\Delta E / E \approx 35 \cdot 10^{-3}$ (Fano factor ≈ 20)

Implementation as a TPC yields position resolution adequate to reconstruct beta decays and the tracks of Compton recoils.

The ratio of ionization to scintillation signals provides neutron-gamma discrimination.

"Intrinsic" Energy Resolution for Ionization at ^{136}Xe Q-Value

Q-value (^{136}Xe $\rightarrow$ ^{136}Ba) = 2480 keV

$W =$ energy per ion/electron pair in xenon gas = 21.9 eV,
but W depends on electric field strength, might be ~24.8 eV

$N =$ number of ion pairs = Q/W

$F =$ Fano factor. Measured in Xe gas: F = 0.13 – 0.17 (assume 0.15)

$$\frac{\Delta E}{Q} = 2.35 \cdot \frac{\sqrt{FN}}{Q} = 2.35 \cdot \sqrt{\frac{FW}{Q}} \approx 2.9 \cdot 10^{-3} \text{ FWHM}$$

Comparison:

Germanium diodes @ 2.5 MeV $\Delta E / E \approx$ 1 – 2·10^{-3} FWHM

Fano Factor of Liquid Xe ~20 $\Rightarrow$ $\Delta E / E \approx$ 3.5·10^{-2} FWHM
(mixed ionization + scintillation)

Absolute Signal Charge Fluctuations

$Q = 2480$ keV

$W = 24.8$ eV

$N =$ number of ion pairs $= Q / W$

$N =$ 2480 x 10^3 eV / 24.8 eV = ~**100,000 electron/ion pairs**

$$\sigma_N = \sqrt{FN}$$

$F = 0.15$

$\Rightarrow \quad \sigma_N = \sqrt{FN} \approx$ 120 electrons rms @ 2480 keV

120 electrons: Electronic noise will dominate in practical configurations

Need internal gain without introducing significant fluctuations.

Energy Resolution Including Gain Fluctuations

If fluctuations are uncorrelated, then

$$\sigma_N = \sqrt{(F + L + G)N}$$

where $F =$ Fano factor = 0.15
$L =$ Loss of primary ionization (set to 0)
$G =$ Fluctuations in gain process

To maintain resolution G must be smaller than F.

Avalanche charge gain introduces excessive noise because early fluctuations are amplified exponentially.

Example: for a wire $G =$ 0.6 – 0.9 $\Rightarrow$ benefit of small F is lost!

In general, avalanche devices can't deliver $G < F$.

Alternative: Electroluminescence

Accelerate electrons in an electric field so that over a certain distance they gain just enough energy to excite optical states – NOT emit secondary electrons.

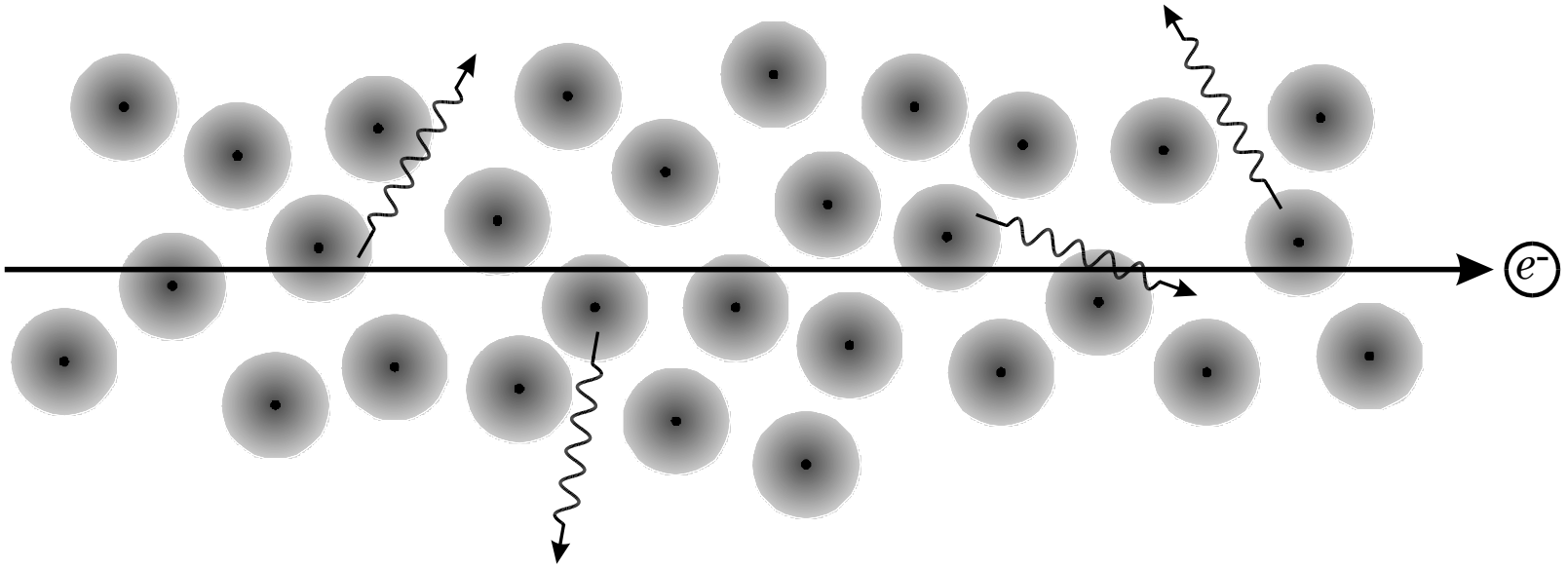

Typically one photon (170 nm $\triangleq$ 7.3 eV) per 8 – 10 V traversed by the electron.

No additional electrons released.

Linearly sequential gain process – photons don't excite additional emissions

$\Rightarrow$ Excitations are independent of one another.

$\Rightarrow$ Initial fluctuations are not magnified.

Principle of Current LBL Chamber

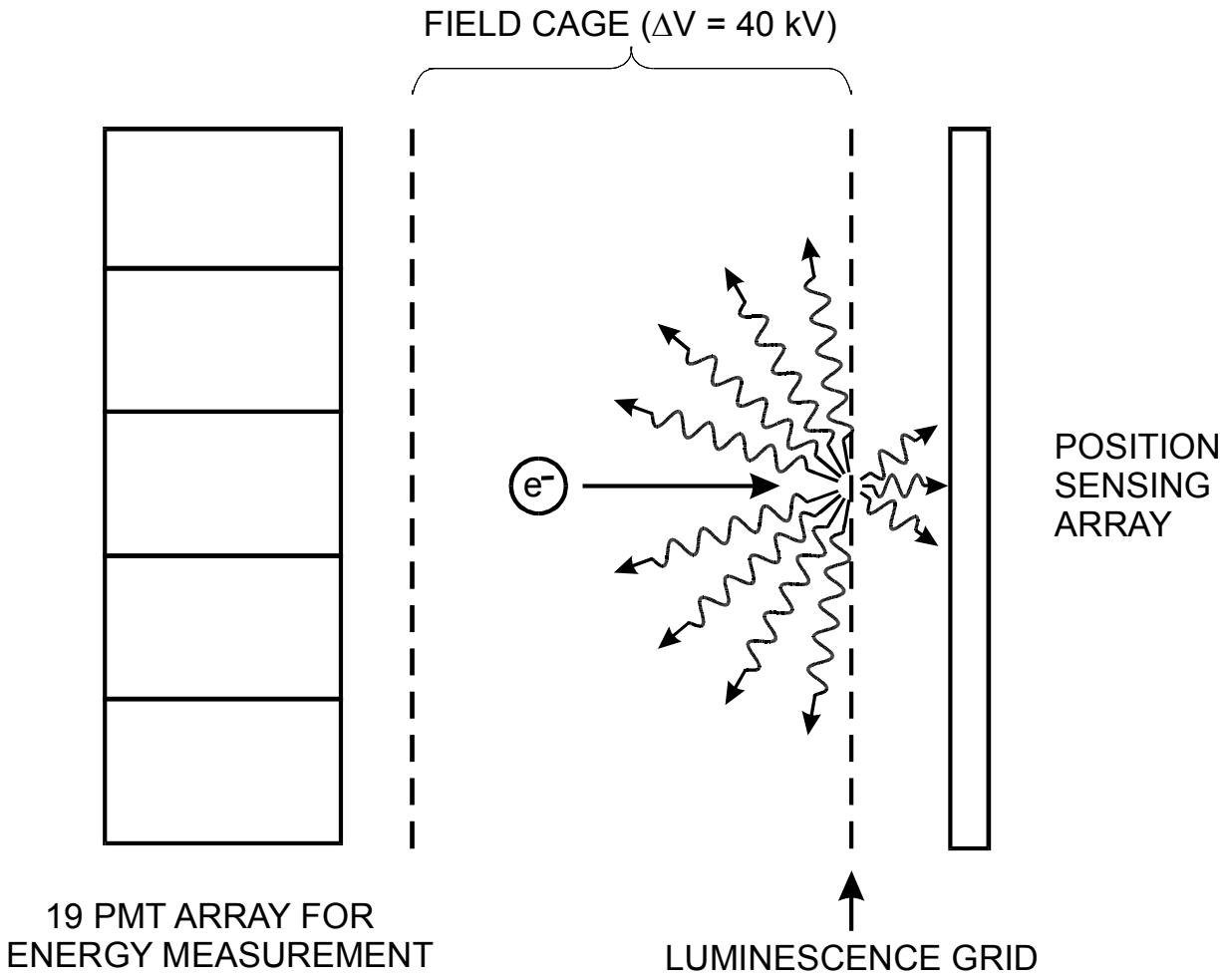

z-coordinate (horizontal) is determined by measuring the drift time of the signal charges. Prompt scintillation provides the start signal.

The duration and form of the energy signals varies greatly, because the drift velocity is about 1 mm/μs.

A track parallel to the readout plane will have a duration determined by the diffusion. This will be about 1 cm, so the signal duration is about 10 μs.

For a track normal to the readout plane, the duration is determined by the length of the track, which for the 2.5 MeV neutrinoless double-beta decay will be up to 160 μs. For gamma calibrations, the duration is even greater.

Typical signal from a 511 keV gamma

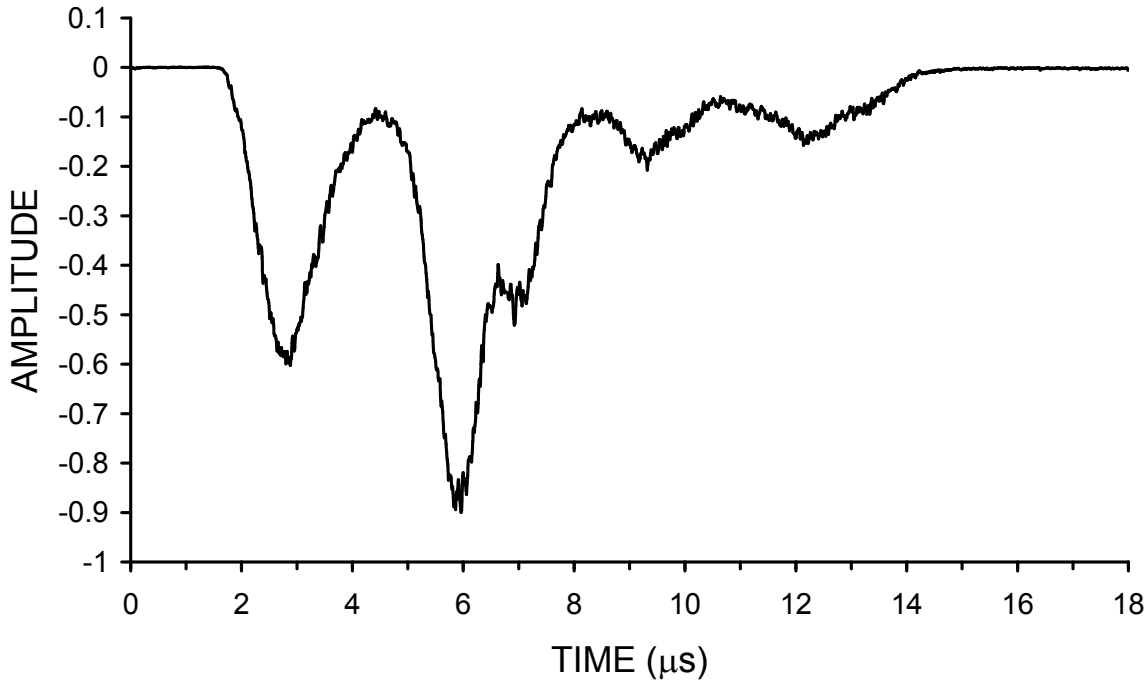

Pulse Processing

⇒ Pulse processing must accurately record the signal charge

⇒ Digital signal processing is the solution

The signals are sampled at a 100 MHz rate and signal charge is determined from the sum of all samples.

This would be straightforward if the ADC would have a gated integrator that provides the signal charge in each sample interval.

However, our test system uses commercial ADCs that only provide an instantaneous amplitude sample.

The single electron PMT output pulse is only about 6 ns in duration.

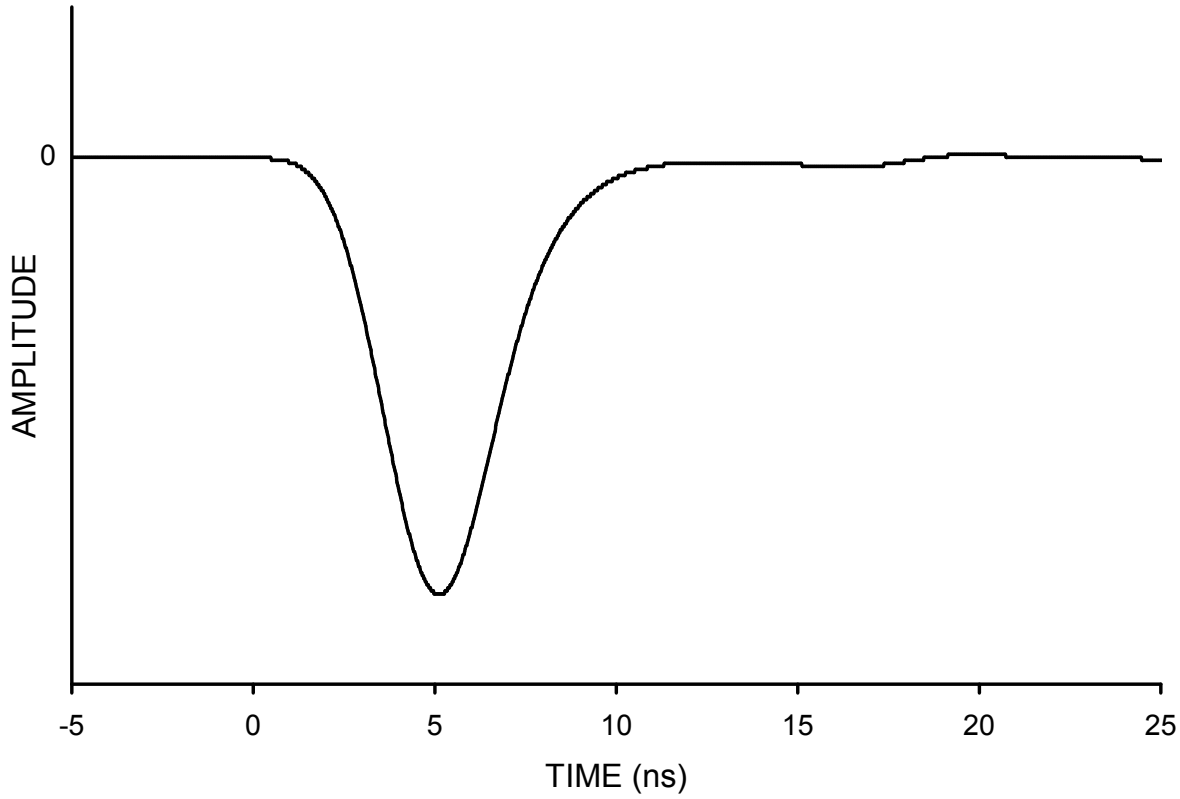

Sampling at 10 ns intervals will miss numerous pulses and for the pulses as are typically recorded at the start of the sampling interval, the rms fluctuation is excessive.

This can be bridged by integrating the signal current from the PMT, so that the pulse fed to the ADC has a width of several samples.

This is easily done by placing a shunt capacitor directly at the PMT anode. It charges quickly, but discharges with the time constant of the capacitance times the load resistance, which is the impedance of the feedline.

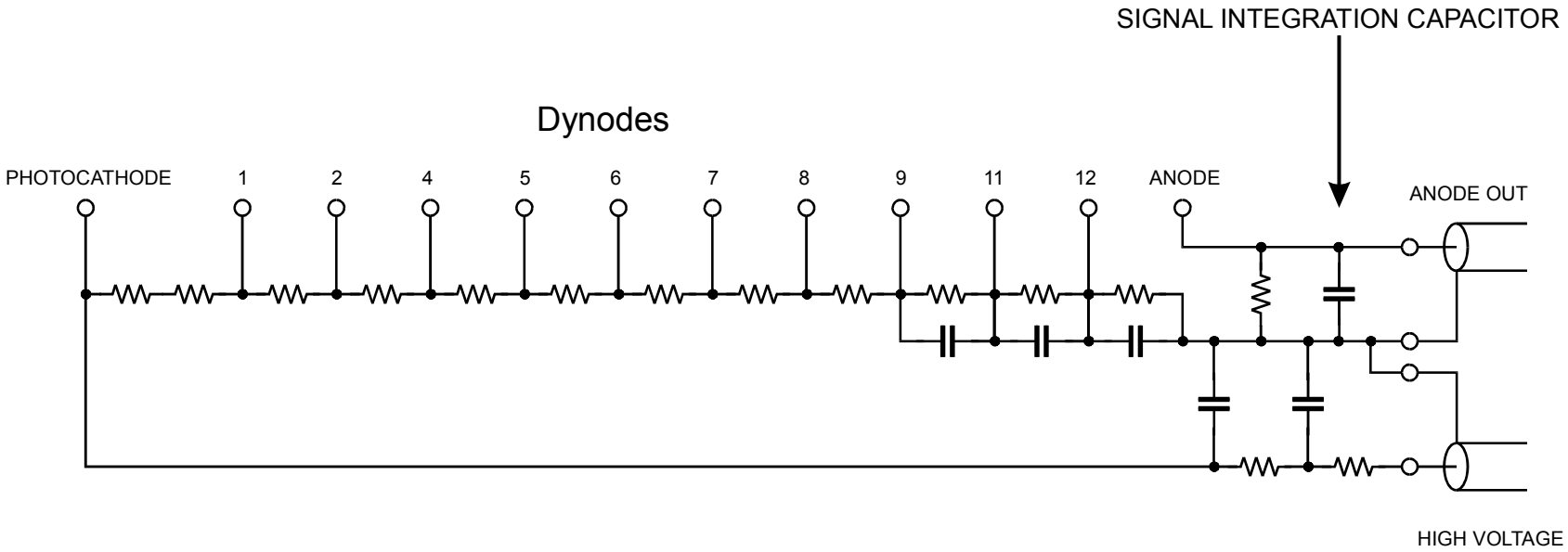

The shunt capacitance reduces the peak voltage applied to the readout electronics, so the electronic noise must be improved (ADCs are commonly high-noise).

A low-noise preamplifier with bandwidth filtering to cut off frequencies greater than ½ of the sampling frequency is used.

Pulse shape fed to the 10 ns sampling ADC – width is multiple samples

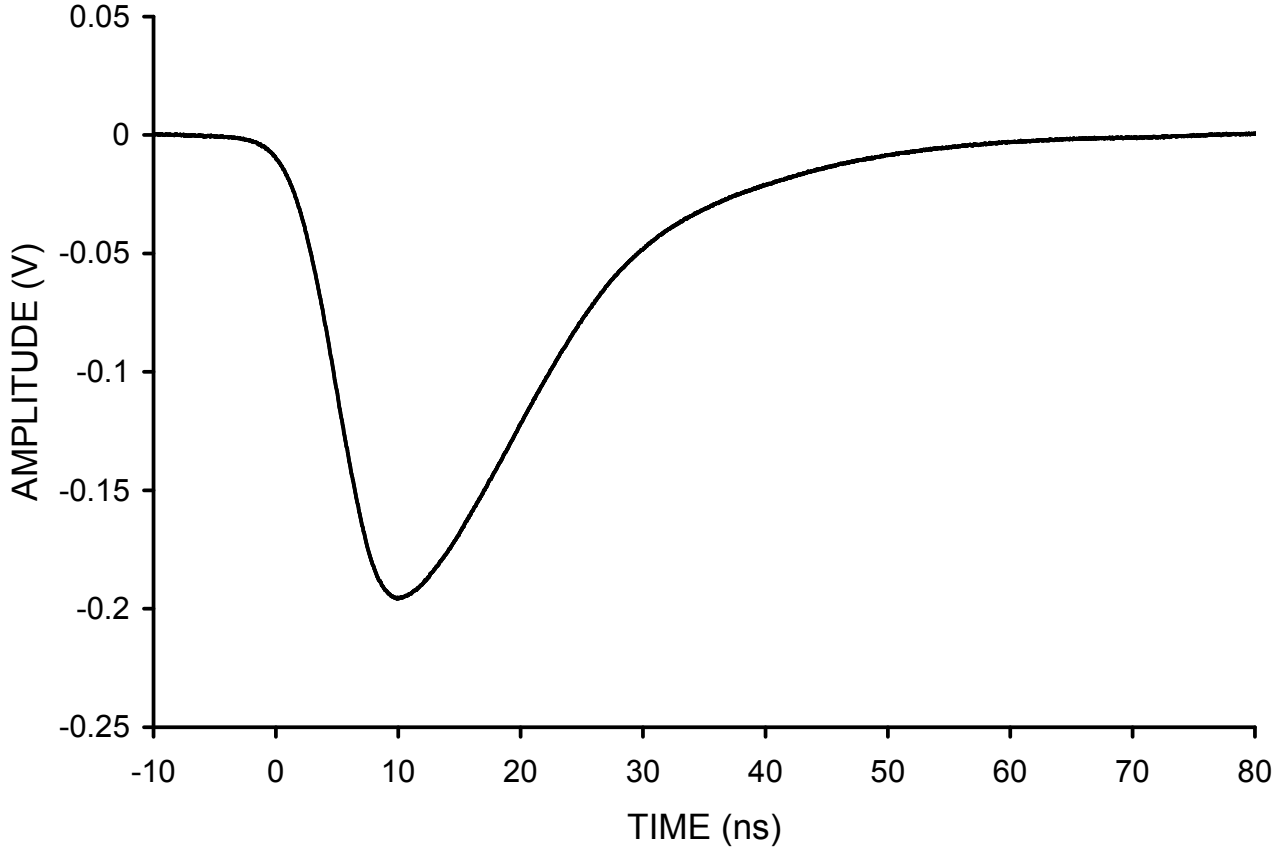

Preamp Frequency Response

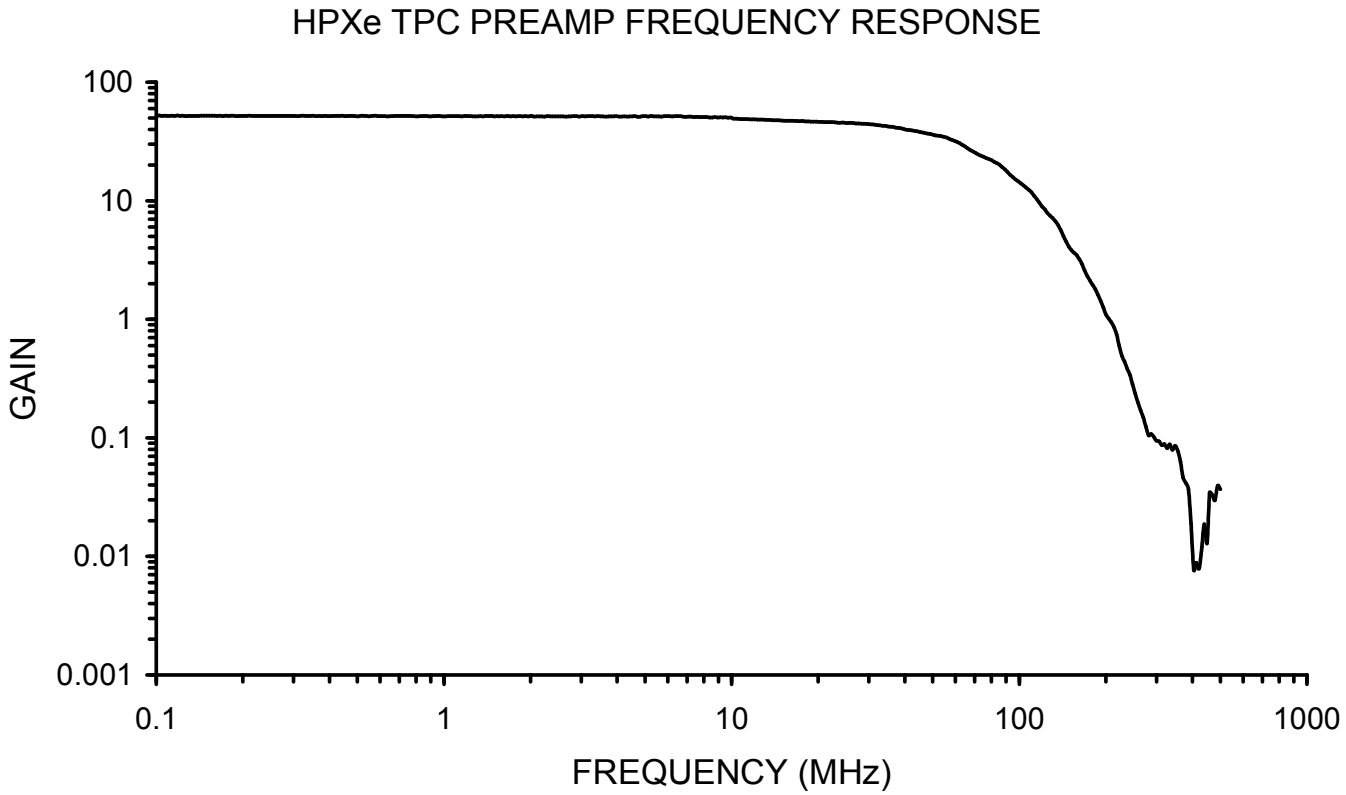

To optimize S/N the preamp cutoff frequency can be matched to the PMT anode decay time constant, but a faster rise time is maintained to evaluate event timing.

In Valencia interference from a local VHF radio station must be attenuated, so a lower cutoff frequency is incorporated.

Initial experimental results are encouraging, but more extensive analysis is required.

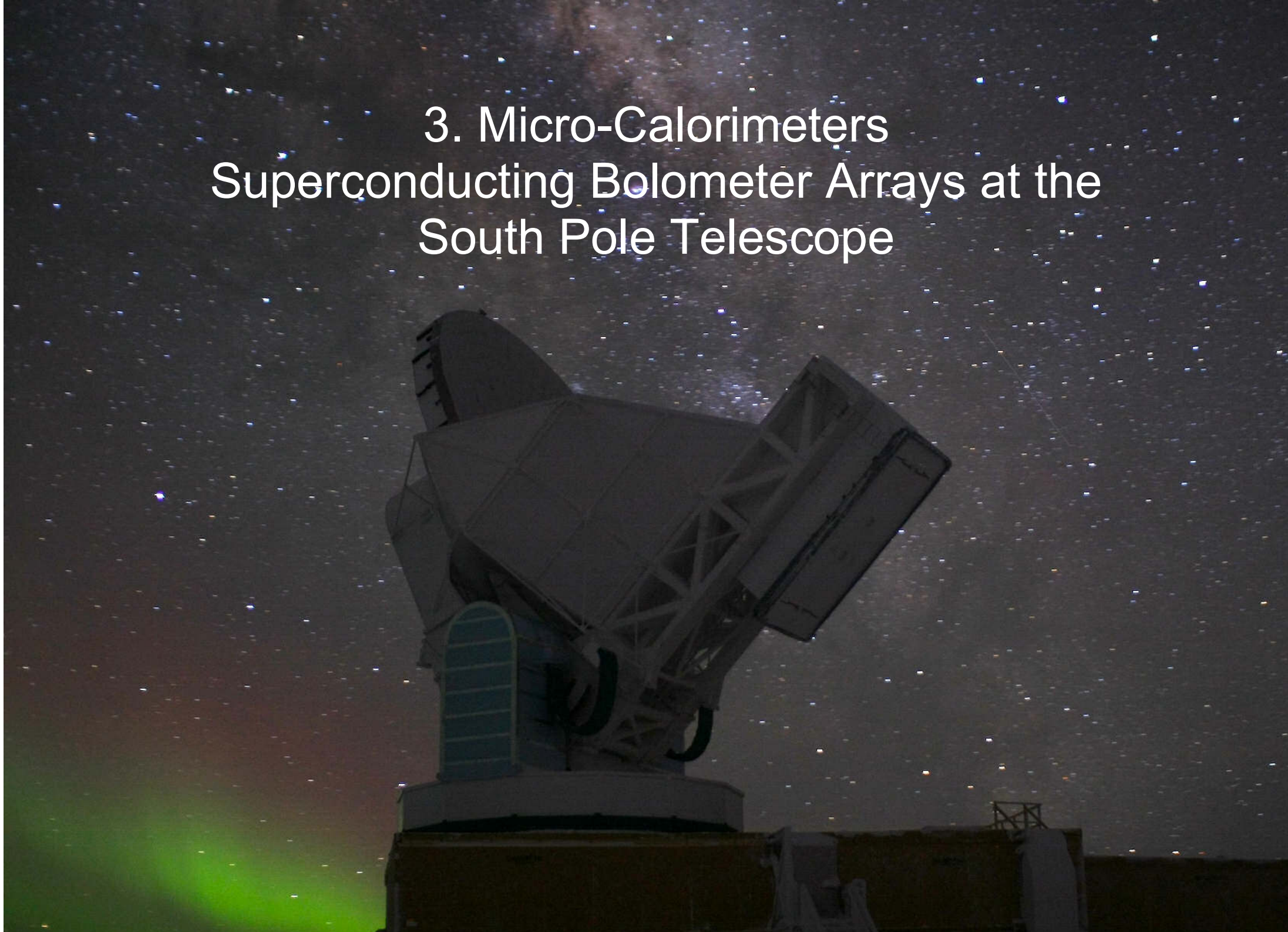

3. Micro-Calorimeters
Superconducting Bolometer Arrays at the South Pole Telescope

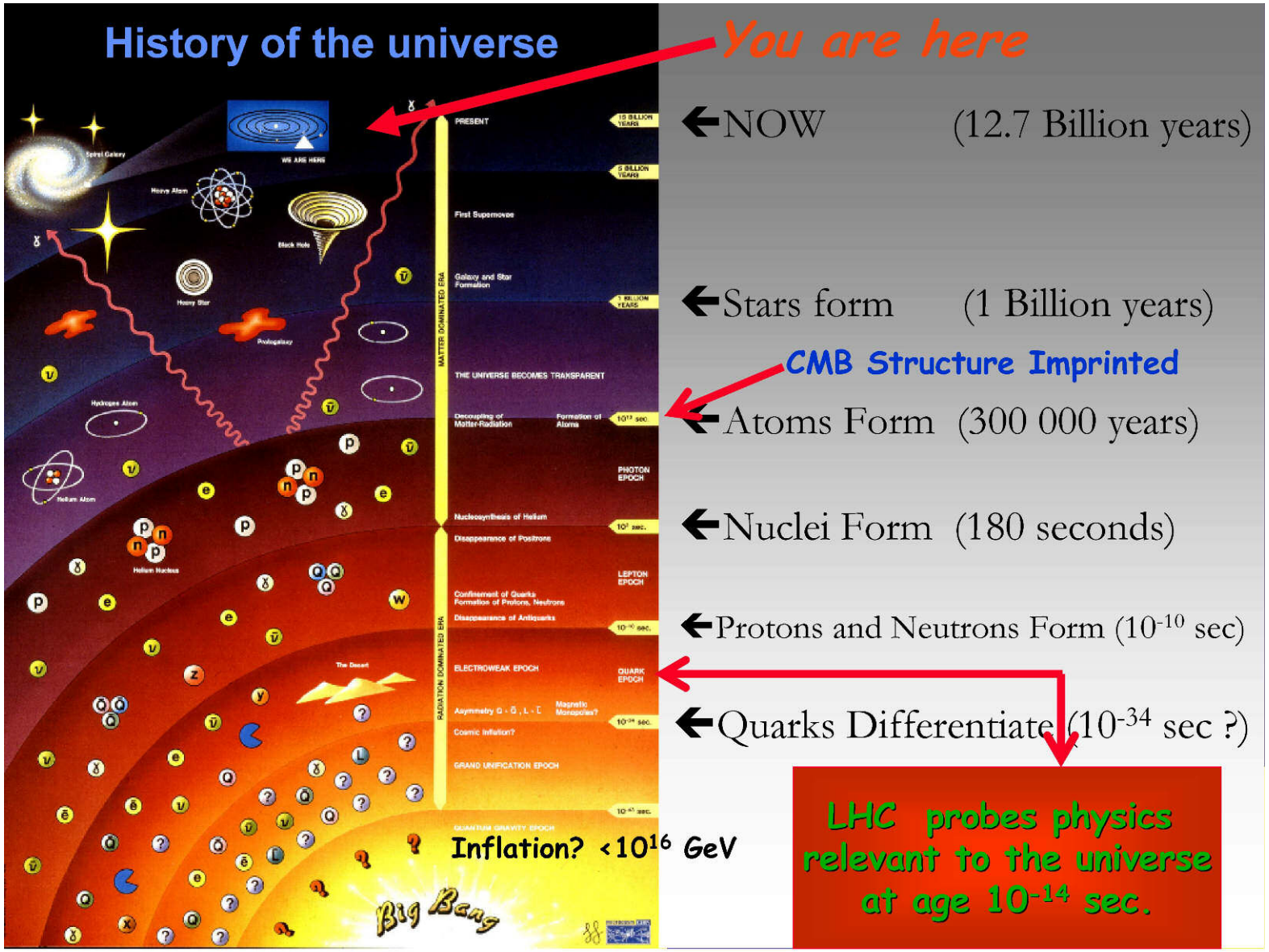
History of the universe
You are here
NOW (12.7 Billion years)
Stars form (1 Billion years)
CMB Structure Imprinted
Atoms Form (300 000 years)
Nuclei Form (180 seconds)
Protons and Neutrons Form (10^{-10} sec)
Quarks Differentiate (10^{-34} sec ?)
LHC probes physics relevant to the universe at age 10^{-14} sec.
Inflation? $<10^{16}$ GeV
Big Bang
PRESENT
First Supernovae
Galaxy and Star Formation
THE UNIVERSE BECOMES TRANSPARENT
Decoupling of Matter-Radiation
Formation of Atoms
PHOTON EPOCH
Nucleosynthesis of Helium
Disappearance of Positrons
LEPTON EPOCH
Confinement of Quarks
Formation of Protons, Neutrons
Disappearance of Antiquarks
ELECTROWEAK EPOCH
QUARK EPOCH
Cosmic Inflation?
GRAND UNIFICATION EPOCH
MATTER DOMINATED ERA
RADIATION DOMINATED ERA

Measuring deviations from the Cosmic Microwave Background (CMB) provides a very sensitive technique to scale the universe for galaxy clusters.

This is helpful to analyze the evolution of the universe to eventually form planets.

Unlike visible light or x-ray measurements, the galaxy cluster signals are independent of redshift (distance, i.e. age)

The CMB has a near perfect black body spectrum (T =2.7K), which peaks at about 150 GHz (mm wavelength)

The equivalent temperature of the cluster signal is <10^{-3} K , so very sensitive detectors are needed.

H_2O in the atmosphere absorbs the relevant radiation and creates moving backgrounds, so experiment locations should be high and dry:

Atacama Plateau in Chile at an altitude of 5100m (“driest desert”)
South Pole at an altitude of 2800 m – very stable weather

More information at spt.uchicago.edu and www-physics.LBL.gov/~spieler.

We use superconducting transition sensors

- Bias thin film superconductor at transition from super- to normal conducting

⇒ Large change in resistance with absorbed power

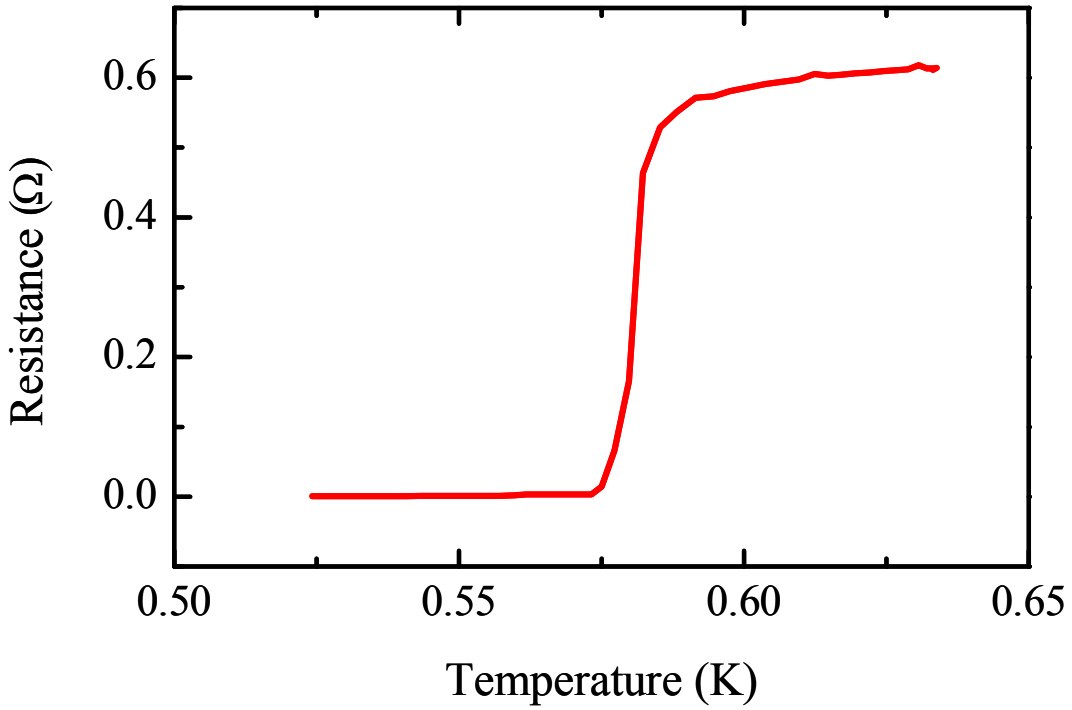

- Thin bi-layers (e.g. Al – Ti) allow tuning of transition temperature

Signal Spectrum in Galaxy Cluster Search

Antenna beam width: 1’ FWHM Scan speed: 10’/s

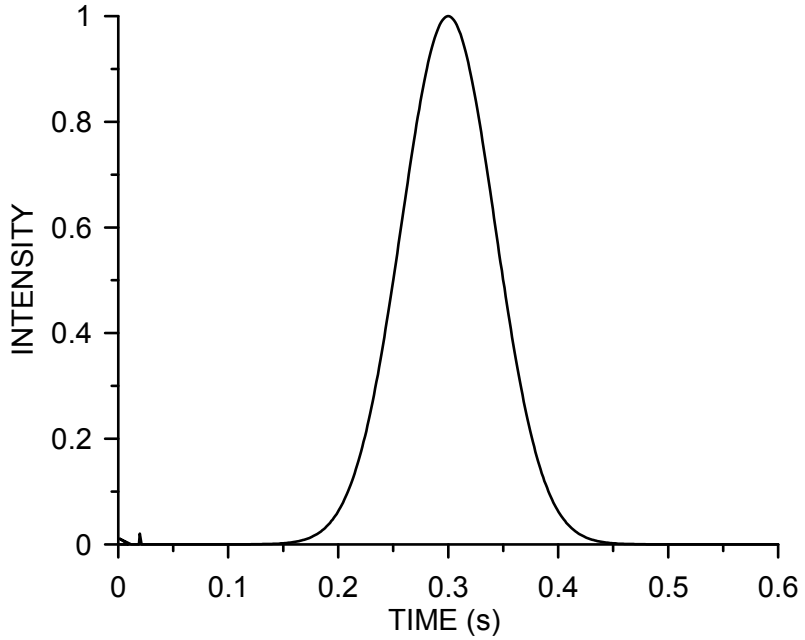

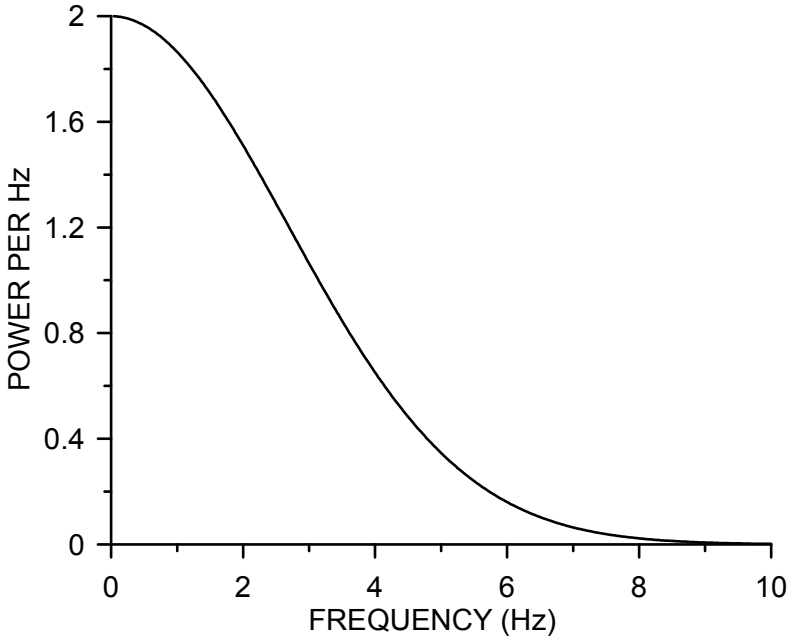

(W. Lu, CWRU)

Typical observations: scan back and forth in azimuth at 0.25 degrees/s, step in elevation

⇒ Maintain Gain Stability + Noise Level down to ~0.1 Hz

Why Bolometers?

Amplifiers (phase coherent systems) are subject to the quantum noise limit.

Minimum spectral noise power density: $\frac{dP}{d\omega} = \hbar\omega$

Follows from uncertainty principle.

(H.A. Haus and J.A. Mullen, Phys. Rev. 128 (1962) 2407-2413)

For a simple derivation see Spieler, *Semiconductor Detector Systems*, pp. 132-133

Bolometers do not preserve phase, so not subject to quantum noise limit.

Large (~1000) detector arrays are needed. They are monolithically integrated.

Superconducting transition sensors require constant voltage bias to optimize stability.

APEX Focal Plane (Jared Mehl) – Initial ~320 element array prior to SPT

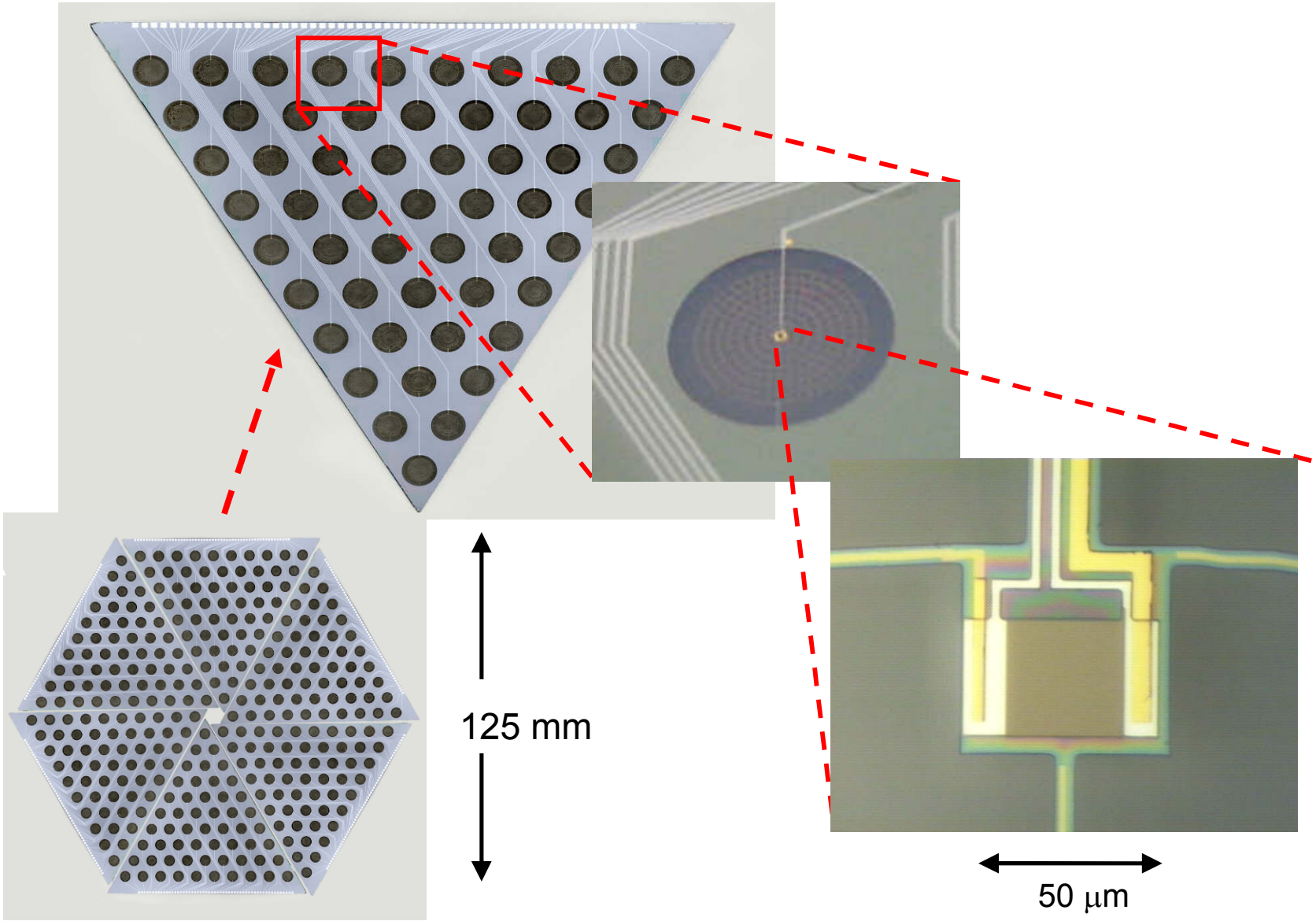

Close-up of spiderweb bolometer

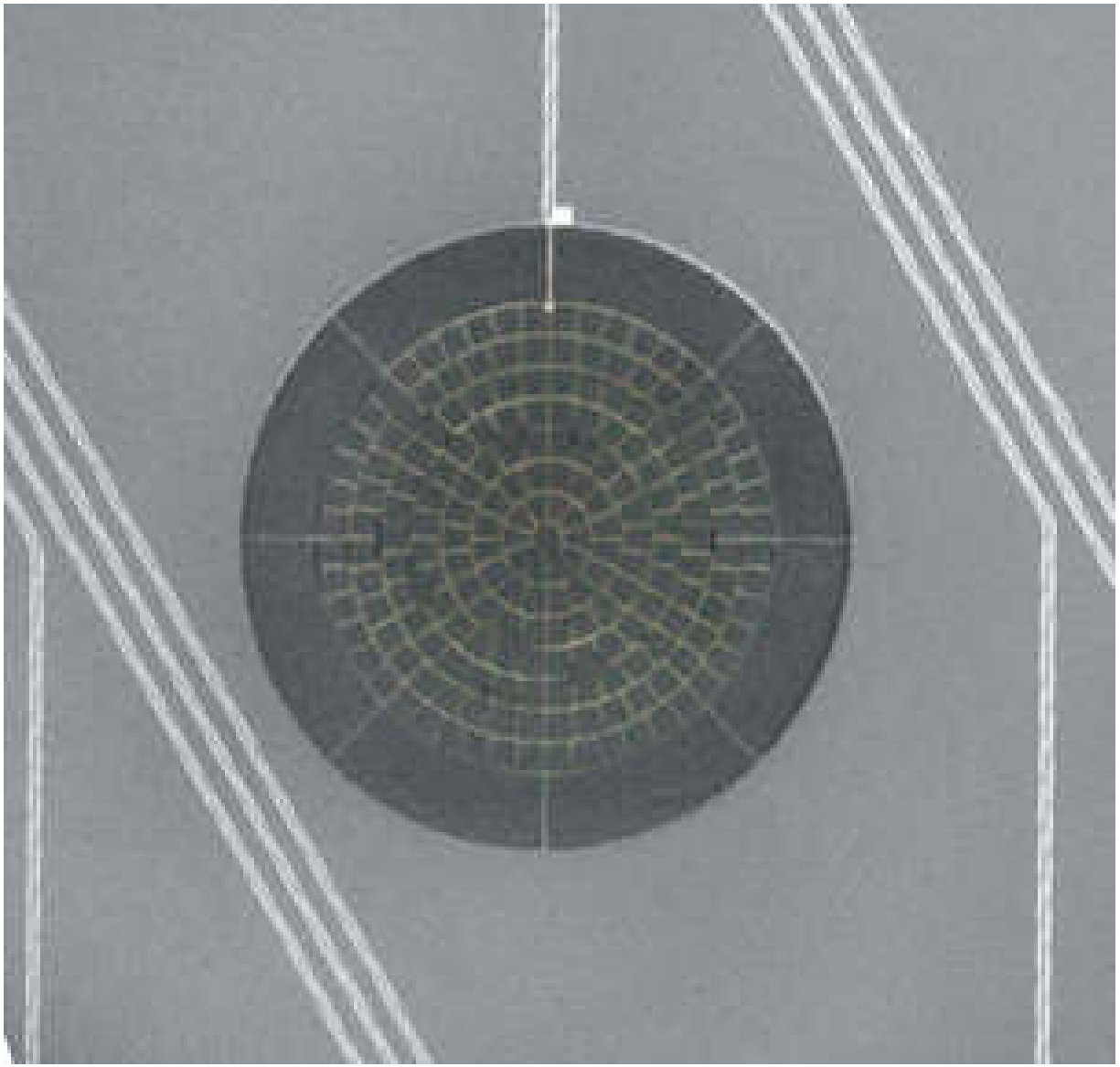

- Constant voltage bias optimizes stability
  This requires that readout impedance $\ll$ bolometer resistance

  bolometer resistance $\approx 1\ \Omega$

  bias resistance $\approx 20\ \mathrm{m}\Omega$

  amplifier input impedance $\approx 10\ \mathrm{m}\Omega$

  1st amplifier stage: SQUID at 4K in shunt feedback configuration. High-frequency feedback loop includes SQUID + warm electronics (300K).

- Typical bolometer bias power: 10 – 40 pW
  (orders of magnitude greater than signal)
- Power Budget on 0.25K stage: <10 μW TOTAL
- Heat conduction through wires to 4K stage acceptable up to ~300 bolometers

  $\Rightarrow$ Larger arrays require multiplexing
- Novel development:

  Frequency-Domain MUX with ZERO additional power on cold stage

  + no noise degradation

Principle of Frequency-Domain Multiplexing

1. High-frequency bias (~100 kHz – 1 MHz)

   Each bolometer biased at different frequency

2. Signals change sensor resistance

   ⇒ Modulate current

   ⇒ Transfer signal spectrum to sidebands adjacent to bias frequency

   ⇒ Each sensor signal translated to unique frequency band

3. Combine all signals in common readout line

4. Retrieve individual signals in bank of frequency-selective demodulators

⇒ High-frequency bias greatly reduces sensitivity to microphonics!
(a major problem for many bolometer systems)

Modulation Basics

If a sinusoidal current $I_0 \sin \omega_0 t$ is amplitude modulated by a second sine wave $I_m \sin \omega_m t$

$$I(t) = (I_0 + I_m \sin \omega_m t) \sin \omega_0 t$$
$$I(t) = I_0 \sin \omega_0 t + I_m \sin \omega_m t \sin \omega_0 t$$

Using the trigonometric identity $2 \sin \alpha \sin \beta = \cos(\alpha - \beta) - \cos(\alpha + \beta)$ this can be rewritten

$$I(t) = I_0 \sin \omega_0 t + \frac{I_m}{2} \cos(\omega_0 t - \omega_m t) - \frac{I_m}{2} \cos(\omega_0 t + \omega_m t)$$

The modulation frequency is translated into two sideband frequencies

$(\omega_0 t + \omega_m t)$ and $(\omega_0 t - \omega_m t)$

symmetrically positioned above and below the carrier frequency ω_0.

All of the information contained in the modulation signal appears in the sidebands; the carrier does not carry any information whatsoever.

The power contained in the sidebands is equal to the modulation power, distributed equally between both sidebands.

Modulation Waveforms and Spectra

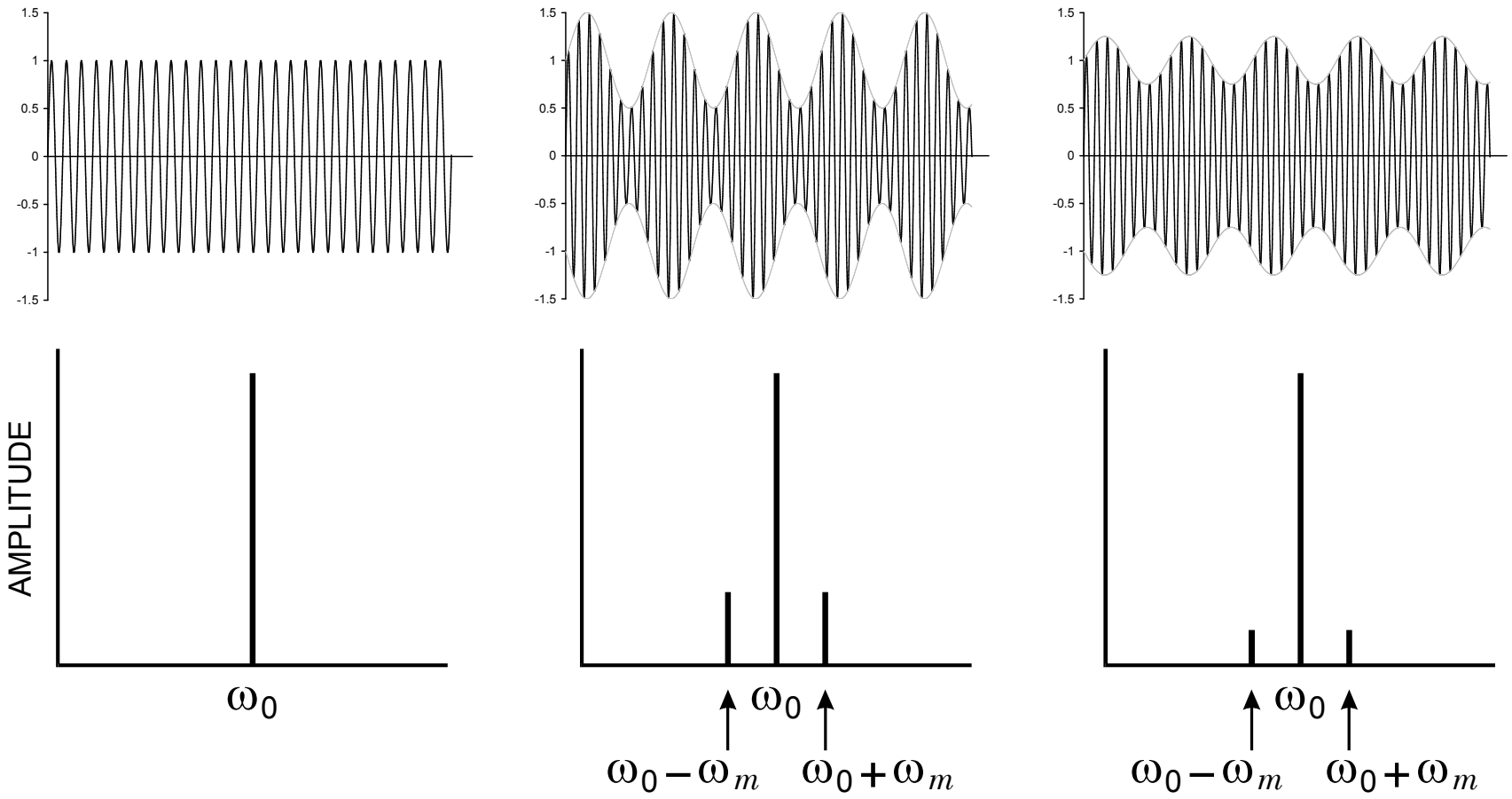

Carrier amplitude remains constant! All signal information in the sidebands.

MUX circuit on cold stage

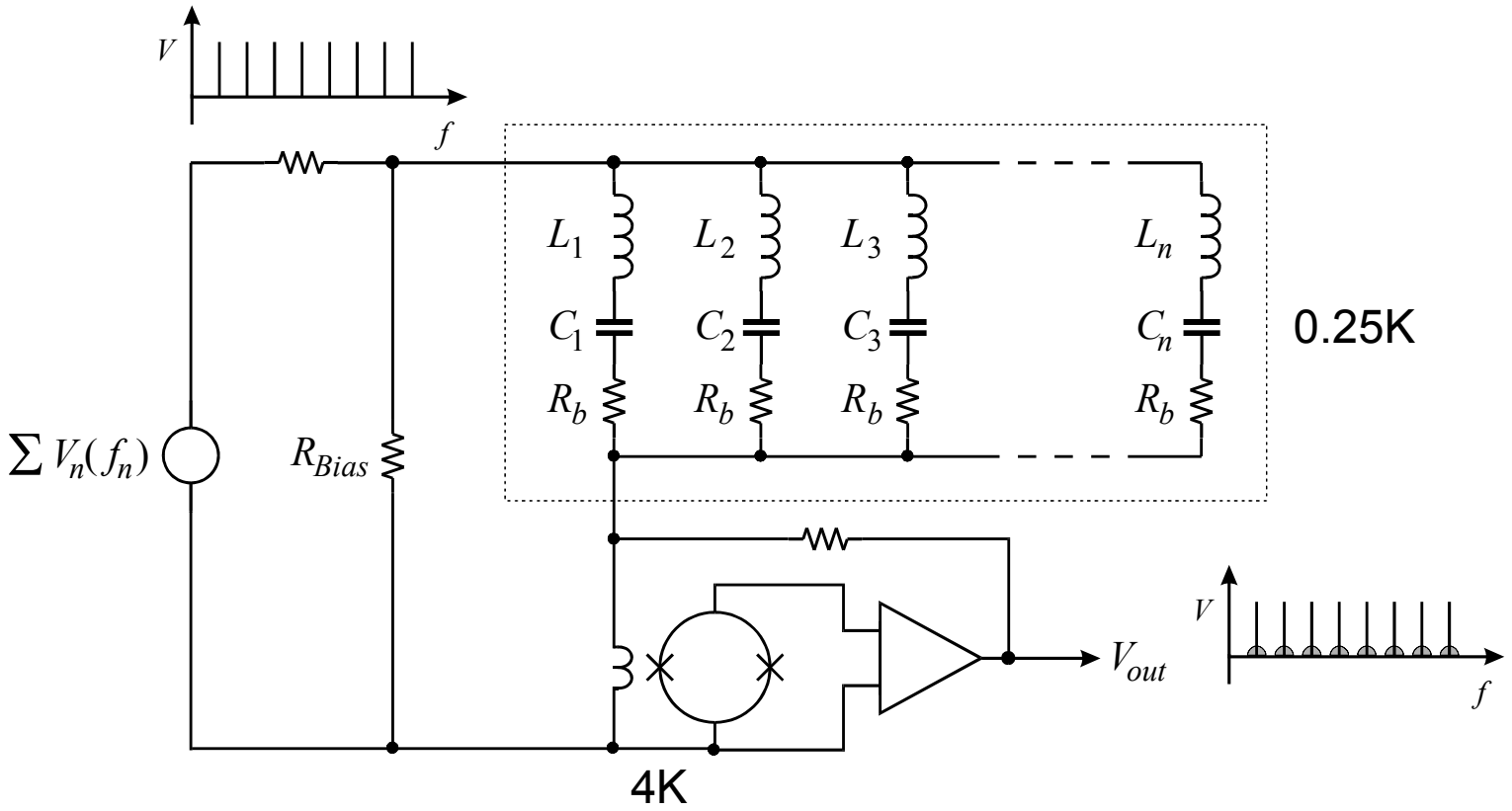

- "Comb" of all bias frequencies fed through single wire.
- Tuned circuits "steer" appropriate frequencies to bolometers and limit noise bandwidth.
- Wiring inductance tuned out at resonance to reduce impedance.
- Current return through shunt-fedback SQUID amplifier (low input impedance).
- No additional power dissipation on cold stage (only bolometer bias power).

System Block Diagram

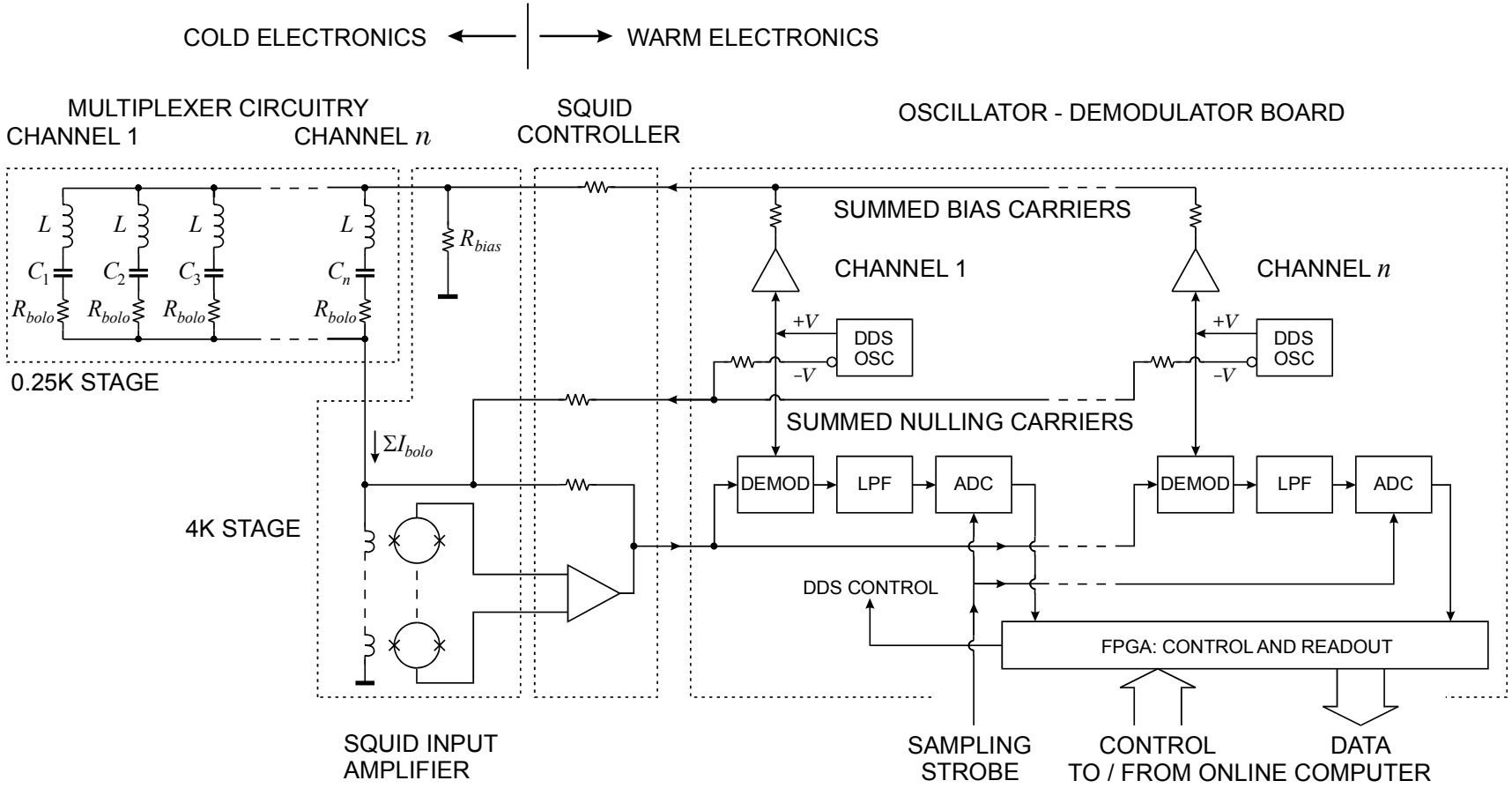

New version uses fully digital processing from the SQUID preamplifier onwards

Matt Dobbs, Eric Bissonnette, and Helmuth Spieler, Digital Frequency Domain Multiplexer for mm-Wavelength Telescopes. IEEE Trans. Nucl. Sci. **NS-55/1** (2008) 21-26

SQUIDs are mounted as arrays of eight in a magnetic shield (4K stage)

SQUID mounting board

SQUIDs mounted on Nb pads
to pin magnetic flux

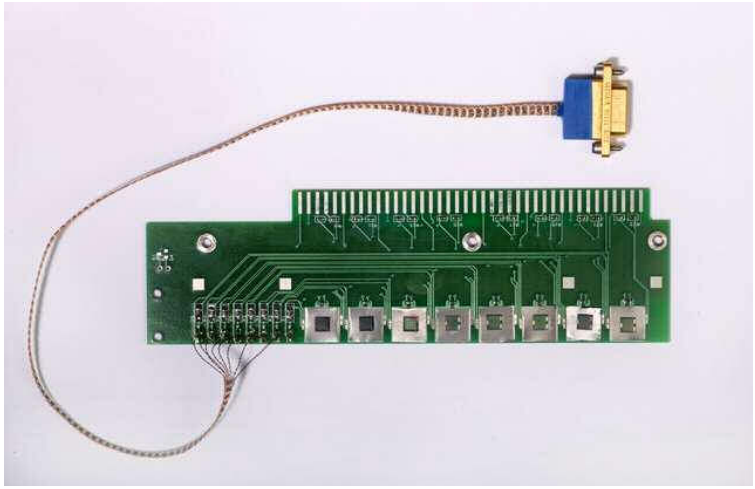

Magnetic Shield
(M. Lueker)

8-channel SQUID Controller

Computer-controlled (FPGA)
SQUID diagnostics
Open/closed loop
Switchable gain

SQUIDs VERY sensitive to pickup (up to GHz), so local shielding of digital circuitry is crucial.

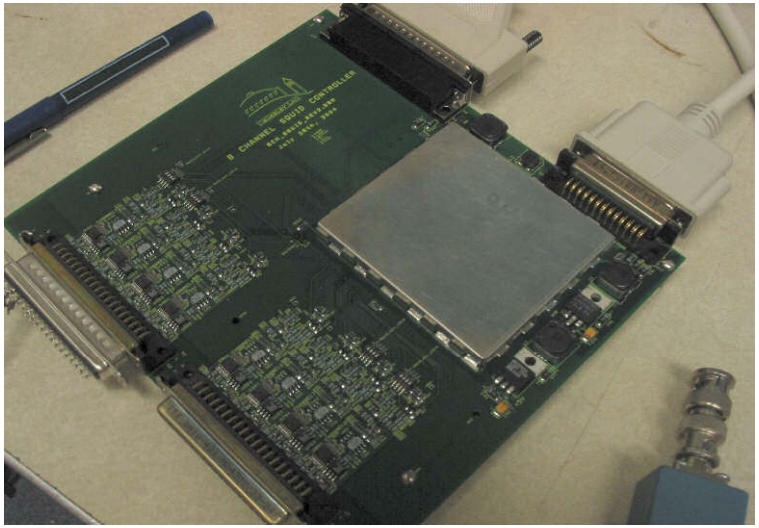

16-channel Demodulator Board

16 individual demodulator channels
1 DDS freq. generator per channel
On-board A/D
Opto-isolated computer interface

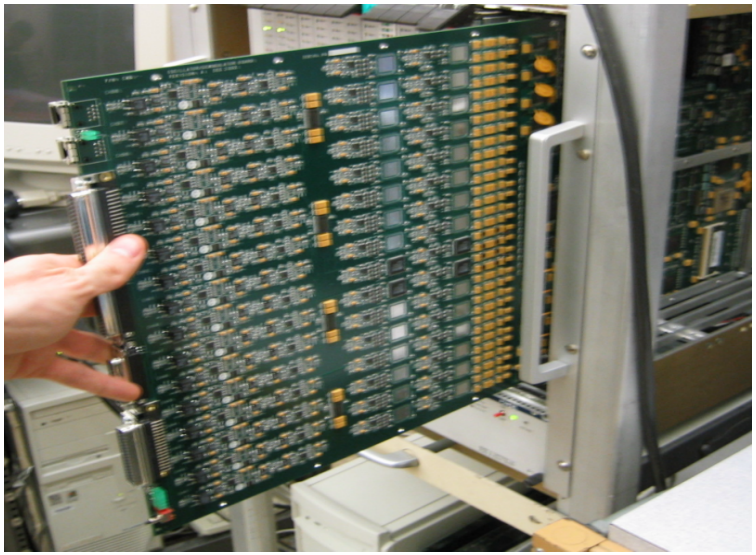

Design at LBNL
(M. Dobbs, J. Joseph, M. Lueker, C. Vu)

High Energy Physics experience essential!

Measured MUX Noise Spectrum at SQUID Amplifier Output
(Trevor Lanting)

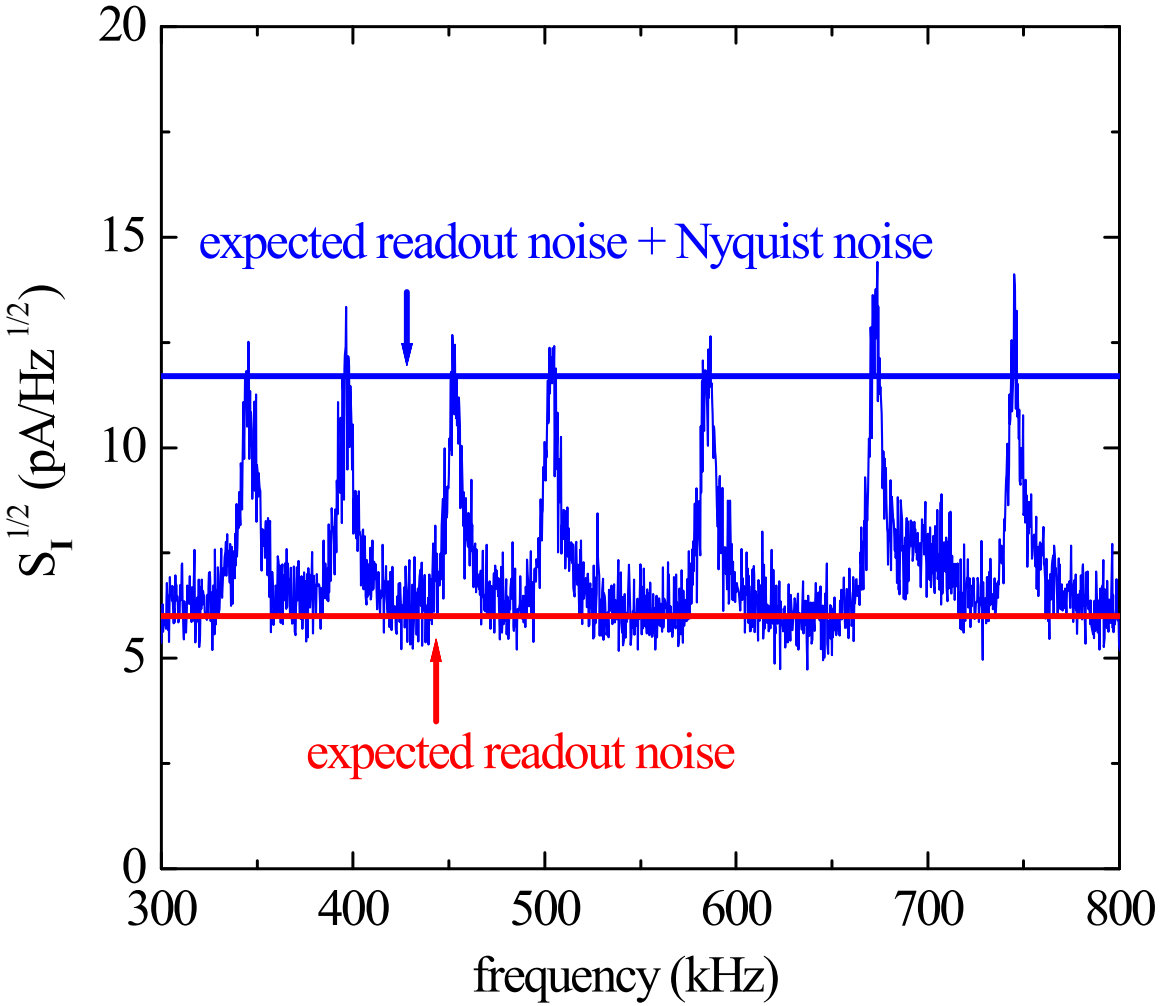

Measured Noise Spectrum in 8-Channel MUX System

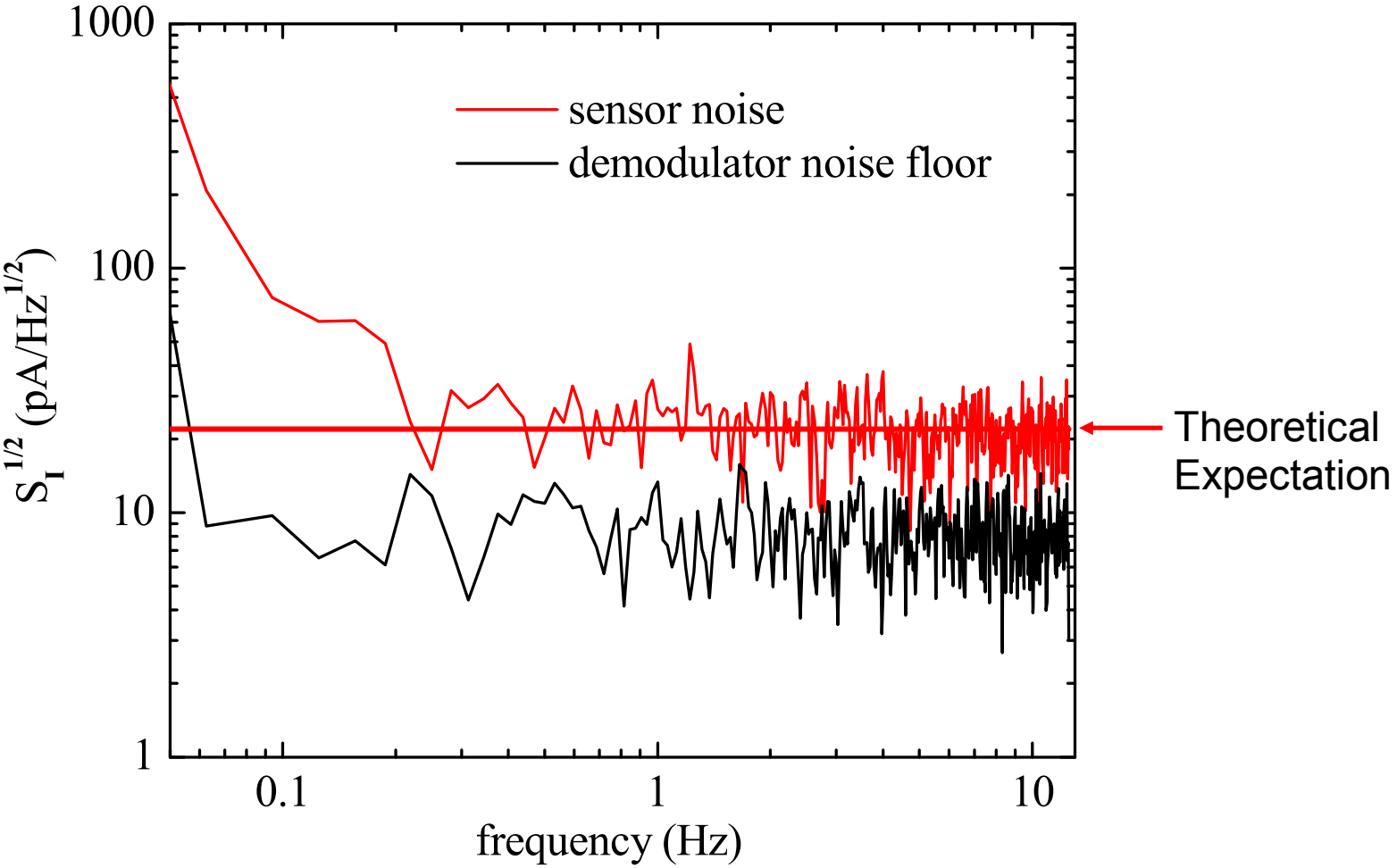

Sensor noise white above 0.2 Hz

(Trevor Lanting)

Cross-Talk < 1%

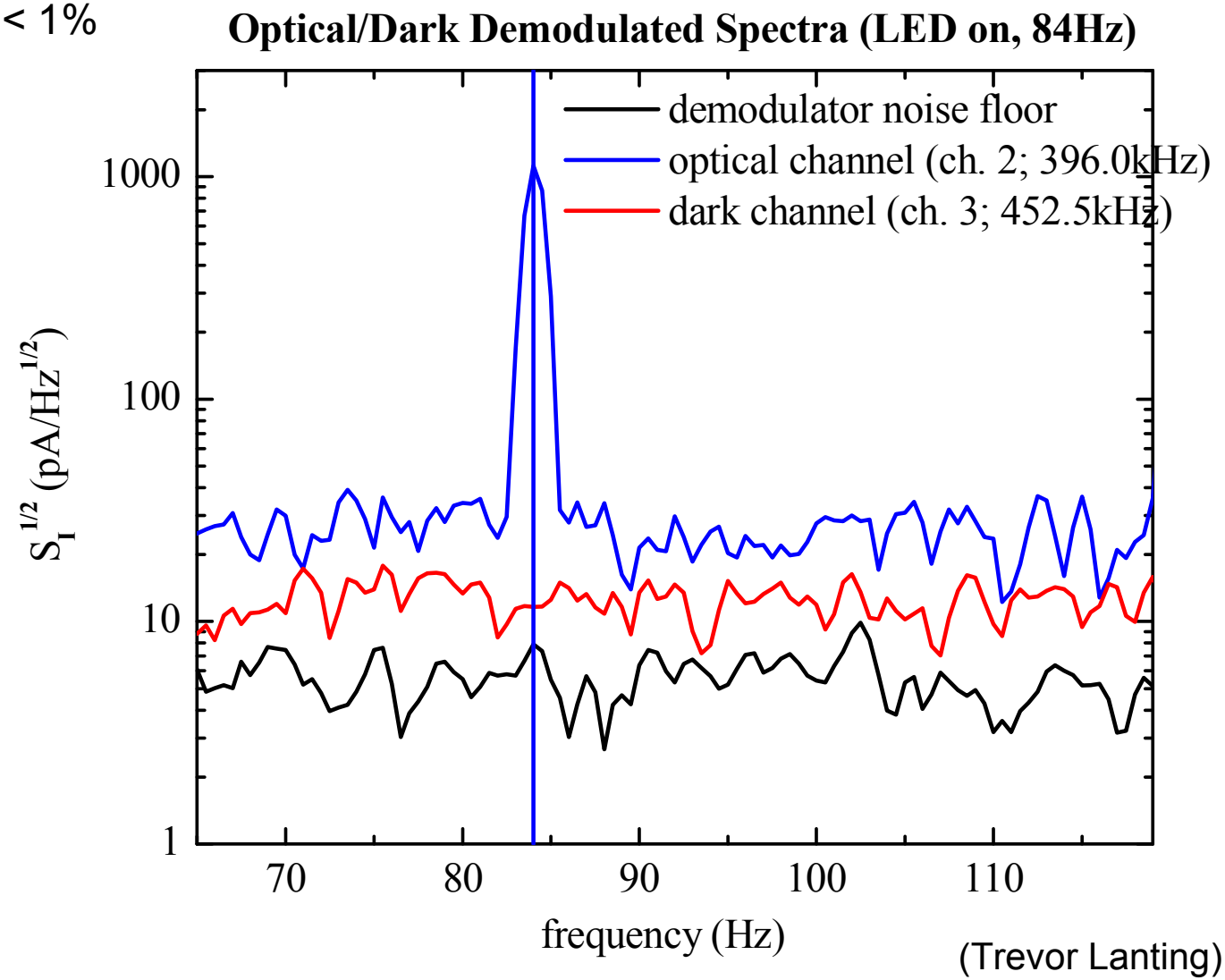

(Trevor Lanting)

Unlike most bolometer systems our noise and overall operational results are within a few % of theoretical simulations.

Detector Configuration

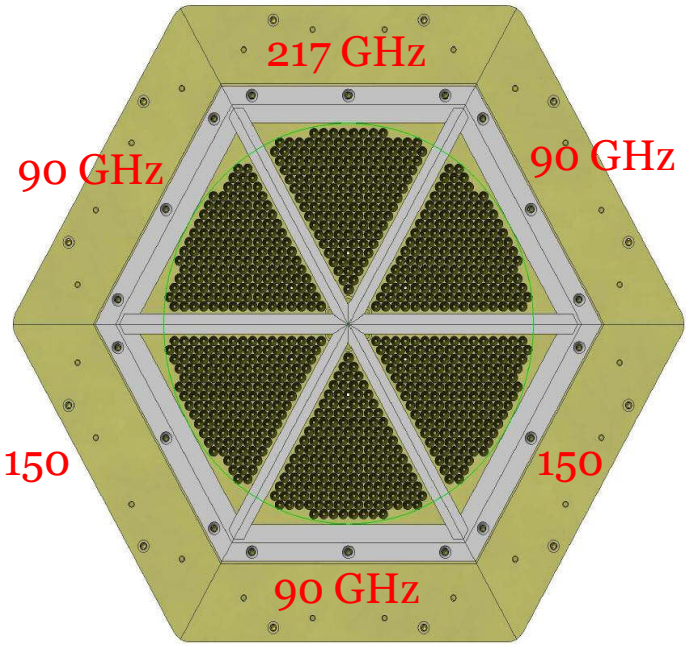

Focal Plane: $T = 0.25\text{K}$

Current configuration:

4 wedges at 150 GHz
1 ea. at 90 and 220 GHz

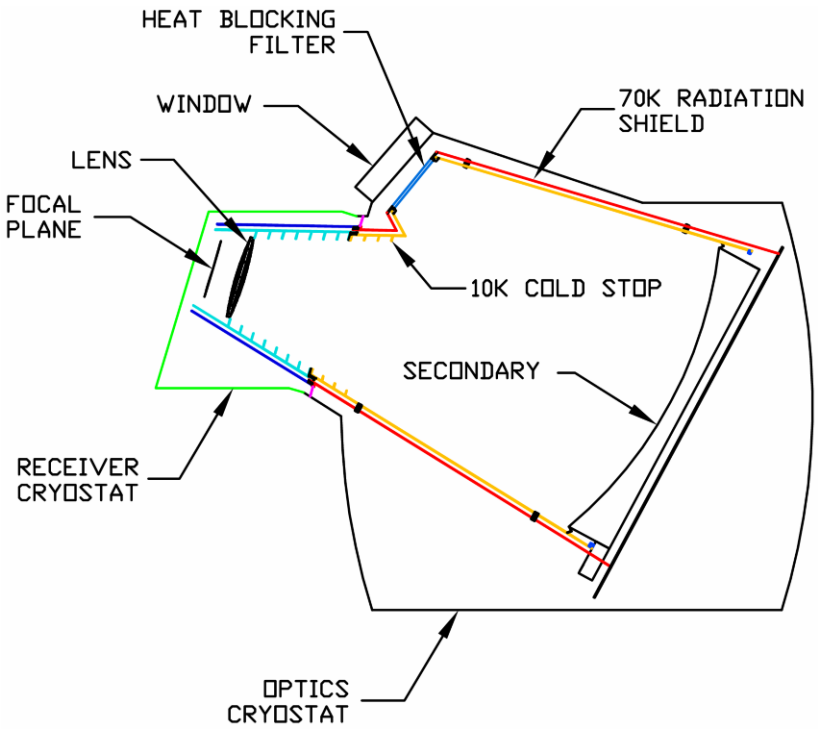

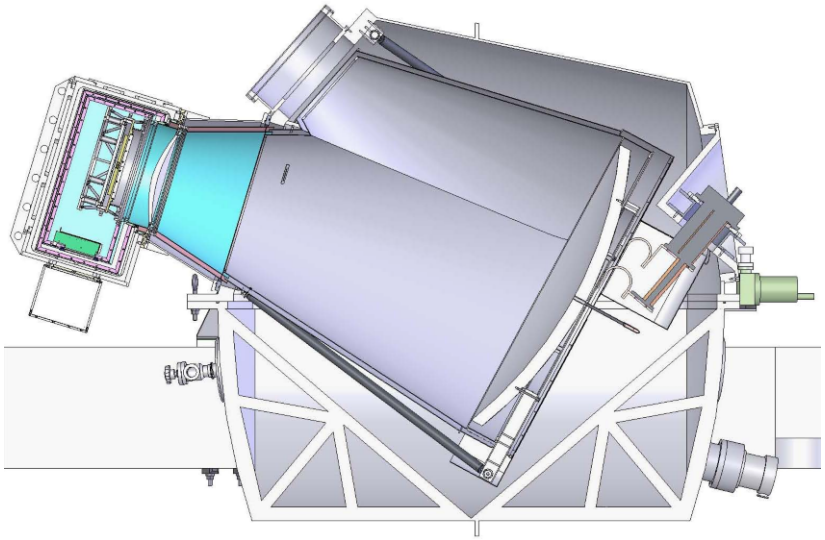

The optics cryostat (white) and receiver cryostat (red) removed from rcvr cabin

Disassembled focal plane for upgrades

Wirebonding replacement SQUIDs

Sometimes some fine tuning is required

Assembled focal plane

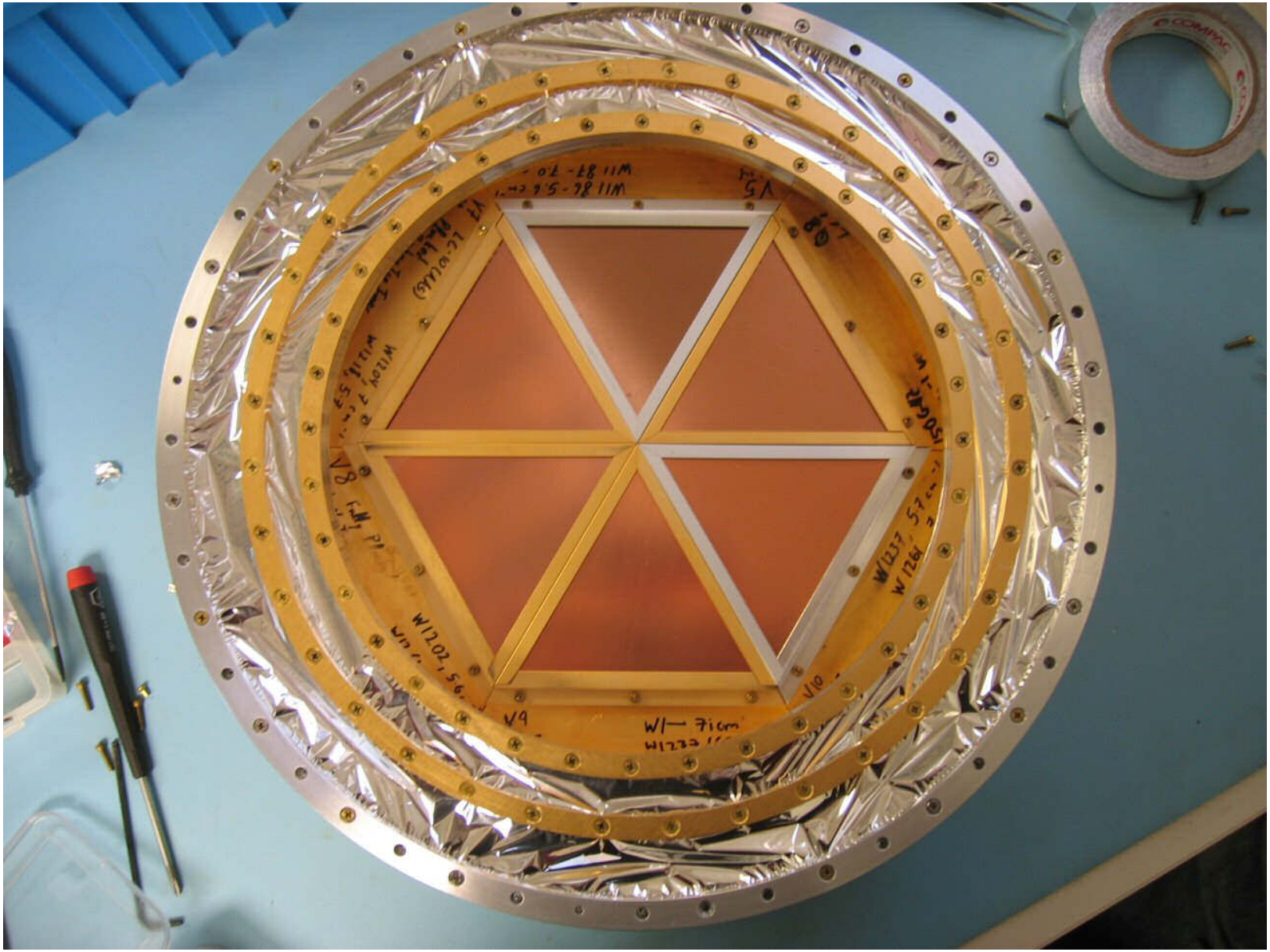

Innards of receiver cryostat

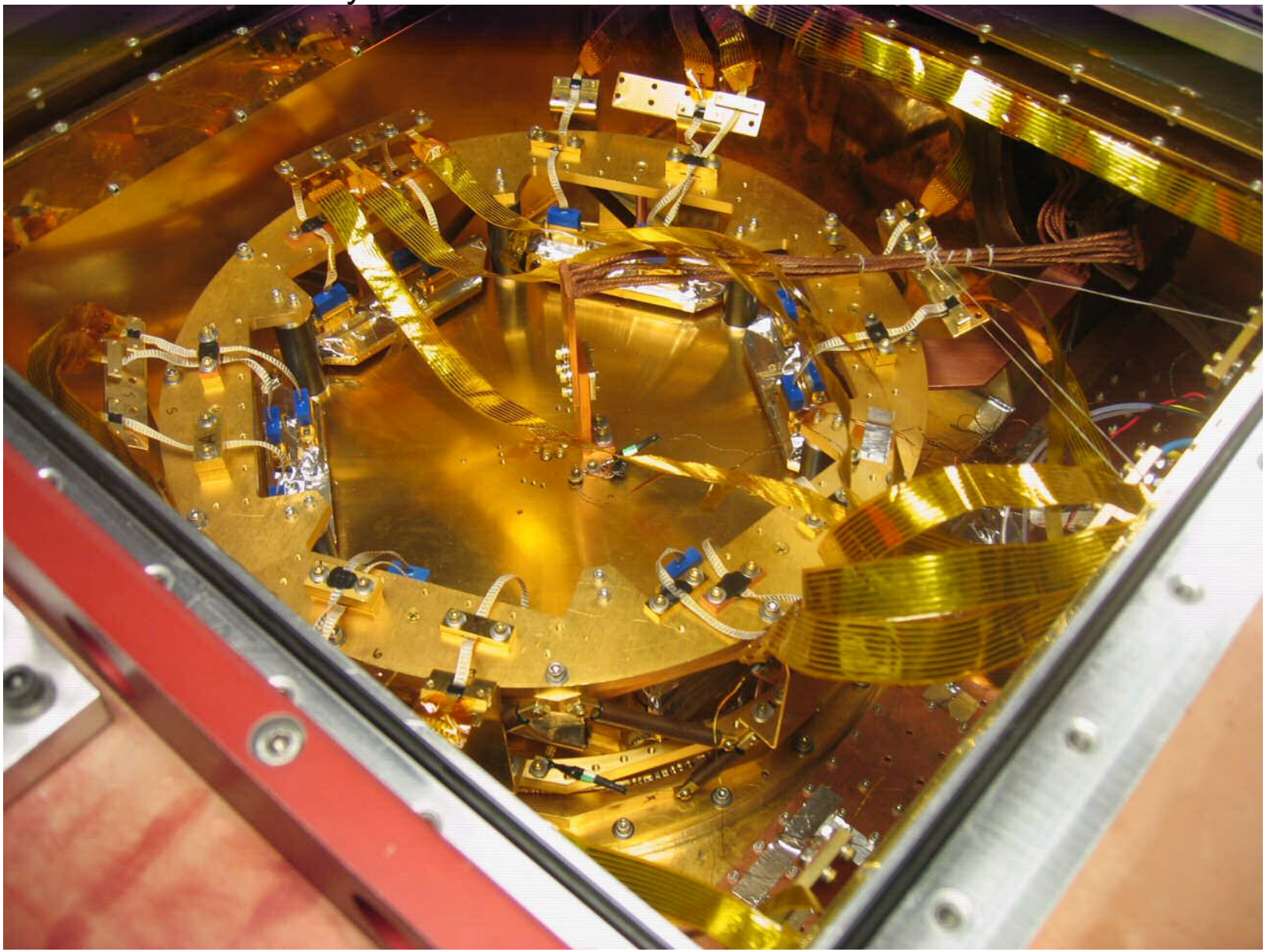

Assembly area

Assembled cryostat beneath the open receiver cabin

Nice summers in München … and nice summers at the South Pole

Summary

- South Pole Telescope in its 5th year of operation, taking data efficiently
- Current CMB experiments achieve 10^2 – 10^3 fold improved sensitivity
- Monolithic fabrication technology provides wafer-scale TES kilopixel arrays
- Frequency-domain MUXing demonstrated

  Zero power dissipation at 0.25K focal plane
  <1% cross-talk
  Very insensitive to vibration
  Negligible increase in noise
  Conceptually simple, but many crucial details

- System incorporates techniques from

  Cryogenics and superconductivity
  RF communications (old and new)
  Low noise analog electronics
  High Energy Physics

- Collaboration between University and National Lab was essential, although not supported by funding agencies (NSF – DOE)

Closing Comments

- Detectors involve a wide range of interacting functions – often conflicting.
- Don't just follow recipes – think physics!
- Statements may sound good, but what counts is whether they are correct.
- The key aspects of detectors and electronics can be recognized if you really understand physics.
- Just talking physics is not good enough – implementing ideas to test their correctness is essential
- Don't blindly accept the results of simulations. Do cross checks!
- Bugs are not just technical, but also intellectual.

Following Confucius, yins at the extreme turn into yangs.

Science projects driven by recipes turn into engineering
and engineering projects driven by physics can turn into science.

The broad range of physics in novel detector development brings you into more science than run-of-the-mill data analysis.